

UCSF

UC San Francisco Electronic Theses and Dissertations

Title

Non-canonical roles for telomerase in T cells and breast cancer cells

Permalink

<https://escholarship.org/uc/item/38n028mr>

Author

Gazzaniga, Francesca Smylie

Publication Date

2013

Peer reviewed|Thesis/dissertation

NON-CANONICAL ROLES FOR TELOMERASE IN T CELLS
AND BREAST CANCER CELLS

by

Francesca Smylie Gazzaniga

DISSERTATION

Submitted in partial satisfaction of the requirements for the degree of

DOCTOR OF PHILOSOPHY

in

Biomedical Sciences

in the

GRADUATE DIVISION

of the

UNIVERSITY OF CALIFORNIA, SAN FRANCISCO

ACKNOWLEDGEMENTS

I dedicate this thesis to my parents who inspired me to become a scientist through invigorating scientific discussions at the dinner table even when I was too young to understand what the hippocampus was. They also prepared me for the ups and downs of science and supported me through all of these experiences.

I would like to thank my advisor Dr. Elizabeth Blackburn and my thesis committee members Dr. Eric Verdin, and Dr. Emmanuelle Passegue. Liz created a nurturing and supportive environment for me to explore my own ideas, while at the same time teaching me how to love science, test my questions, and of course provide endless ways to think about telomeres and telomerase. Eric and Emmanuelle both gave specific critical advice about the proper experiments for T cells and both volunteered their lab members for further critical advice. I always felt inspired with a sense of direction after thesis committee meetings.

The Blackburn lab is full of smart and dedicated scientists whom I am thankful for their support. Specifically Dr. Shang Li and Dr. Brad Stohr for their stimulating scientific debates and “arguments.” Dr. Jue Lin, Dana Smith, Kyle Lapham, Dr. Tet Matsuguchi, and Kyle Jay for their friendships and discussions about what my data could possibly mean. Dr. Eva Samal for teaching me molecular biology techniques and putting up with my late night lab exercises. Beth Cimini for her expertise with microscopy, FACs, singing, and most of all for being a caring and supportive friend. Finally, I would like to thank Dr. Imke Listerman, my scientific partner for most of the breast cancer experiments. She taught me to enjoy and benefit from a scientific collaboration. She was also wonderful mentor while at the same time treating me as a scientific peer and friend.

I would also like to thank my family and friends who helped me maintain a lab/life balance. My brother Zack has always blindly and enthusiastically supported me without any need for understanding what I do. My sisters Marin, Anne, Kate, and Zaz for supporting their nerdy little sister. My nieces and nephews Lilly, Emmy, Garth, Dante, and Rebecca who always put a smile on my face even when experiments fail. My best friends Karen and Cleya who have made life outside of the lab fun with wine, hikes, and too many good times to list. Finally, I would like to thank my fiancé and partner in adventures, Richard Novak, who is always there to talk science, cook dinner, or just make me smile.

CONTRIBUTIONS

I performed the majority of the experiments in the T cell portion of this thesis with the exception of the following experiments: the Gladstone institute performed the microarray, Dr. Richard Novak performed the microarray analysis, and Beth Cimini performed FACs sorting for GFP + cells. The breast cancer portion of the thesis was a team effort. I performed the telomere length analysis and Dr. Imke Listerman performed telomerase expression and activity data described in this thesis. This data was published in (Listerman, I., Sun, J., Gazzaniga, F.S., Lukas, J.J., Blackburn, E.H. 2013. The major reverse transcriptase-incompetent splice variant of the human telomerase protein inhibits telomerase activity but protects from apoptosis. *Cancer Research*. May 1;73(9):2817-28). The majority of the breast cancer portion of this thesis was reprinted from (Gazzaniga, F.S., Listerman, I., Blackburn, E.H. 2013. An investigation of the effects of the telomerase core protein TERT on Wnt signaling in human breast cancer cells. *Molecular Cell Biology*. Epub. Nov 11 2013 doi: 10.1128/MCB.00844-13) in which Listerman and I were co-first authors. I performed the majority of cell culture and the qPCR arrays. Dr. Listerman performed the biochemical and bioinformatic analyses. Both Dr. Listerman and I performed the Wnt reporter assays, stained and imaged cells, and wrote the paper. Pierre de la Grange from Genosplice performed the data analysis correlating telomerase activity and gene expression.

ABSTRACT

Non-canonical roles for telomerase in T cells and breast cancer cells

Francesca S Gazzaniga

Telomerase is a ribonucleoprotein that adds telomeric DNA to the ends of linear chromosomes. It is composed of two core components, the reverse transcriptase component, hTERT, and the RNA template, hTR. In the absence of sufficient telomerase, most differentiated cells experience telomere shortening with each cell division and eventually undergo replicative senescence. Conversely, stem cells and the majority of cancer cells have high telomerase activity, which maintains telomere length allowing them to divide indefinitely. While the role of telomerase in telomere maintenance is clear, recent studies have suggested non-canonical roles for telomerase. The purpose of this thesis is to investigate any non-canonical roles for telomerase in both normal and cancer cells.

The first part of this thesis focuses on the role of telomerase in primary human T cells. T cells are one of the few types of differentiated cells that upregulate telomerase activity upon stimulation. While telomerase activity and T cell proliferation correlate, it is unknown if this upregulation is necessary or even quantitatively coupled to T cell survival. Surprisingly, I find that the telomerase RNA, hTR, actually protects CD4⁺ T cells from apoptosis independent of telomere maintenance or telomerase activity. This is the first report showing a non-telomere role for the telomerase RNA.

The second part of this thesis investigates a controversial mechanism for a non-canonical role for hTERT in Wnt signaling. One study published that telomerase activity promotes Wnt/ β -catenin signaling in mice and HeLa cells. However, another study was unable to reproduce these findings in mice, but did not investigate these findings in cancer cells. Since

Wnt signaling is often dysregulated in breast cancer, we sought to determine if we could independently replicate any hTERT -Wnt/ β -catenin interactions in breast cancer cells. Using genetic, biochemical, and bioinformatic analyses we do not find any data supporting the hypothesis that hTERT promotes Wnt/ β -catenin signaling in breast cancer cells and instead suggest that any published interactions detected are cell line and cell context specific.

We and others have shown hTERT can promote proliferation, protect from apoptosis, and promote mitochondrial function independent of telomere maintenance and/or telomerase activity in a wide variety of cell types. This thesis shows that hTERT does not promote these functions through Wnt/ β -catenin signaling. Furthermore, I show for the first time that hTR also has a non-telomere and non-telomerase role protecting from apoptosis in CD4⁺ T cells. While the importance of telomerase for maintaining telomeres is clear, this thesis shows that both of the telomerase core components have non-canonical roles in cell survival in normal and cancer cells.

TABLE OF CONTENTS

ACKNOWLEDGEMENTS	iii
CONTRIBUTIONS	v
ABSTRACT.....	vi
TABLE OF CONTENTS	viii
LIST OF FIGURES AND TABLES.....	ix
CHAPTER 1: T CELLS.....	1
INTRODUCTION	1
MATERIALS AND METHODS.....	11
RESULTS.....	19
CONCLUSIONS AND DISCUSSION.....	46
FUTURE STUDIES.....	62
CHAPTER 2: BREAST CANCER	65
INTRODUCTION	65
RESULTS.....	74
DISCUSSION.....	100
FUTURE STUDIES.....	105
APPENDIX.....	106
REFERENCES.....	139
LIBRARY RELEASE FORM	148

LIST OF FIGURES AND TABLES

CHAPTER 1

Figure 1. Visualizing telomeres and telomerase structures	9
Figure 2. hTR knockdown induces Bim mediated apoptosis	21
Figure 3. Telomerase knockdown does not induce significant telomere shortening or TIFs in the timeframe of this experiment	24
Figure 4. hTR knockdown does not alter CD4+ T cell type or cytokine release	30
Figure 5. Genes significantly changed with hTR knockdown	34
Figure 6. hTR overexpression protects from dexamethasone induced apoptosis independent of telomerase activity	38
Figure 7. hTERT overexpression increases telomerase activity and induces apoptosis	41
Figure 8. Overexpression of catalytically inactive hTR mutants protects from hTERT-induced apoptosis	43
Figure 9. Models for how catalytically inactive hTR protects from apoptosis	56
Figure 10. Two functions for hTR	59
Table 1. Summary of telomerase activity and susceptibility to apoptosis	45

CHAPTER 2

Figure 1. Endogenous Wnt/ β -catenin target gene induction varies in breast cancer cells	76
Figure 2. Effect of hTERT overexpression on two Wnt/ β -catenin reporters	80
Figure 3. hTERT does not interact with β -catenin or BRG1	83
Figure 4. Effect of hTERT overexpression on Wnt target gene expression in breast cancer cell lines	90

Figure 5. Effect of hTERT overexpression on Wnt pathway gene expression in breast cancer cell lines	93
Figure 6. Effect of hTERT knockdown on Wnt pathway gene expression in SUM149PT and HCC1806 cells	94
Figure 7. Confluency and passage number do not affect telomerase activity	98
Table 1. Significant GO terms for genes close to BRG1 and hTR co-occupied loci in HeLa S3 genome	87
APPENDIX	
Supplementary Figure S1. hTR knockdown, but not hTERT knockdown reduces T cell survival in T cells from six additional donors	106
Supplementary Figure S2. Telomere length and TIF measurements with 53BP1	108
Supplementary Figure S3. shTIN2 acts as a positive control for telomere shortening and detection of TIFs	109
Supplementary Figure S4. hTR knockdown does not affect CD4 ⁺ T cell development from naïve to effector memory T cells in culture	110
Supplementary Figure S5. hTR knockdown reduces T cell survival in culture when starting with naïve T cell population	112
Figure S6. qRT-PCR of several genes identified by the microarray as significantly changed	113
Supplementary Figure S7. Cell counts of Day 15 shRNAs with 72 hours of 5 μ M cortisol treatment	114

Supplementary Table 1. Names and descriptions of plasmids	115
Supplementary Table 2. Primers for qRT-PCR	116
Supplementary Table 3. Genes that correlate with telomerase activity in a panel of breast cancer cells	117

CHAPTER 1: T CELLS

INTRODUCTION

Telomeres and telomerase solve the end replication problem

The linearity of eukaryotic chromosomes generates two potential problems. One of these problems is the end replication problem, which refers to the inability of the DNA replication machinery to completely replicate the 3' ends of parent chromosomes. Therefore, with each cell division, the 5' ends of each daughter chromosome contain less DNA than chromosomes in the previous cell division (Watson, 1972). The other potential problem with linear chromosomes is that their ends, if unprotected, signal as double stranded DNA breaks characterized by γ H2ax foci, phosphorylation of ATM, and 53BP1 foci in the nucleus leading to activation p53 and apoptosis senescence or apoptosis (Harper and Elledge, 2007). Cells attempt to fix DNA breaks through homologous recombination and non-homologous end joining. However if homologous recombination or non-homologous end joining is inappropriately applied to chromosome ends, chromosomes undergo fusion breakage cycles leading to chromosomal instability triggering senescence or causing the acquisition of mutations to lead to cancer (Harper and Elledge, 2007; de Lange, 2009).

Telomeres are DNA repeat/protein complexes that solve both of the problems of linear chromosomes. To prevent genomic loss due to the end replication problem, telomeres act as extra DNA, in humans composed of TTAGGG repeats, at the ends of chromosomes (Blackburn, 2000). Instead of genomic DNA shortening during each round of replication, telomeres can lengthen. To solve the second problem, telomeric DNA associates and folds via interactions with proteins that protect the ends of chromosomes from signaling as double stranded breaks, and thus prevent telomeric degradation and chromosomal rearrangement (Blackburn, 2000, 2001; de

Lange, 2009). The maintenance of telomeres is therefore crucial for normal cell function. Figure 1A shows a metaphase spread of a normal T-cell with chromosomal DNA stained with DAPI and a fluorescent telomere specific PNA probe used to visualize the telomeres at the ends of the chromosomes.

Additional processes besides the DNA end replication problem can result in telomeres becoming shortened: DNA damage due to oxidative damage, to which telomeric G-rich repeats are particularly susceptible, inappropriate recombination events that loop out and shorten the tracts of telomeric DNA repeats, and nuclease actions (Blackburn, 2000; de Lange, 2009). Counteracting these processes, telomerase is a highly specialized type of reverse transcriptase that both elongates and protects telomeres. In humans, the core telomerase contains a reverse transcriptase catalytic subunit, hTERT, and an RNA template, hTR, hTER, or hTERC, and both are associated with additional factors. The catalytic subunit binds telomeres and uses the RNA template to reverse transcribe TTAGGG repeats onto human telomeres. Most adult human cells have very low levels of telomerase activity, and telomerase addition of telomeric DNA appears to be slower than telomeric DNA loss due to cell divisions, oxidative stress, and other factors. Aging in humans is therefore thought to involve, and potentially result from, shortening telomeres, and their eventual loss of protective properties, over time (for references see (Blackburn and Collins, 2011)). Figure 1 B shows a representation of the telomerase core complex adding telomeres.

Telomerase structure and function

To date, fourteen different splice variants of the human telomerase reverse transcriptase, hTERT have been identified (Saebøe-Larssen et al., 2006). As many of these splice variants introduce a premature stop codon or would give rise to a truncated protein, the splicing of

hTERT has been thought to simply regulate telomerase activity. In addition to the full-length splice variant that gives rise to the hTERT protein, at least one of the other splice variants has been shown to be translated into a protein. This splice variant is referred to as the β - splice variant, which is missing the reverse transcriptase domain, but is still able to bind hTR. Expression of the β - splice variant is negatively associated with telomerase activity and is thought to reduce telomerase activity by sequestering hTR (Listerman et al., 2013). Interestingly overexpression of full length hTERT or the β - splice variant in cancer cells reduces cisplatin induced apoptosis suggesting that hTERT might have reverse-transcriptase independent roles (Listerman et al., 2013). However, any other functions of hTERT and its splice variants are still unknown.

Mutations in hTR giving rise to a disease previously called dyskeratosis congenita, and now described as a subset of “telomere syndromes,” described in more detail below, reveal the importance of hTR secondary structure. Generally hTR is composed of a set of conserved telomerase RNA structural features that in humans include a pseudoknot, the CR4/5 domain, and the H/ACA domain (Fig 1C). The pseudoknot contains the RNA template for telomeric addition and binds to hTERT. At least two conformations of the pseudoknot have been identified (Hengesbach et al., 2012; Qiao and Cech, 2008; Yeoman et al., 2010). The conformation depicted in figure 1C shows predicted pseudoknot conformation that is stabilized by hTERT and is required for telomerase activity. Mutations in this domain that disrupt stem formation, such as the dyskeratosis congenita mutant, GC(107-108)AG, disrupt the folding of hTR and reduce catalytic activity (Hengesbach et al., 2012). Another dyskeratosis congenita mutation, the deletion of nucleotides 96 and 97, which would also disrupt stem formation in the pseudoknot, give rise to a mutant hTR that binds hTERT, but cannot add telomeric DNA. Patients with this

mutation have reduced telomerase activity (the residual activity coming from the other, non-mutated hTR gene allele), short telomeres and severe dyskeratosis congenita symptoms (Robart and Collins, 2010). The CR4/5 domain has also been shown to be important for hTERT binding. Specifically, the p6.1 stem-loop structure in the CR4/5 domain is necessary for telomerase activity and TERT binding (Chen et al., 2000; Leeper et al., 2003; Mitchell and Collins, 2000). The dyskeratosis congenita-linked hTR mutation G305A (and other mutations which disrupt the formation of this stem-loop) disrupts the p6.1 stem of the CR4/5 domain and greatly reduces hTR binding to hTERT and telomerase activity (Robart and Collins, 2010). It is unknown if this p6.1 region is only necessary for telomerase activity via TERT binding or if it also contributes to catalytic activity. This region can fold and bind to the RNA template and mutations that disrupt this stem loop structure disrupt the RNA-RNA interaction of the p6.1 stem loop with the template (Ueda and Roberts, 2004). Figure 1 E shows a potential active conformation of hTR with the triple helix pseudoknot structure and the P6.1 stem loop binding to the template and an inactive conformation of hTR in which the pseudoknot folding and the P6.1 folding are disrupted. Finally, the H/ACA domain binds the protein dyskerin (together with dyskerin's associated protein factors), and this binding is essential for hTR accumulation and stability. Mutations in the CR7 region of the H/ACA domain disrupt dyskerin binding and reduce hTR stability. Replacing the H/ACA domain of hTR with only the H/ACA domain of a snoRNA leads to accumulation of hTR if the H/ACA of the snoRNA is the same size and shape as the hTR H/ACA domain. For example, Figure 1 D shows an experimentally designed hTR mutant, in which the pseudoknot of hTR is fused to the H/ACA domain of the U64 snoRNA. This fusion is stably expressed but does not detectably bind hTERT in vitro or have catalytic activity (Fu and

Collins, 2003; Mitchell et al., 1999). Figure 1 C shows a diagram of the secondary structure of hTR and its predicted binding of hTERT and dyskerin.

The similarity of the hTR H/ACA domain to the H/ACA domain for snoRNAs suggests that hTR might act as or interact with snoRNAs. snoRNAs are small nucleolar non-coding RNAs that complex with ribonucleoproteins to make post-transcriptional modifications of RNAs. snoRNAs are comprised of two main classes: C/D box snoRNAs, which methylate other RNAs, and H/ACA box snoRNAs, which bind dyskerin and pseudouridylylate other RNAs. These modifications can affect the stability and potentially the functionality of the modified RNA. For example, the P6.1 hairpin of hTR can be pseudouridylylated and this modification affects the structure of this hairpin and catalytic activity (Kim et al., 2010). While each snoRNA appears to have a specific RNA target for modification, it remains unclear how to identify snoRNA targets. Furthermore, snoRNAs are dysregulated, and often downregulated in cancer and this dysregulation is thought to contribute to carcinogenesis (Esteller, 2011). Since the telomerase RNA contains an H/ACA domain and binds dyskerin it is possible that the telomerase RNA might function as an H/ACA snoRNA. However any targets for hTR acting as an H/ACA snoRNA have not been identified.

Telomerase in mouse models and human disease

The importance of sufficient, yet well-regulated, telomerase activity is highlighted in mouse models and human disease. For example, mice with telomerase genetically knocked out show decreased cell proliferation, compromised immune function, premature aging, and eventual loss of fertility coordinate with telomere shortening (Goytisolo and Blasco, 2002). Clearly showing the importance of sufficient telomerase activity in humans, haploinsufficiency for telomerase, caused by either hTR or hTERT mutations, causes premature loss of immune

function, fibroses and cancer predisposition (collectively called “telomere syndromes”) (Armanios and Blackburn, 2012; Blasco, 2005). Shorter telomeres and lower telomerase activity are typically measured in peripheral blood mononuclear cells (PBMCs); both are associated with diseases of aging and hence may be biological markers for aging in the general population (Armanios, 2013; Weng et al., 1997). While these examples clearly indicate the importance of sufficient telomerase activity, too much telomerase activity is also damaging, as cancer cells commonly acquire very high levels of telomerase activity (Shay and Bacchetti, 1997) and overexpression of telomerase in mice leads to increased incidence of cancer (Artandi et al., 2002). Furthermore, somatic mutations located in the hTERT promoter that cause only an ~2-fold increase in hTERT expression in reporter cell lines are the most prevalent mutations found in melanomas and brain cancers, and frequent in other human cancers as well (Horn et al., 2013; Huang et al., 2013; Killela et al., 2013). A similar germline hTERT mutation causes melanoma with 100% penetrance in mutation carriers in a recently studied kindred (Horn et al., 2013). Understanding mechanisms regulating telomerase levels and activity is an important step in understanding how to treat diseases of both compromised and enhanced telomerase activity.

The role of telomerase in T cells

In general, proliferating cells, such as stem cells, progenitor cells and the majority of cancer cells, contain high telomerase activity. However most differentiated cells have undetectable to minimal telomerase activity (Kim et al., 1994; Morrison et al., 1996). Lacking sufficient telomerase activity, differentiated normal cells such as fibroblasts replicate until their telomeres become critically short, at which point the cells enter senescence (Harley et al., 1990). In most cell types hTERT appears to be the limiting factor for telomerase. In fact fibroblasts

express hTR, but not hTERT, though it is unclear why cells without telomerase activity would express the telomerase RNA template (Feng et al., 1995).

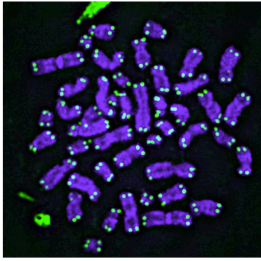
In the hematopoietic system T cells, like other differentiated cells, have very low levels of telomerase activity in a resting state (Broccoli et al., 1996; Morrison et al., 1996; Weng et al., 1996). Upon stimulation, however, T cells rapidly proliferate and telomerase activity, hTERT mRNA, and hTR levels increase. As proliferation slows, telomerase activity, hTERT mRNA, and hTR levels also drop (Kosciolek and Rowley, 1999; Liu et al., 1999; Weng et al., 1996, 1997). Furthermore when T cell proliferation is hindered by cortisol treatment, actinomycin D, cycloheximide, or Herbimycin A, telomerase activity is also reduced (Choi et al., 2008a; Weng et al., 1996). While T cell proliferation and telomerase activity track, it is unknown whether telomerase activity is necessary or even quantitatively coupled to this proliferative response. The ability of helper T-cells to proliferate is one measure of their function since helper T-cells activate killer T-cells and other immune cells to combat infections (reviewed in (Zhu and Paul, 2008)). Since telomerase activity is upregulated in helper T-cells during cell proliferation, understanding the role of telomerase in T-cell proliferation is important in understanding normal T-cell function.

Low telomerase in resting Peripheral Blood Mononuclear Cells (PBMCs) is associated with chronic stress and aging related disease (Epel et al., 2004). Conversely, meditation and healthy lifestyle changes are associated with increases in resting PBMC telomerase activity and decreased measures of psychological distress (Daubenmier et al., 2012; Lavretsky et al., 2013) and decreased LDL in PBMCs of men with low risk prostate cancer (Ornish et al., 2008). While these studies, which were done in healthy individuals, suggest that telomerase activity levels are important for maintaining health and presumably proper immune function, they only show an

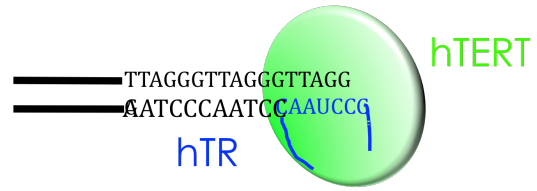
association between telomerase and disease or other states. The purpose of this study was to determine if telomerase activity is necessary for proper immune cell function or is instead a consequence of other factors that can affect disease development or states. Unexpectedly, we found that while the level of telomerase activity is important for CD4+ T cell survival, it is specifically hTR that protects CD4+ T cells from apoptosis in a telomere and telomerase activity independent manner.

Figure 1

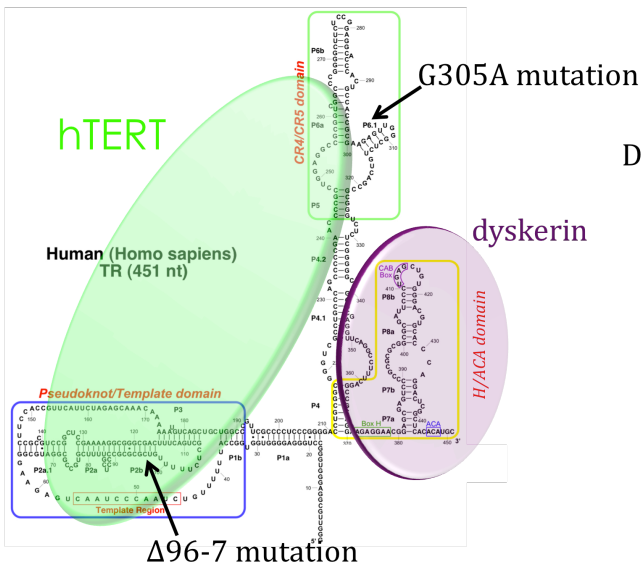
A



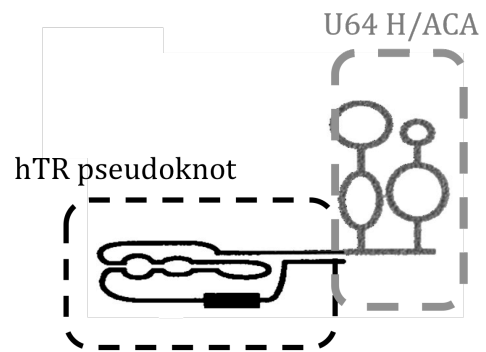
B



C



D



E

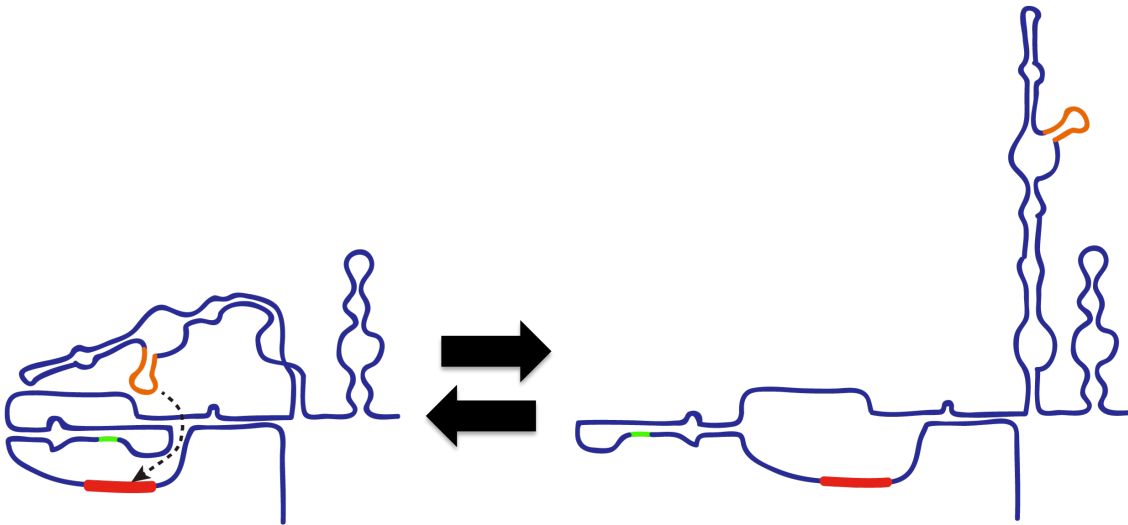


Figure 1. Visualizing telomeres and telomerase structures. **A)** Chromosomes from a metaphase spread of CD4⁺ T cells. Chromosomal DNA labeled with DAPI (purple). Telomeres labeled with fluorescent telomeric PNA probe (green). Image taken at 100X. Brightness and contrast and coloring were adjusted in FIJI. **B)** Representation of the telomerase core complex adding telomeres. hTR represented in blue. hTERT represented in green. Telomere represented in black. **C)** Telomerase RNA secondary structure is composed of three domains. The pseudoknot domain, the CR4/5 domain, and the H/ACA domain. hTERT represented by the green oval binds the pseudoknot domain and the CR4/5 domain. Dyskerin binds the H/ACA domain. The $\Delta 96-7$ and G305A mutations that produce catalytically inactive hTR are indicated with black arrows. Image adapted from (Chen et al., 2000) **D)** Secondary structure representation of the hTR-U64 fusion RNA composed of the hTR pseudoknot (black) and the U64 H/ACA domain (gray). Image adapted from (Fu and Collins, 2003). **E)** Potential hTR conformations. hTR switches between a catalytically active state (left) and a catalytically inactive state (right). In the catalytically active state, the P6.1 stem loop (orange) forms an RNA-RNA interaction with the template (red) and the pseudoknot folds into a triple helix. The catalytically inactive state exists transiently in WT hTR or can be permanent in hTR mutants. Mutations such as the $\Delta 96-7$ (green) in hTR disrupt stem binding in the pseudoknot, which unfolds the pseudoknot. Mutations in the P6.1 stem/loop such as G305A disrupt the P6.1 template interaction.

MATERIALS AND METHODS

Cell culture

Human buffy coats from 9 healthy donors between 17 and 25 years old were purchased from Stanford Blood Center. PBMCs were isolated from buffy coat by centrifugation with Ficoll-Paque Plus (GE Healthcare 17-1440-02) according to the manufacturer's instructions. CD4⁺ T cells were isolated from PBMCs using either the Untouched CD4⁺ T cell Isolation Kit II Human (Miltenyi 130-091-155), Naïve CD4⁺ T Cell Isolation Kit II (Miltenyi 130-094-131), the Dynabeads Untouched Human CD4 T cell Isolation Kit (Life Technologies 11346D), or the Human Dynabeads CD4 Positive Isolation Kit (Life Technologies 11331D) according to the manufacturer's instructions. CD4 T cells were cultured in 24 well dishes at 1 million cells/ml. Cells were stimulated 24 hours after isolation with 50 µl of Dynabeads Human T Cell Activator CD3/CD28 (Life Technologies 111.32D) per 1 million CD4⁺ T cells and cultured in RPMI with 10% FBS (Hyclone), 1% Penicillin and Streptomycin, and 1% glutamine with 10 ng/ml IL-2 (Sigma 12644-10UG). Cells were transduced in triplicate with lentivirus 24 hours after stimulation by centrifuging with titered virus to a volume of 1 ml at 800g for 30 min at 37°C with 8µg/ml polybrene. Viral supernatant was removed and cells were resuspended in 1ml of fresh media with 10 ng IL-2. 2 µg/ml of Puromycin was added 24 hours after transduction and kept in culture during the course of the experiment. Cells were split at day 6 and split and restimulated at day 12. When cells were split, they were resuspended in fresh media, IL-2, and puromycin. In the experiments in which the cells were transduced with two different lentiviruses, the second virus was added 24 hours after the second stimulation. Live cells and percent live cells determined by trypan blue exclusion were counted with the TC-20 Automated Cell Counter (BioRad). All centrifugation excluding viral transduction was performed at 4°C at

4000 rpm for 5 min. Dexamethasone (Sigma D4902) treatment was 1 μ M concentrations for 72 hours.

Plasmids and lentivirus

The lentiviral vector system was provided by Dr. Trono (University of Geneva, Geneva Switzerland, (Zufferey et al., 1997)). Lentivirus and shRNA expression vectors were prepared as described previously (Li et al., 2004). The following lentiviruses were generated from those previously described in (Li et al., 2004) but the CMV promoter was replaced with EF1alpha promoter driving either Puromycin resistance or GFP: Empty vector, shScramble, shTR1. shTERT was generated in the same lentiviruses based on the target sequence from (Gazzaniga et al., 2013). shTR2 was generated based on a previously published target sequence (Kedde et al., 2006). shBIM was generated based on the previously published target sequence (Del Gaizo Moore et al., 2007). The CMV-Luciferase-IRES-GFP and CMV-TERT-IRES-GFP vectors were generated from pHR vector described in (Li et al., 2004). The CMV-GFP-IRES-puromycin and CMV-TERT-IRES-puromycin lentiviruses were described in (Gazzaniga et al., 2013). The hTR overexpression constructs were generated by PCR amplification of U3hTR500 from the following plasmids from Dr. Collins (University California Berkeley, Berkeley CA) and cloned into the pHR vector with eflalpha driving puromycin resistance, pBS'U3-hTR-500, pBS'U3- Δ 96-7-500, pBS'U3-C204G-500, pBS'U3-G305A-500, pBS'U3-hTR-U64-500 (Fu and Collins, 2003; Robart and Collins, 2010). See Supplementary Table 1 for names of all plasmids.

Lentivirus was titered by qRT-PCR. Viral RNA was extracted using the QiaAmp Viral RNA mini kit (Qiagen) according to the manufacturer's instructions. Viral RNA was treated with 2.5 Units of Dnase 1 and 10X Incubation buffer (Roche) for 15 minutes at room temperature and

then inactivated by incubating at 75 C for 10 min. qRT-PCR was performed according to the manufacturer's instructions with the Brilliant II Sybr Mix (Stratagene) in a 20 μ l reaction with 5 μ l of RNA and 0.1 μ M of the following primers to detect the W element in the lentivectors, forward primer for W element: 5' - CATGCTATTGCTTCCCGTATGGCT -3', reverse primer for W element: 5' - ACAACGGGCCACAACCTCCTCATAA - 3'. A standard curve of 150 million, 15 million, 1.5 million, 150 thousand, 15 thousand copies of the shScr1 plasmid was generated to quantify relative concentrations of lentiviral vectors. Samples were run on the Mx3000P (Stratagene) with the following cycles: 50 C for 30 min, 95 C 10 min, (95 C for 30 sec, 55 C 1 min, 72 C for 30 sec) for 40 cycles, 95 C for 1 min, 55 C for 30 sec, 95 C for 30 sec. Relative viral concentrations were determined.

Flow cytometry

Cell cycle state was measured by staining with Vibrant DyeCycle Green (Life Technologies) according to the manufacturer's instruction. Dead cells were stained with Live/Dead Fixable Red Dead Cell Stain Kit (Life Technologies) according to the manufacturer's instruction. To determine the percent of naïve vs. central memory vs. effector memory CD4⁺ T cells, 1x10⁵ cells per condition in triplicate were stained with 0.2 μ l anti-CD4 APC (eBioscience 17-004.8-42), 0.1 μ l anti-human CD45RA PerCP-CY5.5 (eBioscience 45-0458-42), and 3 μ l PE anti human CD197 (CCR7) (BD Pharmingen 552178) in 30 μ l 0.5% BSA in PBS on ice for 20 min. Cells were washed with 0.5% BSA in PBS and resuspended in 400 μ l RPMI for analysis by flow cytometry. To determine the percent of CD25⁺ and IFN γ producing CD4⁺ T cells, 1x10⁵ cells per condition in triplicate were stimulated with 5 μ l CD3 CD28 Dynabeads (Life Technologies) in 100 μ l RPMI for 23 hours. Protein release was inhibited by incubation with 10 ng of BerfeldinA

(Sigma) for 1 hour at 37°C. Cells were washed with PBS and stained with 0.2µl anti-CD4 APC (eBioscience 17-004.8-42) in 30 µl of 0.5%BSA in PBS on ice for 20 min. Cells were washed with 0.5% BSA in PBS and fixed with 100 µl 2% PFA in PBS for 10 minutes at room temperature. Cells were washed with PBS and permeabilized with 30 µl permeabilization buffer (0.5% BSA, 0.05% Saponin, 0.01% NaN₃ in PBS) for 30 minutes at room temperature. Cells were washed with permeabilization buffer and stained with 0.5 µl anti-human IFN γ PerCP-CY5.5 (eBioscience 45-7319-42), 0.5 µl anti human IL-2 PE (eBioscience 12-7029-42) in 30 µl 0.5%BSA in PBS at room temperature for 30 minutes. Cells were washed with 0.5% BSA in PBS and resuspended in 400 µl RPMI for analysis by flow cytometry. All centrifugation steps were performed at 4000 rpm for 4 minutes. Stained cells were analyzed with the BD FACSCalibur (BD Biosciences) and quantified with CellQuestPro. GFP+ cells were sorted using the FACS Aria (BD Biosciences).

Apoptosis

Apoptosis was measured in triplicate with the Caspase –Glo 3/7, Caspase-Glo 8, Caspase –Glo-9 kits (Promega) according to the manufacturer’s instructions. Luminescence was read by the Veritas Microplate Luminometer (Turner Biosystems).

Telomere Repeat Amplification Protocol

Relative telomerase activity was determined by the real-time quantitative telomere repeat amplification protocol RQ-TRAP (Wege et al., 2003). Briefly cells were extracted at 1,000 cells/µlof 1X CHAPS buffer (10mM Tris HCl, pH 7.5; 1 mM MgCl₂; 1 mM EGTA; 0.1 mM Benzamidine; 5 mM β -mercaptoethanol; 0.5% CHAPS; 10% glycerol) for 30 min on ice and

centrifuged for 20 minutes at 4C at 14,000 rpm and supernatant was transferred to a new tube. Each TRAP reaction was performed in triplicate with 5µlof cell extract and 15µlof master mix (1X TRAP buffer; 8 ng/ul TS primer; 4 ng/ul ACX primer; 30% glycerol; 0.5X SYBR green (Invitrogen S7563); 2.5 mM total dNTPs). 10X TRAP buffer: 200 mM Trish HCl, pH 8.3; 15 mM MgCl₂; 630 mM KCl; 0.5% Tween 20; 10 mM EGTA). TS Primer: 5- AAT CCG TCG AGC AGA GTT – 3'. ACX primer: 5' - GCG CGG CTT ACC CTT ACC CTT ACC CTA ACC - 3'. Reactions were incubated at 30C for 30 minutes then PCR amplification was performed on a Lightcycler 480 (Roche Applied Systems) with the following cycling conditions: 95 C 2 min followed by 50 cycles of 95 C 1 sec, 50 C 7 sec (single acquisition) and 72 C 10 sec. The second derivative max Cp per reaction was compared to a standard curve of serial dilutions of 293T extracts (2500, 500, 100, 25, 5 cells/reaction).

Quantitative RT-PCR

hTR RNA levels and mRNA levels were measured as described in (Listerman et al., 2013). RNA was extracted (Qiagen RNA mini kit) and cDNA was synthesized using 2µgRNA, 500 ng of random primers (Invitrogen 48190-011), 0.5 mM dNTPs, 1X First-Strand Buffer, 5 mM DTT, and 100 U of Superscript III (Invitrogen 18080-044) in a 40µlreaction according to the manufacturers instructions. cDNA was diluted 1:4 with water and 4µlof cDNA was amplified in 10 µl reactions containing LightCycler 480 DNA SYBR Green I Master (Roche Applied Science 04887352001) and 0.5-1 µmol/L final concentration of each primer. See Supplementary Table 2 for list of primers used. Quantitative RT-PCR was performed on the LightCycler 480 (Roche Applied Science) with the following cycling parameters: 95 C for 5 min then 50 cycles of 95 C 10 sec, 60 C 20 sec, 72 C 20 sec (single acquisition), then a melting curve of 95 C 5 sec, 65 C 1

min, 98 C acquisition. The second derivative max was used to identify transcript copy number and normalized to the housekeeping gene GAPDH (Livak and Schmittgen, 2001).

IF-PNA-FISH

Cells were mounted on coated glass Cytoslides (5991056 Thermo Scientific) by centrifugation with the CytoSpin (Thermo Scientific) at 800 rpm for 3 min. Cells were fixed with 4% PFA for 10 min and permeabilized with 0.5% NP-40 in PBMS for 20 min. Immunostaining was performed with the primary antibodies anti-phospho histone H2A.X (05-636, Millipore) or pAb anti 53BP1 (NB 100-304, Novus Biochemicals) and the secondary antibody AlexaFluor 594 (Molecular Probes) Primary antibodies were diluted 1:500, secondary antibodies were diluted 1:750. DNA was visualized with 4',6-diamidino-2-phenylindole (DAPI, Life Technologies). IF was followed by telomere FISH as described in (Diolaiti et al., 2013) without pepsin treatment. The telomeric PNA probe used was FAM-OO-ccctaaccctaaccctaa (Panagene) at 0.5µg/ml. All images were obtained using a Deltavision RT deconvolution microscope (Applied Precision) with the 100x/1.4N PlanApo objective (Olympus). Images were acquired in 0.5 µM increments, deconvoluted, Z-projected in Softworx (Applied Precision), and adjusted for brightness and contrast in FIJI (Schindelin et al., 2012). Telomeric and DNA damage foci and telomeric and DNA damage integrated intensity were measured with CellProfiler image analysis software (www.cellprofiler.org; pipelines available on request).

Microarray

RNA was extracted with the Qiagen RNA mini kit. cDNA synthesis and hybridization to the GeneChip Human Gene ST 1.0 Array (Affymetrix 901086) was performed by the Gladstone Genomis Core (Gladstone Institutes, San Francisco CA).

Antibodies and Western Blot analysis

Cells were lysed in 1x RIPA buffer plus 2x Roche Protease Inhibitor Cocktail (Roche #11836170001), 2 mM PMSF, 2 mM DTT, 1x Halt Protease and Phosphatase Inhibitor Cocktail (Thermo Scientific # 78441), and 10% glycerol on ice for 30 min and flash frozen in liquid nitrogen. 50 ng of protein with ½ volume Lemmli Sample Buffer (BioRad 161-0737) was heated at 85C for 10 min then loaded onto a 15% Tris-HCl precast polyacrilamide gel (BioRad 161-1157). Gels were run at 50 v for 1 hour, then 80 v for 1.5 hours in Tris/Glycine/SDS buffer (BioRad 161-0772). Gels were transferred onto Hybond-P PVDF 0.45 micron membrane (GE Healthcare RPN303F) in TG buffer (BioRad 161-0772) plus 20% methanol at 100 v for one hour. Blots were blocked in TBS-T (Tris buffered Saline, pH 7.6 plus 0.1% Tween-20) and 5% BSA for hour. Membranes were incubated over night in TBS-T with 5% BSA and primary antibody at 4C overnight. Membranes were washed in TBS-T with 5% BSA for 15 min three times and then incubated with the appropriate secondary IgG-horse radish peroxidase (HRP) conjugate in TBS-T with 5% BSA for one hour. Membranes were washed with TBS-T for 15 minutes three times and then treated with either the Western Lightning Plus ECL kit (Perkin Elmer NEL103001EA) or the SuperSignal West Femto Kit (Thermo Fisher 34095). Signals were captured and developed using CL-X Posure Film (Thermo Scientific 34091). Blots were stripped in 100 mM β - mercaptoethanol, 2% SDS, and 62.5 mM Tris, pH 6.8 at 60 C for 30 min,

rinsed twice with TBS-T, washed twice with TBS-T for 15 minutes and blocked and reprobed as described above.

The following primary antibodies were used: Rabbit anti-Bid (human) at 1:1000 (Cell Signaling Technology 2002), Rabbit anti-Bim at 1:1000 (Cell Signaling Technology 2819), Rabbit anti-Puma at 1:1000 (Cell Signaling Technology 4976), Rabbit anti-Bad at 1:1000 (Santa Cruz Biotechnology sc-943), mouse anti-p53 (Abcam PAb 240), and mouse anti-GAPDH at 1:20,000 (Millipore MAB374). The following secondary antibodies were used goat anti-rabbit at 1:2000 (Jackson ImmunoResearch 111-035-144) and sheep anti-mouse (Jackson ImmunoResearch 515-035-003) at 1:2000 p53 and 1:10,000 for GAPDH.

Statistical analysis

All statistical analysis was performed using Prism (GraphPad Software). Significant differences were assessed by either one-way ANOVA or by unpaired t-tests as indicated. A cut off of $p < 0.05$ was used to determine significance.

RESULTS

hTR knockdown induces the intrinsic apoptotic pathway

Since telomerase activity tracks with T-cell proliferation upon activation, we sought to determine if telomerase activity is necessary for this proliferation response. Telomerase activity was knocked down in primary human CD4⁺ T cells by lentiviral vectors targeting hTERT or hTR. Figure 2A shows the experimental timeline with respect to telomerase activity of stimulated CD4⁺ T-cells in culture. During the first round of stimulation, shRNAs targeting hTERT and hTR begin to reduce telomerase activity. At day twelve telomerase activity is low in all conditions and the cells are split and restimulated. Three days after restimulation, telomerase activity is knocked down by approximately 80% with shTERT, shTR1, and shTR2 (Fig. 2B). Figure 2C shows that at day 3 restimulation, shTERT significantly reduces TERT mRNA levels but has no effect on hTR levels. Similarly shTR1 and shTR2 significantly reduce hTR levels but have no effect on hTERT mRNA levels. These results indicate that telomerase activity can be knocked down by about 80% with shTERT, shTR1, or shTR2 and that knocking down one core component of telomerase does not affect the transcription of the gene encoding the other in T cells.

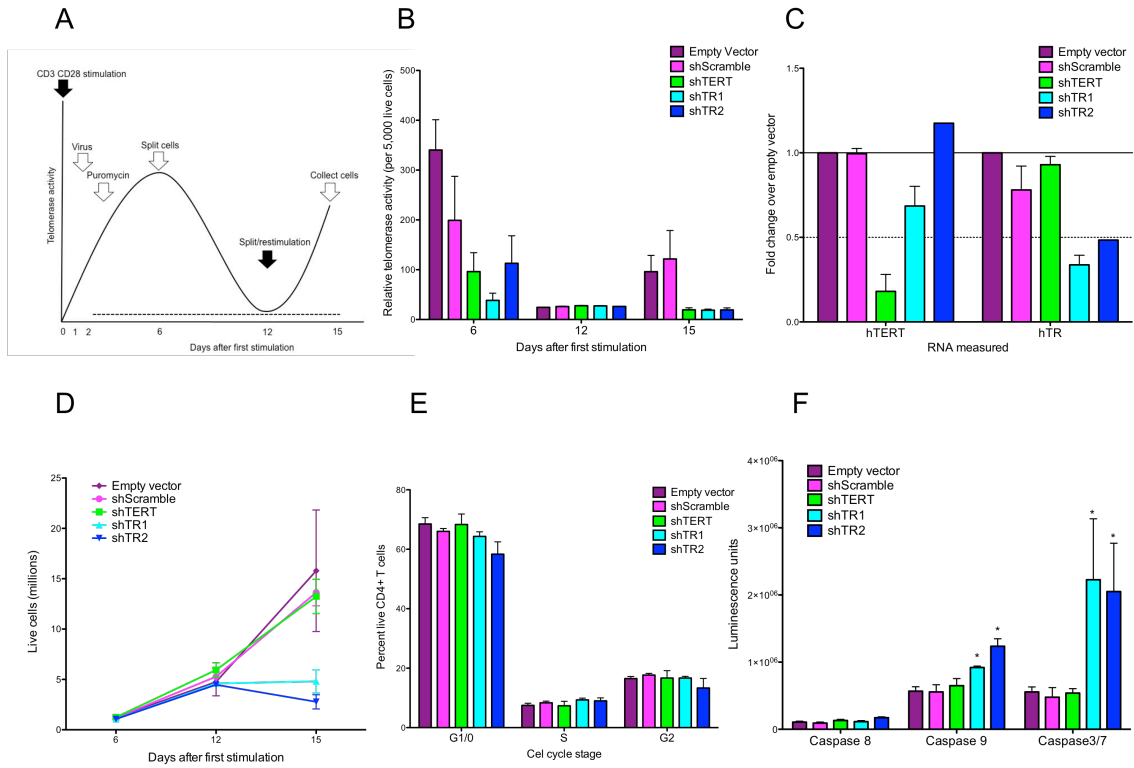
Unexpectedly, at day 3 restimulation, there are significantly less live cells measured by trypan blue with hTR knockdown compared to empty vector, shScramble, or shTERT (Fig. 2D). This result has been repeated in 6 additional donors in 9 additional experiments shown in Supplementary Figure S1A-1. This reduction in live cells is not due to an effect on proliferation since progression through the cell cycle is not disrupted as shown by DyeCycle green incorporation (Fig. 2E). Instead, hTR knockdown, but not hTERT knockdown, induces

apoptosis measured by caspase 3/7 and 9 activity (Fig. 2F), indicating that the intrinsic apoptotic pathway is activated with hTR knockdown.

To determine how the intrinsic pathway is activated by hTR knockdown, we measured the protein levels of the apoptotic proteins, Bim, Bad, Bid, Puma, and p53. We found that both Puma, which triggers upregulation of Bim, and Bim, which triggers Caspase 9 activation, are upregulated with hTR knockdown compared to shScramble and shTERT (Fig. 2G). However p53 is not upregulated, suggesting that PUMA is triggered through p53 and DNA damage independent mechanisms (Erlacher et al., 2006b; Yu and Zhang, 2008). Knockdown of Bim followed by subsequent knockdown of hTR results in more live cells compared to the control Empty Vector followed by knockdown of hTR (Figure 2H), suggesting that Bim is at least partially responsible for apoptosis induced by hTR knockdown. These results indicate that hTR knockdown induces Bim mediated apoptosis through p53 independent activation of Puma in CD4+ T cells.

To determine how hTR knockdown induces Bim mediated apoptosis we investigated the following hypotheses: hTR knockdown induces telomere shortening and/or telomere damage, hTR knockdown alters CD4+ T cell cytokine production, hTR protects from apoptosis through a telomere independent role, hTR knockdown induces apoptosis by increasing TERT unbound to hTR.

Figure 2



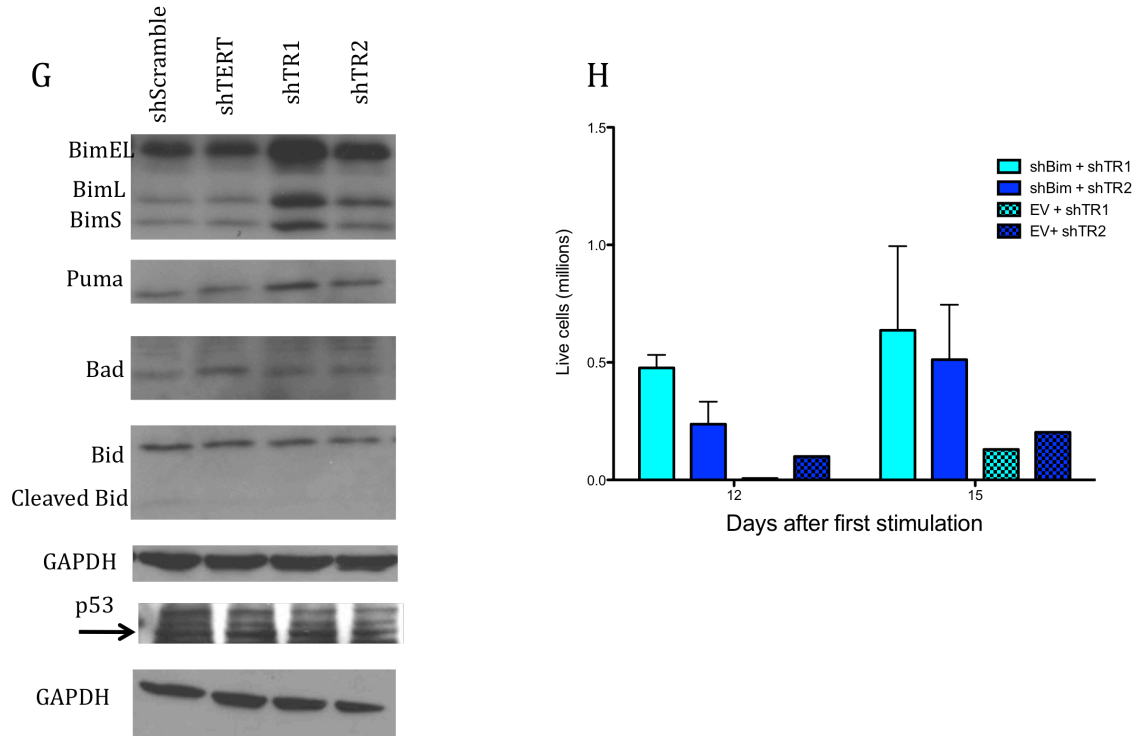


Figure 2. hTR knockdown induces Bim mediated apoptosis. **A)** Experimental timeline with respect to telomerase activity of stimulated CD4+ T cells in culture. X axis shows time in culture, Y axis represents telomerase activity of T cell in culture. CD4+ T cells are isolated from Buffy coat. 24 hours later cells are stimulated with CD3 CD28 Dynal beads (day 0). Lentivirus with control or shRNAs targeting telomerase with puromycin resistance are added at day 1. Puromycin is added at day 2 and kept in culture throughout the experiment. Cells are split at days 6 and 12 and restimulated at day 12. Most analysis was performed at day 15 (day 3 restimulation). **B)** Telomerase activity. Telomerase activity in CD4+ T cells is significantly knocked down at day 15 with shTERT, shTR1, and shTR2 compared to controls. Error bars show standard deviation of biological triplicates. Representative example of 10 different experiments performed in triplicate **C)** RNA levels. hTERT mRNA and hTR RNA levels in CD4+ T cells are significantly knocked down with respective shRNAs at day 15. Error bars show

standard deviation of the average of two experiments **D)** Live cell counts. Cell proliferation measured by trypan blue exclusion is significantly reduced with hTR knockdown. Error bars show standard deviation of biological triplicates. Representative example of 10 different experiments. **E)** Cell Cycle. Stages in cell cycle measured by DyeCycle green at day 15 are not affected by telomerase knockdown. Error bars show standard deviation of biological triplicates **F)** Caspase 8, 9, 3/7 activity at day 15. Caspase activity is measured by luminescence. hTR knockdown induces significant Caspase 9 and 3/7 activity. Error bars represent standard deviation of biological triplicates. Representative example from 4 different Caspase 3/7 experiments. One-way ANOVA was performed for each caspase. *represents $p < 0.05$ **G)** Western blot measuring Bim, Puma, Bad, Bid, p53 in shScramble, shTERT, shTR1, shTR2 cells at day 15 show Puma and Bim induction with hTR knockdown. **H)** Cell counts. Bim knockdown followed by hTR knockdown increases cell survival measured by trypan blue exclusion compared to empty vector knockdown followed by hTR knockdown.

Apoptosis induced by hTR knockdown is telomere length and damage independent

Short or deprotected telomeres trigger a p53 DNA damage response to induce apoptosis or senescence (de Lange, 2009). Since total p53 levels were not upregulated with hTR knockdown and telomerase activity was significantly knocked down for only 3 days, short or damaged telomeres seem to be an unlikely trigger for hTR knockdown induced apoptosis. However as to date the only known function of hTR has been to add telomeric repeats in complex with hTERT, we sought to directly test the hypothesis that hTR knockdown induces DNA damage through telomere shortening. We measured telomere length and the amount of Telomere DNA damage Induced Foci (TIFs) by ImmunoFluorescence Peptide Nucleic Acid Fluorescence in Situ Hybridization (IF-PNA FISH). Telomere length was determined by measuring the integrated intensity of telomeric PNA foci at days 6, 12, and day 3 restimulation. In the timeframe of this experiment, telomere length was not significantly shorter in shTERT, shTR1, or shTR2 cells compared to no virus, empty vector, and shScramble (Fig. 3A, Fig. S2A). To account for the possibility that the shortest telomeres are not detected in this method we also measured the amount of telomeres/area. If telomeres were shortening to an undetectable level in those with hTR knockdown, we would expect less telomeres/area in those cells. However we do not see a significant difference in the amount of telomeres/area in any of the conditions (Fig. 3B, Fig S2B). As a positive control for telomere shortening we knocked down TIN2, one of the telomere scaffold proteins, which resulted in significant telomere shortening and less telomeres/area 14 days in culture (Fig S3A,B). These results indicate that hTERT or hTR knockdown does not induce significant telomere shortening in the timeframe of this experiment.

Although hTR knockdown did not induce telomere shortening in this timeframe, it is possible that hTR knockdown induces DNA damage at the telomere independent of telomere length. Since telomeric DNA damage triggers 53BP1 and gH2ax signaling (de Lange, 2009), we measured co-localization between 53BP1 or gH2ax and telomeres. Co-localization between a telomeric signal and a DNA damage signal is referred to as a TIF (Telomere DNA damage Induced Foci). If hTR knockdown induced apoptosis through increased DNA damage at the telomere, there would be an increase in TIFs with hTR knockdown. However, hTR knockdown did not induce an increase in 53BP1 or gH2ax TIFs/telomere or TIFs/DNA damage foci (Fig. 3C, D, Fig. S2C,D). Furthermore hTR knockdown did not increase the total amount of 53BP1 or gH2ax foci regardless of localization (Fig. 3E, Fig. S2E). As a positive control, shTIN2 increased TIFs/telomere, TIFs/53BP1 foci, and actually reduced total 53BP1 foci/area in this timeframe, indicating that a larger fraction of 53BP1 foci reside at the telomere with TIN2 knockdown (Fig. S3C, D, E). These results indicate that hTR knockdown does not induce apoptosis through telomere shortening or by induction of the telomeric DNA damage response in the timeframe of this experiment.

Figure 3

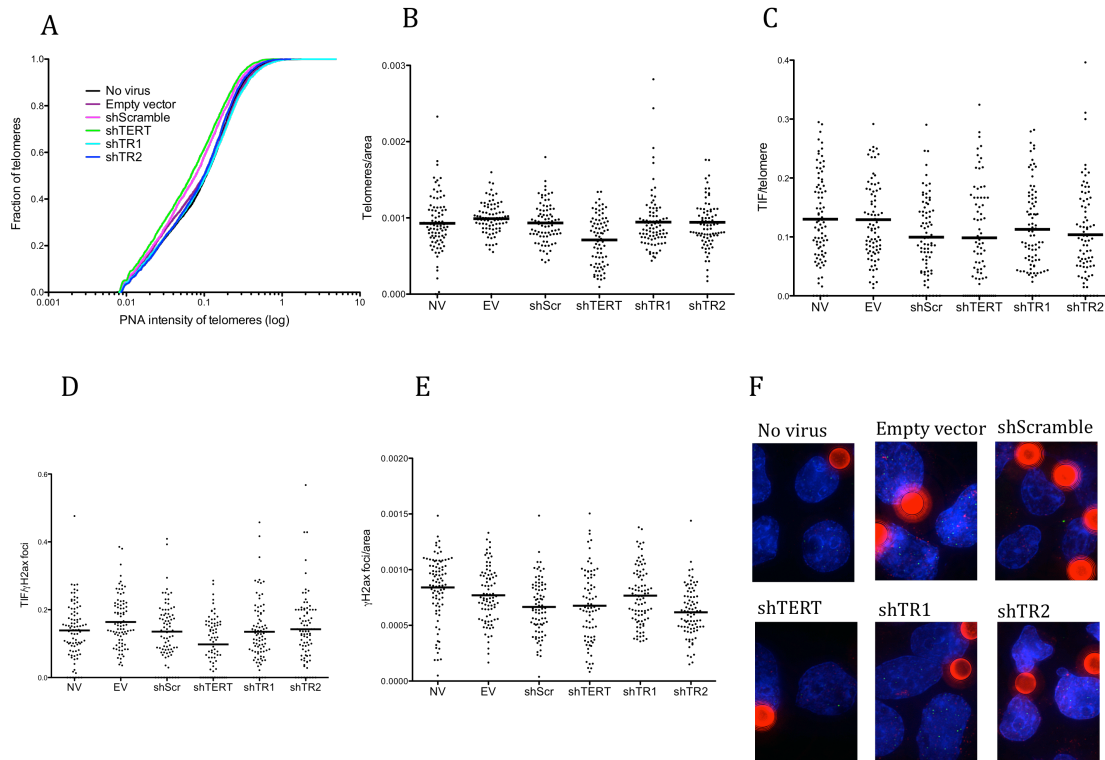


Figure 3. Telomerase knockdown does not induce significant telomere shortening or TIFs in the timeframe of this experiment. **A)** Telomere lengths. Cumulative frequency of telomere lengths measured by PNA intensity reveals that hTR knockdown does not significantly reduce telomere lengths compared to no virus (NV), empty vector (EV), or shScramble **B)** Telomeres/area. Telomeres/area are not significantly less with hTR knockdown than controls indicating that hTR knockdown does not result in telomeres too short to be detected. **C)** TIFs/telomere. TIFs/telomere measured by co-localization of γ H2ax foci and PNA foci are not significantly different between conditions **D)** TIFs/ γ H2ax foci. TIFs/ γ H2ax foci do not significantly differ between conditions **E)** γ H2ax foci/area. γ H2ax foci/area in shTR are not significantly different from NV, EV, shScramble, and shTERT. **F)** Representative images of stained cells. Blue Dapi,

Green: Telomeric PNA, Red: γ H2ax, Large red circles: CD3CD28 Dynal beads. Statistical significance was assessed using one way ANOVA and Dunn's multiple comparison test with a significance cutoff of $p < 0.05$ in Prism (GraphPad).

hTR knockdown induces apoptosis in both naïve and memory T cells without affecting cytokine production

To determine if hTR knockdown induces apoptosis in all CD4⁺ T cells or only in a specific subtype, the ratios of naïve, central memory, effector memory, and Th1 cells were measured by flow cytometry. Figure 4A shows that hTR knockdown does not affect the ratio of naïve to central memory to effector memory CD4⁺ T cells, nor does hTR knockdown affect the progression from naïve to effector memory in culture (Fig. S4). Furthermore, the reduction in live cells at day three restimulation occurs when starting with either a mix of naïve and memory T-cells or when starting with only naïve CD4⁺ T-cells (Fig. S5). We conclude that hTR knockdown induces apoptosis in both memory and naïve CD4⁺ T cells. Figure 4B shows that hTR knockdown does not affect the ratio of CD4⁺ CD25⁺ cells producing IFN γ (activated Th1), CD4⁺ CD25⁺ IFN γ ⁻(Treg), CD4⁺ CD25⁻ IFN γ ⁺ (differentiated Th1), or CD4⁺ CD25⁻ IFN γ ⁻ (non-Th1). While the culture conditions with IL2 added bias towards Th1 CD4⁺ T cells, we conclude that hTR knockdown does not selectively skew the development of these cells.

To determine if hTR effects the production of other cytokines other than IFN γ , a media switch experiment was performed. Two days after restimulation, the medium from the cells with hTERT or hTR knockdown was switched with control shScramble cells and vice versa. After 24 hours of the switched medium, no effect on apoptosis was detected by caspase 3/7 activity in the shScramble cells in shScramble medium, shTERT medium, or shTR medium indicating that hTERT or hTR knockdown does not trigger cells to produce pro-apoptotic factors. However, cells with hTR knockdown, but not hTERT knockdown, displayed a slight but reproducible reduction in caspase activity with shScramble medium than in their own medium. This slight reduction in caspase with shScramble media might be due to the amount of live cells producing

pro-inflammatory cytokines in the shScramble condition instead of hTR knockdown cells producing less pro-inflammatory cytokines. There are more live cells in the shScramble condition than shTR condition, therefore more cells are producing pro-inflammatory cytokines, and therefore the medium from those cells contains more pro-inflammatory cytokines that protect from apoptosis compared to a medium with less live cells producing cytokines (Fig. 4C). Similarly, shRNAs with a GFP marker instead of puromycin were used to knockdown hTERT and hTR. As expected hTR knockdown results in less live GFP+ cells three days after restimulation, confirming the results when hTR is knocked down with a puromycin lentivector (Fig. 4D). These results indicate that hTR knockdown also reduces cell survival in the absence of puromycin treatment. If hTR knockdown alters cytokine production to induce apoptosis then neighboring cells in the same medium without hTR knockdown (non-GFP cells) should also undergo apoptosis. Figure 3D shows that the ratio of dead non-GFP cells does not change with hTR knockdown, indicating that hTR knockdown does not trigger the cell to release pro-apoptotic factors and instead induces apoptosis by mechanisms intrinsic to the cell.

Figure 4

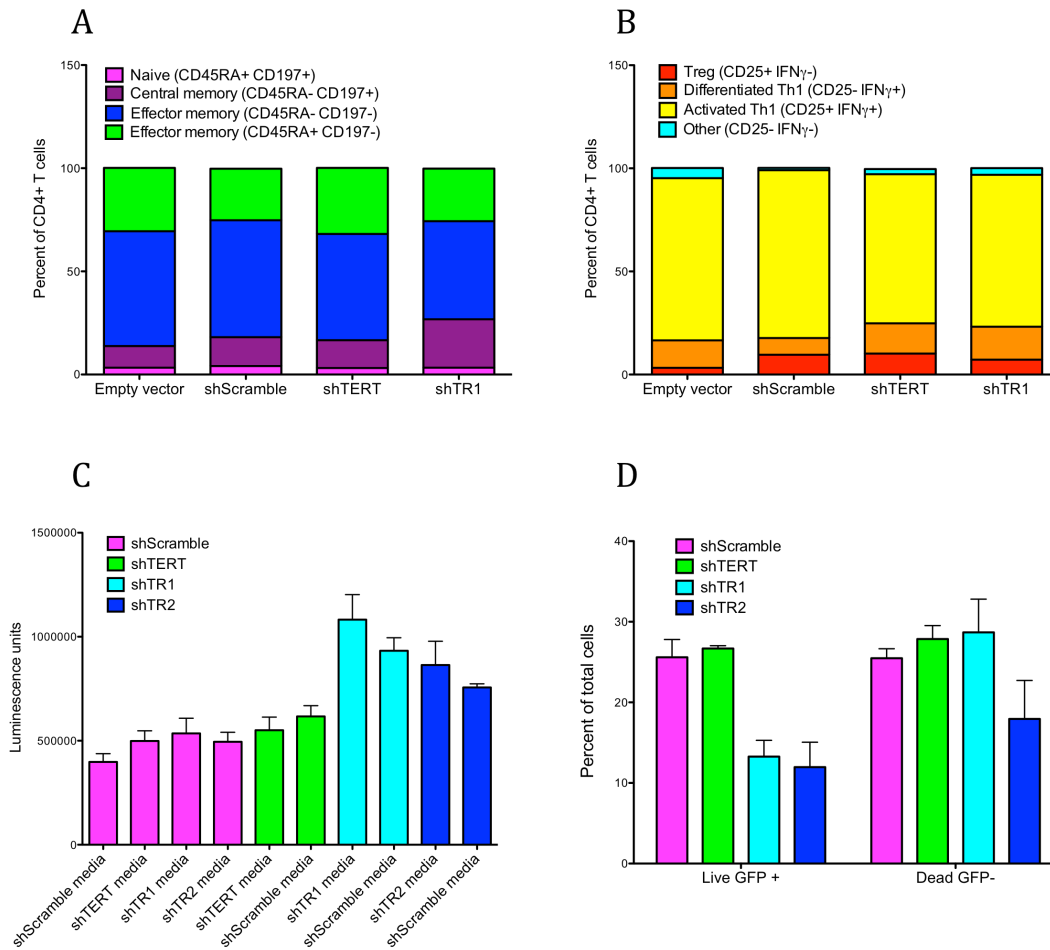


Figure 4. hTR knockdown does not alter CD4⁺ T cell type or cytokine release. **A)** Cells were stained with anti-CD4⁺ APC, anti-CD45RA⁺ PerCp Cy5.5, anti-CD197 PE and analyzed by flow cytometry. Ratios of naïve, central memory, and effector memory do not significantly change with hTERT or hTR knockdown compared to empty vector or shScramble. **B)** Cells were stained with anti-CD4⁺ APC, anti-IFN γ PerCp Cy5.5, anti-II2 PE and analyzed by flow cytometry. Ratios of Treg, activated or differentiated Th1, and non-Th1 cells do not change with

hTERT or hTR knockdown compared to empty vector or shScramble **C)** Caspase 3/7 activity from media switch experiment. Media from cells with shTERT, shTR1, shTR2 were switched with media from cells with shScramble at 3 days after restimulation. No change in apoptosis was seen with 24 hours of switched media when shTERT or shTR media was added to shScramble cells. Slight decrease in apoptosis measured when shScramble media added to shTR cells. Luminescence was normalized to blank with no cells **D)** Percent of cells stained with GFP+ or Live/Dead red. Lentiviral vectors with GFP marker instead of puromycin resistance were used to knockdown TERT, TR or Scramble. While less GFP+ cells were observed with TR knockdown compared to Scramble or shTERT, no change in GFP- dead cells was observed suggesting that cells undergoing apoptosis by hTR do not release factors to induce apoptosis in surrounding cells without hTR knockdown. Dead cells were stained with Live/Dead red kit. All experiments in this figure were performed in triplicate and repeated with another donor. Statistical significance was assessed in A and B with one-way ANOVA and significance cut off of $p < 0.05$.

hTR knockdown causes minimal effects on gene transcription

Since our results suggest that hTR knockdown does not induce apoptosis through telomere damage or by altered cytokine production, we performed a gene expression microarray analysis to identify any genes altered by hTR knockdown that might induce apoptosis. While more genes were significantly altered with hTR knockdown than hTERT knockdown compared to shScramble, most of these genes either were not significantly changed or appeared to be triggered by shRNAs or lentivirus in general, and thus were not specific to hTR knockdown when validated by subsequent qRT PCR experiments (examples in Fig. S6). Three immune genes remained significantly upregulated with hTR knockdown: CXCL10, CXCL11 and IL6 (Fig. 5A). Notably IL6 is significantly upregulated in shTERT, and in the shTRs compared to shScramble but significantly downregulated when compared to no virus and empty vector. Since CXCL10 and CXCL11 are chemokines that attract T cells and do not necessarily induce apoptosis in T cells (Groom and Luster, 2011), and since the experiments described above did not suggest any extrinsically produced triggers of apoptosis, we conclude that these genes might be a result of apoptosis instead of a trigger. We also conclude that hTR does not appear to induce apoptosis at the transcriptional level.

Interestingly the microarray revealed several snoRNAs that are significantly affected by hTR knockdown when compared to hTERT knockdown (Fig. 5B). While a direct link between these snoRNAs and apoptosis is unknown, it is possible that the telomerase RNA acts as a snoRNA or is involved in the snoRNA pathway. Since many snoRNAs are downregulated in cancer, its possible that an interaction between hTR and the snoRNA pathway might protect cells from apoptosis (Esteller, 2011). More studies must be done to understand snoRNA functions in general and if hTR is involved with snoRNAs. However, since hTR contains an H/ACA domain

similar to H/ACA snoRNAs and binds dyskerin like H/ACA snoRNAs, it is reasonable to hypothesize that hTR might act as a snoRNA.

Figure 5

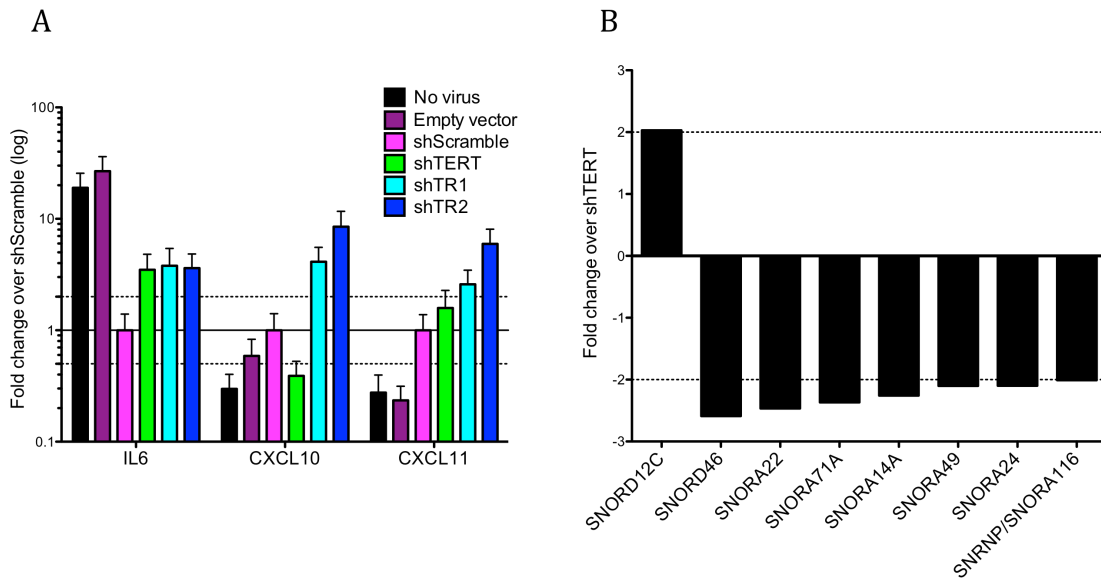


Figure 5. Genes significantly changed with hTR knockdown. **A)** RNA levels. Only three genes identified by the microarray were validated by subsequent qRT-PCR experiments to be significantly upregulated with hTR knockdown compared to shScramble. IL6 is significantly upregulated compared to shScramble, but significantly downregulated when compared to no virus or empty vector in hTERT and hTR knockdown cells. CXCL10 and CXCL11 are chemokines that are significantly upregulated with hTR knockdown compared to no virus, empty vector, shScramble, and shTERT. **B)** RNA levels. snoRNAs identified by microarray analysis to be significantly changed with hTR knockdown compared to hTERT knockdown. All experiments were performed in triplicate and significance was assessed by fold change values greater than 2 fold with $p < 0.05$.

hTR overexpression protects from dexamethasone induced apoptosis independent of hTERT binding

Since hTR knockdown induces Bim mediated apoptosis, we tested the hypothesis that hTR protects from apoptosis. To test this hypothesis, we overexpressed hTR in the presence or absence of dexamethasone, a steroid that induces Bim mediated apoptosis in T cells (Erlacher et al., 2006a; Heidari et al., 2012). We also tested different mutants of hTR to determine which part of hTR is necessary for protection from apoptosis. Overexpression of hTR increases telomerase activity suggesting that either hTERT exists in the cell without hTR or hTR overexpression stabilizes hTERT protein (Fig. 6A). As expected, overexpression of several catalytically inactive mutants of hTR, described in Figure 1, does not increase telomerase activity Figure 6A. The $\Delta 96-7$ mutation in which the nucleotides 96 and 97 are missing from hTR was previously shown to bind hTERT but confer no catalytic activity. The G305A point mutation in which a guanidine is replaced with an adenosine at position 305 in hTR was previously published to have no catalytic activity and poorly bind hTERT (Robart and Collins, 2010). While overexpression of G305A shows no increase in catalytic activity in our experiments, the degree of overexpression is so high that we cannot exclude the possibility of some level of binding to hTERT. The hTR-U64 fusion RNA consists of the wild type pseudoknot of hTR, but the H/ACA domain of hTR is completely replaced with the H/ACA domain of the similarly sized snoRNA U64 (Figure 1D) (Fu and Collins, 2003). This fusion RNA is catalytically inactive. In the absence of apoptosis induced by dexamethasone, overexpression of any hTR variant does not affect cell growth or apoptosis suggesting that while a level of hTR is necessary to prevent apoptosis, more hTR does not protect T cells from the baseline level of apoptosis in culture.

To determine if hTR overexpression protects from apoptosis when Bim mediated apoptosis is induced, we overexpressed hTR and mutants in the presence of dexamethasone. An optimized level of dexamethasone was determined for each donor. If dexamethasone induced apoptosis in shScramble but not no-virus cells, then dexamethasone-induced apoptosis could be protected by various overexpressed RNAs described below. However if the concentration of dexamethasone killed no virus cells in addition to shScramble virus cells, the degree of apoptosis was too high and could not be rescued. For the donor presented below, 1 μ M dexamethasone was used.

Figure 6E shows only the G305A mutation protects from dexamethasone induced apoptosis indicating that not only is telomerase activity unnecessary for protection from apoptosis, but also active telomerase might actually prevent hTR from inhibiting apoptosis. To test if WT hTR in the absence of activity can prevent apoptosis we overexpressed hTR and hTR mutants in cells with hTERT knocked down (Fig 6F). Interestingly, knocking down hTERT even without overexpressing hTR prevents apoptosis induced by dexamethasone. Furthermore, shTERT also protects from hydrocortisone-induced apoptosis (Fig. S7), while shScramble alone or shTR alone do not protect. These results suggest that knocking down hTERT reduces the amount of catalytically active hTR allowing endogenous levels of catalytically inactive WT hTR to protect from apoptosis. Furthermore, overexpression of WT or G305A in the presence of hTERT knockdown both protected from dexamethasone induced apoptosis again suggesting that WT hTR protects from apoptosis in a catalytically inactive state. Interestingly overexpression of the hTR-U64 fusion RNA with knockdown of hTERT still did not protect from dexamethasone induced apoptosis. Since knocking down hTERT alone protects from apoptosis, these results suggest that the hTR-U64 fusion interferes with the ability of endogenous WT hTR to protect

from apoptosis. We conclude from these findings that catalytically inactive hTR protects from dexamethasone-induced apoptosis and that the hTR-U64 fusion RNA interferes with this protection.

Figure 6

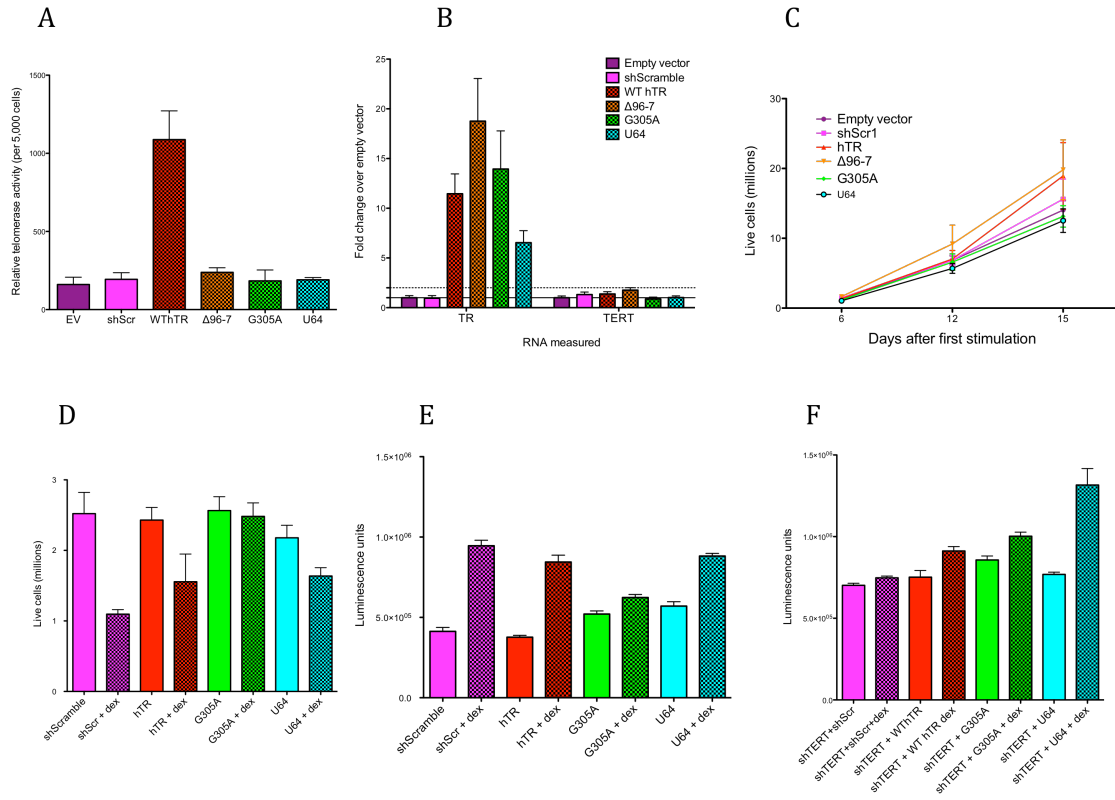


Figure 6. hTR overexpression protects from dexamethasone induced apoptosis independent of telomerase activity. **A)** Telomerase activity. WT hTR overexpression increases telomerase activity whereas the Δ96-7 and G305A mutant hTRs or a U64 fusion RNA with the hTR pseudoknot fused to the H/ACA domain of U64 do not increase telomerase activity. Error bars show standard deviation of biological triplicates **B)** RNA levels of hTR overexpression represented as fold change over empty vector. Error bars show standard deviation of PCR triplicates **C)** Live cell counts. Cell survival is not affected by overexpression of any of the hTR mutants. Error bars show biological triplicates. **D)** Live cell counts with dexamethasone treatment. 1 μM dexamethasone reduces live cells in shScramble, WT hTR overexpression, and

hTR-U64 fusion overexpression, but not with G305A overexpression. Error bars represent biological triplicates **E)** Caspase 3/7 activity. Caspase activity measured by luminescence. Only the G305A mutation prevents dexamethasone-induced apoptosis. Luminescence normalized to background levels. Error bars represent biological triplicates **F)** Caspase 3/7 activity. When hTERT is knocked down, shScramble, WT and G305A protect from dexamethasone induced apoptosis, but the U64 fusion does not. Error bars represent biological triplicates.

Overexpression of hTERT but of not the catalytically inactive β - hTERT induces apoptosis

Since our data suggest that hTR in an inactive state protects from apoptosis, overexpressing hTERT could reduce the amount of endogenous inactive hTR by binding to hTR and increasing telomerase activity and thus is predicted increase apoptosis. To test this hypothesis we overexpressed full length hTERT or the β - splice variant of hTERT which binds hTR, but is missing the catalytically active site (Listerman et al., 2013). hTERT overexpression, but not β - overexpression increases telomerase activity and reduces T cell survival by increasing apoptosis (Fig 7A-D). Since we have shown that telomerase activity is increased with either hTERT overexpression or hTR overexpression, we measured RNA levels of hTERT and hTR when either is overexpressed to determine if hTR and hTERT co-regulate each other. Figure 7E shows that hTERT or hTR overexpression does not affect the transcription of the other. Since hTERT overexpression does not increase hTR expression, and hTERT overexpression increases telomerase activity, hTR must exist in the cell unbound to hTERT. Since hTERT overexpression increases apoptosis, these results suggest that overexpressed hTERT binds hTR, reduces the levels of catalytically inactive hTR, and prevents hTR from protecting from apoptosis. Since overexpression of the β - splice variant, which binds hTR, but has no activity, does not induce apoptosis, binding to hTERT does not render hTR unable to protect from apoptosis. Instead, these results suggest that hTR can be bound to hTERT, but must be catalytically inactive to be able to prevent apoptosis.

Figure 7

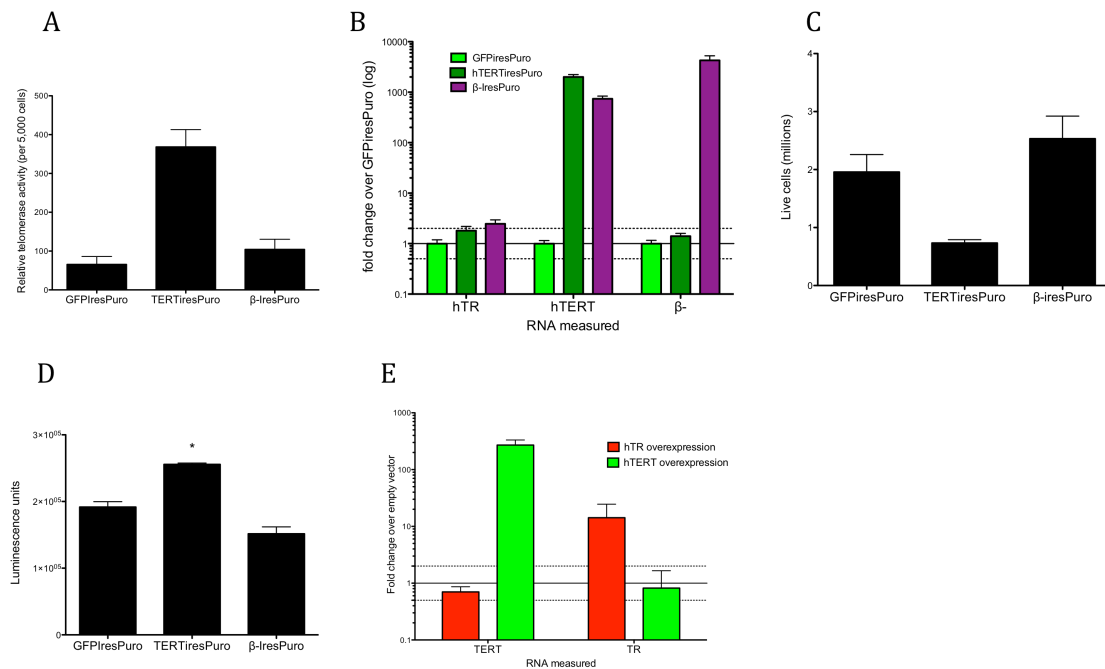


Figure 7. hTERT overexpression increases telomerase activity and induces apoptosis. **A)** Telomerase activity. hTERT overexpression but not overexpression of the β - splice variant increases telomerase activity. Error bars show standard deviation of biological triplicates **B)** RNA levels. Neither hTERT overexpression or overexpression of the β - splice variant affect hTR levels. hTERT overexpression increases total hTERT mRNA, but does not increase the β - splice variant. Overexpression of the β - splice variant increases β - splice variant mRNA and total hTERT levels, probably due to the increase in β - splice variant. Error bars show standard deviation of PCR triplicates. **C)** Cell counts. hTERT overexpression but not overexpression of the β - splice variant results in less live cells and increased **D)** apoptosis measured by Caspase3/7 at day 12 in culture. Error bars show standard deviation of biological triplicates. * represents statistical significance of $p < 0.05$ assessed by one-way ANOVA **E)** RNA levels. Overexpression of hTERT does not affect expression of hTR. Overexpression of hTR does not affect expression of hTERT. Error bars show standard deviation of PCR triplicates.

Catalytically inactive hTR mutants protect from hTERT-induced apoptosis

Since hTERT overexpression induces apoptosis, we sought to determine if co-overexpression of hTERT and hTR mutants could prevent hTERT-induced apoptosis. Co-overexpression of hTR and hTERT increased telomerase activity and increased apoptosis compared to co-overexpression of GFP and hTR (Fig 8A). Interestingly co-overexpression of either of the catalytically inactive hTR mutations, $\Delta 96-7$ or G305A, protected from hTERT-induced apoptosis, while overexpression of the the wild type hTR or of the hTR-U64 fusion did not (Fig. 8D). Since the catalytically inactive mutants, but not WT, protected from hTERT-induced apoptosis, these results suggest that hTR in a catalytically inactive state can prevent hTERT-induced apoptosis. In a catalytically active state, hTR cannot protect from apoptosis. Since the hTR-U64 fusion also did not protect from apoptosis, these results suggest that the 3' portion of hTR is necessary to protect from hTERT-induced apoptosis. Table 1 shows a summary of the different hTERT and hTR mutants and their effects on apoptosis.

Figure 8

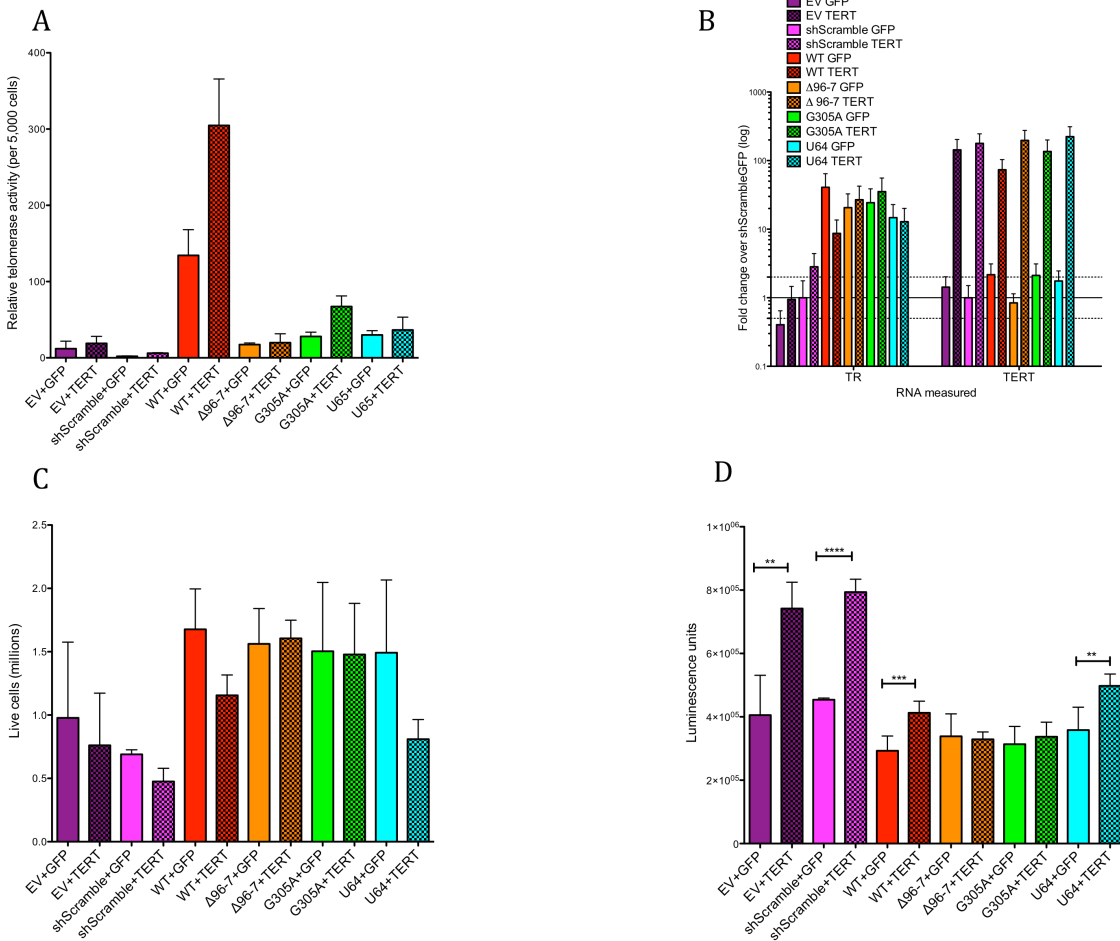


Figure 8. Overexpression of catalytically inactive hTR mutants protects from hTERT-induced apoptosis. **A)** Telomerase activity. hTR overexpression increases telomerase activity. hTERT+hTR overexpression increases telomerase activity even more. Cells with two viruses have less telomerase activity than cells with one virus, but hTERT overexpression does increase telomerase activity in EV and shScramble controls. Overexpression of the catalytically inactive mutants Δ96-6, G305A, or hTR-U64 fusion does not increase telomerase activity. **B)** RNA levels. hTR RNA levels are overexpressed with hTR overexpression vectors compared to empty

vector and shScramble. hTERT levels are overexpressed with hTERT vector compared to GFP.

C) Cell counts. hTERT overexpression reduces live cells when co-overexpressed with empty vector, shScramble, WT hTR, and hTR-U64. Overexpression of the catalytically inactive mutants $\Delta 96-7$ or G305A increase cell survival with hTERT overexpression. **D) Caspase 3/7 activity measured by luminescence.** hTERT overexpression induces apoptosis when co-expressed with an empty vector, shScramble, WT hTR, and hTR-U64 fusion. Overexpression of the catalytically inactive mutants $\Delta 96-7$ and G305A protect from hTERT induced apoptosis. Significance assessed by unpaired t-test. ** represents $p < 0.01$, *** represents $p < 0.001$, **** $P < 0.0001$.

Table 1. Summary of telomerase activity and susceptibility to apoptosis

RNA name	Telomerase activity	Activation-induced apoptosis	Dexamethasone-induced apoptosis	hTERT-induced apoptosis
shScramble	normal	normal	susceptible	susceptible
shTERT	decreased	normal	resistant	
shTR1,2	decreased	increased		
WT hTR	increased	normal	susceptible	susceptible
Δ 96-7	catalytically inactive	normal	resistant	resistant
G305A	catalytically inactive	normal	resistant	resistant
hTR-U64	catalytically inactive	normal	susceptible	susceptible
hTERT	increased	increased		
β -hTERT	catalytically inactive	normal		

CONCLUSIONS AND DISCUSSION

We have shown that hTR knockdown, but not hTERT knockdown, induces Bim mediated apoptosis in activated human CD4+ T cells. We have found that Bim upregulation is accompanied by PUMA upregulation, a protein that triggers Bim and can be triggered either by the p53 mediated DNA damage response or by DNA damage independent stressors in T cells (Erlacher et al., 2006b; Yu and Zhang, 2008). While the most obvious explanation for hTR knockdown induced apoptosis would have been a telomere shortening induced DNA damage response, we find that hTR knockdown induces apoptosis independent of telomere damage and in fact hTR only protects from apoptosis when not catalytically active. To our knowledge, these results suggest the first non-telomere function for the telomerase RNA. Based on the data generated in this thesis we propose a model in which the telomerase RNA in a catalytically inactive state (at least canonically catalytically inactive) protects T cells from apoptosis. Below we outline the results and rationale for this model.

hTR knockdown induces apoptosis independent of telomere shortening or damage

In the presence of endogenous telomerase, lymphocytes undergo replicative senescence accompanied by telomere shortening and an increase in TIFs in vitro (Chebel et al., 2009). Depending on culture conditions and age of donors, this replicative senescence can occur between 40 days to 27 weeks in culture (Chebel et al., 2009; Perillo et al., 1989; Röth et al., 2005). CD4+ T cells with telomerase activity knocked down by overexpression of a dominant negative hTERT, survived in culture for up to 30-50 days (Röth et al., 2005). The experiments in the present study were performed in primary human T-cells from healthy donors under 25

years of age, and T cells were cultured for no longer than eighteen days. While the shRNAs targeting either shTERT or shTR begin to reduce telomerase activity during the first round of stimulation, telomerase activity is not significantly reduced (80%) until 3 days after restimulation (15 days in culture total). Therefore in our experiments, it seems unlikely that the telomeres shortened enough to trigger a DNA damage response even with telomerase knockdown. Indeed our IF-PNA-FISH results show that the telomeres are not significantly shorter with telomerase knockdown in the timeframe of this experiment. We also tested the hypothesis that regardless of telomere shortening, hTR knockdown triggers a DNA damage response at the telomere. Short or de-protected telomeres can trigger apoptosis through the 53BP1, gH2ax DNA damage response (de Lange, 2009; Li et al., 2004). However we do not find an increase in TIFs marked by either 53BP1 or gH2ax with hTR knockdown in these experiments. These results complement our biochemical findings that p53 is not upregulated with hTR knockdown and suggest that hTR knockdown induces apoptosis independent of classic telomere shortening or telomere DNA damage signaling.

hTR knockdown induces apoptosis without affecting the ratio of CD4+ T cell types or cytokine production

Since PUMA can also be triggered by other stressors such as cytokine withdrawal (Erlacher et al., 2006b; Yu and Zhang, 2008), we tested the hypothesis that hTR knockdown alters cytokine production in CD4+ T cells. When medium from cells with either hTERT or hTR knockdown was switched with shScramble, no effect on apoptosis was seen in shScramble cells with either shTERT or shTR medium suggesting that cells with hTR knockdown do not secrete factors to induce apoptosis. A statistically insignificant but reproducible decrease in apoptosis

was measured in shTR cells with shScramble medium suggesting that the shScramble medium might have more pro-inflammatory cytokines than shTR medium. However this result could be a reflection of the reduction in live cells producing cytokines with shTR cells compared to shScramble cells. More pro-inflammatory cytokines exist in medium from shScramble cells because there are more live cells. We used a second method to test if shTR cells are producing pro-apoptotic factors by using lentiviral vectors with a GFP marker instead of puromycin resistance. At day 6 the amount of GFP+ cells was similar in all conditions. As expected, GFP+ cells were significantly reduced at day 3 restimulation with hTR knockdown, confirming the results in cells with the puromycin marker that cells with hTR knockdown do not survive as well as those with control virus. The percent of dead non-GFP cells was similar for control and hTR knockdown suggesting that cells with telomerase knockdown do not release pro-apoptotic factors. These results suggest that hTR knockdown induces apoptosis by a mechanism intrinsic to the cell.

hTR knockdown minimally affects gene transcription

We performed a microarray analysis to compare gene expression in cells with hTR knockdown compared to hTERT knockdown and controls, to identify any genes that might explain how hTR knockdown induces apoptosis. While many cytokines and chemokines were identified by the microarray, most of these genes appeared to be affected by virus or shRNAs in general instead of specifically to shTR. Interestingly, several snoRNAs were identified by the microarray as significantly changed with hTR knockdown compared to hTERT knockdown. Since the second half of hTR contains a snoRNA like H/ACA domain, and hTR binds dyskerin, like snoRNAs, it is possible that hTR could be involved in a snoRNA pathway directly or

indirectly involved with apoptosis. At a minimum, the microarray data suggest that hTR knockdown does not appear to trigger apoptosis through transcriptional changes. Since hTR has a snoRNA domain and hTR knockdown affects several snoRNA levels, it is possible that hTR knockdown induces apoptosis post-transcriptionally by interacting with the snoRNA pathway.

hTR protects from apoptosis when catalytically inactive

Since hTR knockdown, but not hTERT knockdown induces apoptosis independent of telomere shortening or damage, we tested the hypothesis that hTR has a non-telomere related function to protect from apoptosis.

To test the hypothesis that hTR protects from apoptosis, and if so, which part of hTR is necessary for this protection, we triggered Bim-mediated apoptosis by dexamethasone treatment and overexpressed different hTR mutants. Surprisingly, we found that in the presence of endogenous hTERT and hTR, only the catalytically inactive G305A mutant protects from dexamethasone-induced apoptosis while overexpression of WT hTR, the hTR-U64 fusion, or control viruses do not. Since overexpression of WT hTR increases telomerase activity, and overexpression of G305A does not, these results suggest that not only is catalytic activity unnecessary to protect from apoptosis, but also catalytically active hTR actually appears unable to protect from apoptosis. The G305A mutant was previously published to have poor binding to hTERT, however in our experiments the degree of overexpression is so high that we cannot exclude the possibility of G305A binding to hTERT at some level (Robart and Collins, 2010). Therefore, these results only suggest that catalytically inactive hTR protects from apoptosis and do not reveal whether binding to hTERT affects the ability of hTR to protect from apoptosis.

Since the hTR-U64 fusion RNA does not protect from apoptosis we conclude that the second half of hTR, which is missing from the hTR-U64 mutant, is necessary to prevent apoptosis.

hTERT is not necessary for hTR protection from apoptosis

The above results suggest that catalytically inactive hTR protects from apoptosis. Since normal cells do not naturally contain the catalytically inactive G305A mutant hTR, we wanted to test if WT hTR in a catalytically inactive state can protect from apoptosis. To render WT hTR catalytically inactive, we knocked down hTERT. In the presence of both hTERT knockdown and dexamethasone, the WT and the catalytically inactive G305A hTR are equally effective at protecting from apoptosis. Furthermore, knocking down hTERT without overexpressing hTR also protects from apoptosis. We interpret these results as follows: knocking down hTERT renders more of the endogenous hTR catalytically inactive (by not being bound to hTERT), and thus able to protect from apoptosis. These results show that WT hTR when catalytically inactive can protect from apoptosis and that hTERT binding is not necessary for either WT hTR or G305A to protect from apoptosis.

Interestingly, overexpressing the hTR-U64 fusion does not protect from apoptosis in the presence of hTERT knockdown. hTERT knockdown without overexpression of any hTR variant protects from apoptosis, presumably by increasing the amount of endogenous catalytically inactive hTR. Therefore, in the presence of hTERT knockdown, overexpression of the catalytically inactive hTR-U64 fusion would not affect the levels of catalytically inactive hTR and as a result, should protect from dexamethasone-induced apoptosis. Instead hTERT knockdown with overexpression of the catalytically inactive hTR-U64 fusion does not protect from dexamethasone-induced apoptosis. We hypothesize that hTR-U64 competes with

endogenous hTR for the pathway in which catalytically inactive hTR protects from apoptosis. Since both the H/ACA portion of hTR (which is replaced by the U64 dyskerin binding domain in the hTR-U64 fusion) and the U64 H/ACA domain bind dyskerin, we hypothesize that a 3' hTR region, potentially including the CR4/5 domain along with the H/ACA region that can bind to dyskerin, but not per se the binding of hTR to dyskerin, is involved in protecting from apoptosis. Many snoRNAs that bind dyskerin target a specific RNA for pseudouridylation, which in turn affects the stability of the RNA (Esteller, 2011). It is thus also possible that hTR when bound to dyskerin, but not catalytically active, targets a specific RNA for modification that is involved in apoptosis. Future studies identifying any targets of hTR acting as a snoRNA bound to dyskerin might identify how hTR knockdown triggers apoptosis.

hTERT overexpression induces apoptosis

The above results suggest that the 3' half of hTR is necessary to prevent apoptosis, that this protection from apoptosis only occurs in a catalytically inactive state, and that neither hTERT binding nor dyskerin binding is necessary or sufficient for hTR to protect from apoptosis. However they do not distinguish between a model in which hTERT binding to hTR hinders the ability of hTR to protect from apoptosis or a model in which hTERT unbound to hTR promotes apoptosis.

Overexpression of hTERT increases telomerase activity suggesting that hTR exists in the cell unbound to hTERT. Interestingly overexpression of hTERT, but not of the β - splice variant of hTERT, which binds hTR but has no enzymatic activity, induces apoptosis. These data appear to contradict previous studies that have found that hTERT overexpression extends replicative lifespan in lymphocytes (Menzel et al., 2006; Röth et al., 2003, 2005). We believe that

differences in culture conditions and experimental time lines could account for these discrepancies. The previously published studies start measuring population doublings with hTERT overexpression 10 days after transduction and continue up to over 300 days in culture. We measure apoptosis 8 days after hTERT virus is added to cells. It is possible that hTERT overexpression might initially induce apoptosis and then extends lifespan through better telomere maintenance in long-term culture. Furthermore, these studies detect very low levels of telomerase activity in GFP control transduced cells. Our studies show much higher levels of telomerase activity in control cells. These differences could potentially be explained by the level of activation. When T cells are more strongly activated, there is an increase in proliferation, telomerase activity, and activation induced cell death. The level of activation in the previous studies might not have been strong enough to induce a high enough level of activation-induced death. Therefore in those studies hTERT overexpression extends lifespan by adding more telomeres. In contrast, in the current studies with stronger lymphocyte activation, hTR in an inactive form is necessary to prevent activation-induced (or dexamethasone-induced) cell death.

Our result that hTERT overexpression induces apoptosis at this point could have been explained by either of the two models. The first model is that hTERT overexpression increases catalytically active hTR, thus reducing catalytically inactive hTR rendering it unable to protect from apoptosis. In this case, the β - splice variant of hTERT does not affect apoptosis since, while it binds to hTR, it is missing the catalytic site and thus does not reduce catalytically inactive hTR. The other model is that hTERT overexpression is high enough to both soak up endogenous hTR to increase telomerase activity and exist unbound to hTR to promote apoptosis. In this case the β - splice variant is missing the portion of hTERT that, when unbound to hTR,

triggers apoptosis. To distinguish between these two models we co-overexpressed hTERT with hTR mutants.

Catalytic activity, not hTERT binding inhibits hTR from protecting from apoptosis

Co-overexpression of WT hTR with hTERT increases telomerase activity two fold compared to WT hTR overexpression alone, but does not rescue apoptosis induced by hTERT overexpression. These results could be interpreted as follows: co-overexpression only increases catalytically active hTR (as seen by the increase in telomerase activity) and not catalytically inactive hTR; therefore co-overexpression of WT hTR and hTERT cannot protect from apoptosis since there is no increase catalytically in inactive hTR. Another interpretation is that overexpression of hTR is not enough to bind up all the overexpressed hTERT, allowing any hTERT unbound to hTR to promote apoptosis. However co- overexpression of either the catalytically inactive mutants $\Delta 96-7$ or G305A protect from apoptosis induced by hTERT overexpression. If the second model were correct, then the catalytically inactive mutants, which are expressed at similar levels to WT hTR, would also not protect from apoptosis as they would not be able to soak up all of overexpressed hTERT. Instead, the catalytically inactive mutants protect from hTERT induced apoptosis, suggesting that hTR in an inactive state protects from hTERT induced apoptosis. Since at least the $\Delta 96-7$ mutant is able to bind hTERT, as is potentially the G305A mutant when expressed at the high levels achieved in these experiments, these data also suggest that it is only catalytic activity, and not binding to hTERT that inhibits the ability of hTR to protect from apoptosis. The hTR-U64 fusion does not protect from hTERT induced apoptosis suggesting once again that some element in the 3' half of hTR is necessary for protection from apoptosis.

Proposed model for non-canonical role for hTR in protection from apoptosis

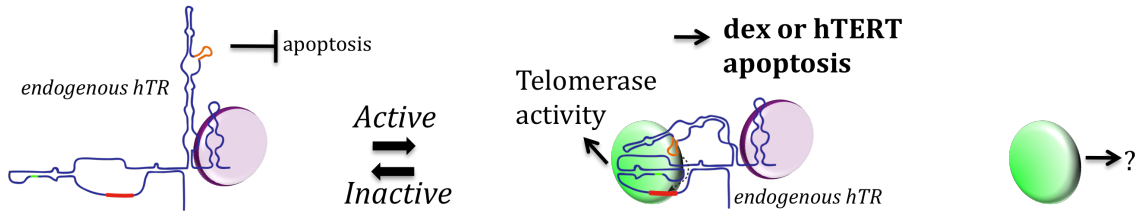
In summary, we suggest a model in which hTR protects from apoptosis specifically when in a catalytically inactive state. Data exist for the telomerase RNA being able to assume more than one conformational state (Hengesbach et al., 2012; Qiao and Cech, 2008; Ueda and Roberts, 2004; Yeoman et al., 2010). We propose that hTR (whether bound to hTERT or not) can dynamically convert between active and inactive conformations and that hTR, when bound to hTERT in an enzymatically functional ribonucleoprotein (but not in an enzymatically non-active ribonucleoprotein complex) pushes the distribution of the hTR forms toward its active conformation. The mutations used in this study that protect from apoptosis are predicted to disrupt the active conformation of the hTR pseudoknot ($\Delta 96-7$) (Hengesbach et al., 2012; Qiao and Cech, 2008; Robart and Collins, 2010), or disrupt the P6.1 stem-loop formation, disrupting hTERT binding and P6.1 binding to the template (G305A) (Robart and Collins, 2010; Ueda and Roberts, 2004). These mutations would force hTR to exist only in an inactive conformation. This inactive conformation might allow hTR to bind other factors to prevent apoptosis and/or affect the localization of hTR to protect from apoptosis. Figure 10 shows two potential conformations and functions of hTR.

When catalytically active hTR is increased in the cell, protection from dexamethasone-induced apoptosis does not occur. However, when catalytically inactive hTR is increased (by G305A overexpression or hTERT knockdown), dexamethasone does not induce apoptosis. The catalytically inactive state in which TR protects from apoptosis does not require TERT binding as hTR can protect from dexamethasone induced apoptosis when hTERT is knocked down. However, binding to hTERT does not inhibit the ability of hTR to protect from apoptosis as the

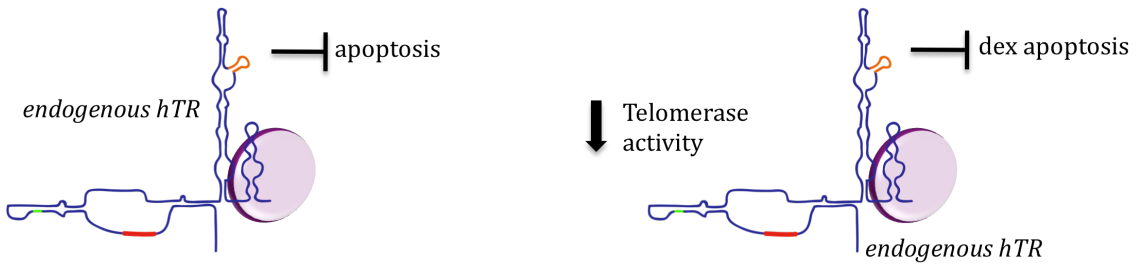
catalytically inactive mutant $\Delta 96-7$, which binds hTERT but has no activity, can protect from hTERT- induced apoptosis. These results suggest that hTERT binding does not inhibit hTR from interacting with the pathway involved in preventing apoptosis. Instead, activity prevents hTR from protecting from apoptosis. Our model also suggests that the second half of hTR containing the hTR A/ACA domain is necessary to protect from apoptosis as the hTR-U64 fusion in which the hTR H/ACA domain is replaced with the U64 H/ACA domain does not protect from dexamethasone or hTERT induced apoptosis. Furthermore hTR-U64 actually appears to compete with endogenous hTR for the pathway in which catalytically inactive hTR protects from apoptosis when hTERT is knocked down. These results suggest that not only is the second half of hTR necessary for protection from apoptosis, the pathway in which hTR protects from apoptosis must also interact with U64. Figure 9 presents a model summary of experiments interpretations of how and when hTR protects from apoptosis. Figure 10 presents a model for the proposed two roles and conformations of hTR at endogenous levels in the cell.

Figure 9

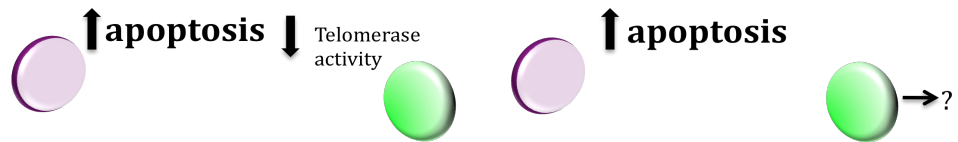
A Endogenous



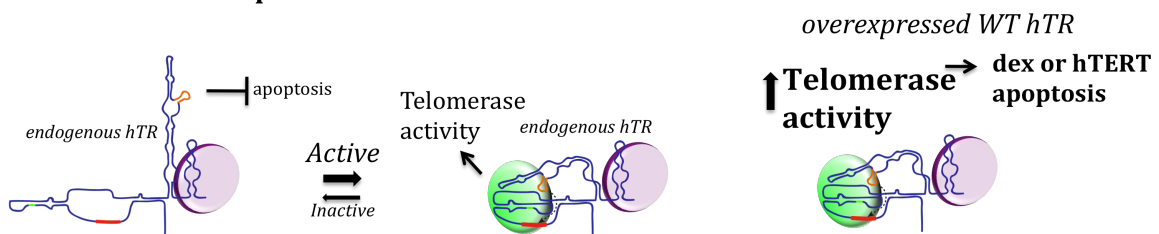
B hTERT knockdown



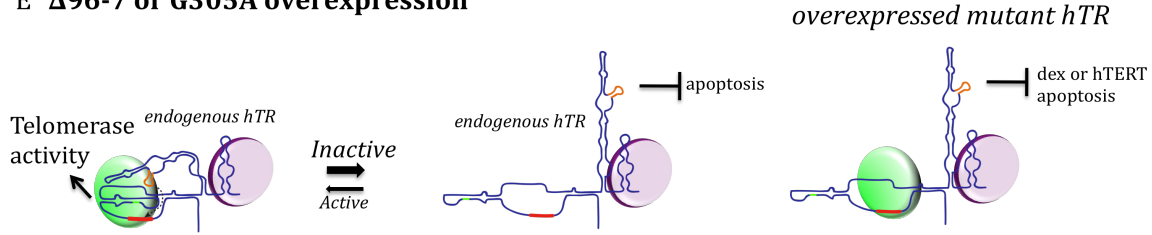
C hTR knockdown



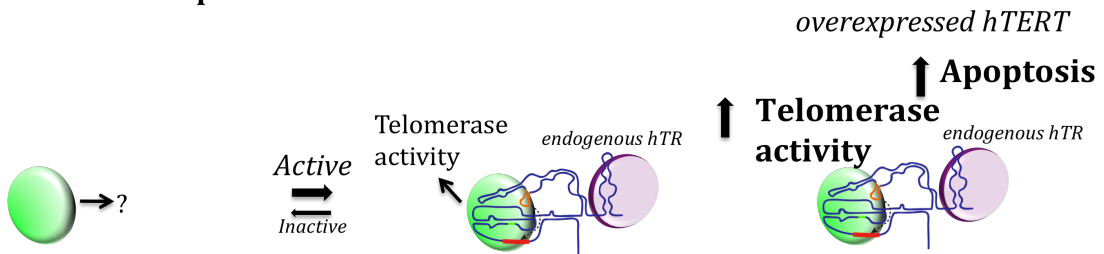
D WT hTR overexpression



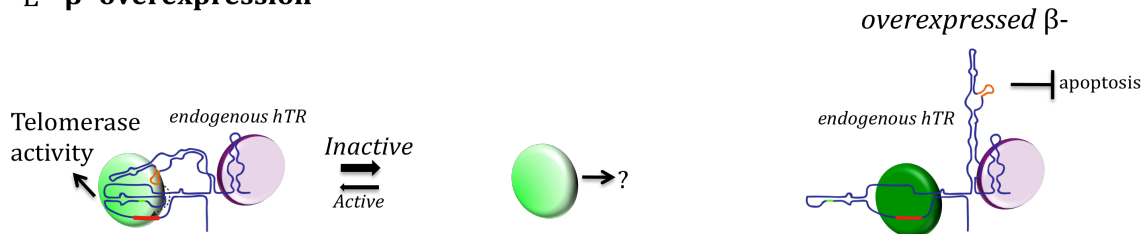
E Δ96-7 or G305A overexpression



G hTERT overexpression



E β- overexpression



Key



Figure 9. Models for how catalytically inactive hTR protects from apoptosis. **A)** At endogenous levels of hTR and hTERT, catalytically inactive hTR (unbound to hTERT) protects from activation-induced apoptosis. hTERT might exist unbound to hTR and perform a non-telomere role. At endogenous levels of hTR, cells are still susceptible to dexamethasone or hTERT-induced apoptosis. **B)** hTERT knockdown reduces telomerase activity and does not affect catalytically inactive hTR levels. There is no effect on activation-induced apoptosis, and in fact, hTERT knockdown actually protects from dexamethasone or hydrocortisone induced apoptosis by increasing catalytically inactive hTR. **C)** When hTR is knocked down, telomerase activity decreases and inactive hTR decreases. Not enough hTR exists to protect from activation-induced apoptosis. **D)** WT hTR overexpression. When WT hTR is overexpressed telomerase activity increases either due to hTR binding unbound hTERT or by hTR stabilizing hTERT protein. hTR overexpression has no effect on activation-induced apoptosis. hTR overexpression does not increase inactive hTR so hTR overexpression does not protect from dexamethasone or hTERT-induced apoptosis. **E)** Δ 96-7 or G305A hTR mutant overexpression. Δ 96-7 and G305A overexpression do not increase telomerase activity and only increase inactive hTR. These mutants are therefore able to protect from dexamethasone or hTERT-induced apoptosis. **F)** hTR-U64 fusion overexpression. The hTR-U64 fusion RNA does not increase apoptosis or bind hTERT. It does not protect from dexamethasone or hTERT-induced apoptosis suggesting that the 3' half of hTR is necessary to protect from apoptosis. **G)** hTERT overexpression. hTERT overexpression increases telomerase activity by reducing the amount of inactive endogenous hTR. Reducing the levels of endogenous inactive hTR increases apoptosis. **H)** β -hTERT overexpression. Overexpressing β -hTERT does not increase telomerase activity and therefore does not reduce the amount of inactive hTR, and thus does not affect apoptosis.

Figure 10

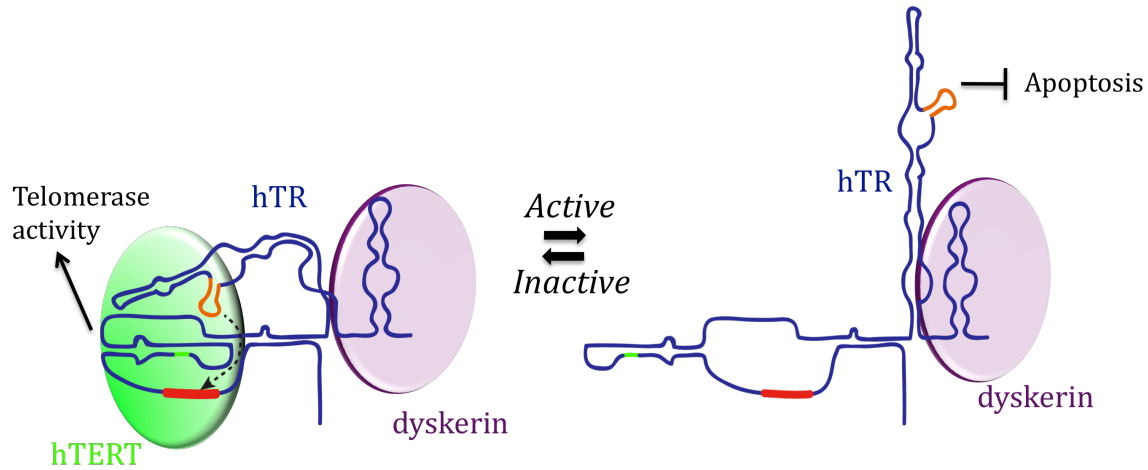


Figure 10. Two functions for hTR. hTR and hTERT complex to form catalytically active telomerase to maintain telomeres. In this catalytically active conformation, the P6.1 stem loop (orange) interacts with the template (red). hTR also functions in a catalytically inactive state (shown here as unbound to hTERT) to prevent apoptosis. In a catalytically inactive state, hTR and potentially the P6.1 stem loop, may be able to bind other factors to protect from apoptosis. Dyskerin is depicted as it is necessary for hTR accumulation, but some other binding partner might be involved with hTR to prevent apoptosis.

Non-canonical roles for telomerase

Many studies have suggested non- telomere roles for hTERT in proliferation, apoptosis, and mitochondrial function (for references see (Gazzaniga et al., 2013)). It should not be surprising that hTR also has a non-telomere function in cell survival. In fact other normal cells such as fibroblasts have hTR but no hTERT (Harley et al., 1990) suggesting that hTR has a non-telomere role. The telomerase components could act as a sensor for proliferation: when hTR is abundantly expressed, enough hTR exists in the cell to both be bound to hTERT and catalytically active for telomere maintenance and to be unbound to hTERT or bound but catalytically inactive to prevent apoptosis. When TR is low, apoptosis is induced to prevent replication without telomerase.

To our knowledge, this is the first study to show that hTR has a non-telomere and non-telomerase activity role within the cell. While hTERT appears to be the limiting factor for telomerase activity in most cells, a role for the telomerase RNA unbound to hTERT or not in a catalytic state, has not previously been identified. Since many studies on the telomerase core components are performed in cancer cells, it is possible that this role of protection from apoptosis was missed since cancer cells contain mutations to escape apoptosis.

Both late generation TERT^{-/-} or TERC^{-/-} mice show bone marrow and lymphocyte proliferation defects, however these defects are most likely due to short telomeres. Earlier generation TERC^{-/-} mice with longer telomeres appear healthy. However, to our knowledge early generation TERC^{-/-} mice have not been tested for viral challenges or infections (Goytisolo and Blasco, 2002). Our model would predict that in a state of high immune activation, the lymphocytes in these early generation TERC^{-/-} mice might undergo more apoptosis and respond differently to immune activation than WT mice. Our model also predicts that human disease

states of telomere syndromes might differ for hTR catalytically dead mutants versus hTR loss mutants, and might differ from hTERT insufficiency mutants. Telomere shortening obviously contributes to disease severity, and therefore later generation individuals tend to present worse telomere syndrome phenotypes than individuals with the same mutation from an earlier generation. However, in some cases the first diagnosis in the family is severe. To date, clinical evidence suggest that telomere syndromes caused by mutations in dyskerin, which decrease hTR levels present as more severe with the first diagnosis (Armanios and Blackburn, 2012). We propose that mutations in dyskerin that reduce hTR levels cause more severe telomere syndromes through two mechanisms: telomere shortening due to low telomerase AND increased lymphocyte apoptosis due to reduced hTR levels. Indeed the most common cause of death in telomere syndrome patients is bone marrow failure (Armanios and Blackburn, 2012).

The ability of a lymphocyte to proliferate upon activation and undergo apoptosis to regulate expansion is essential for proper immune function. Many levels of regulation at both gene and protein levels are in place to insure a proper proliferative response. The roles of small RNAs in this response are just beginning to be understood. For example, lncRNAs were just recently shown to regulate gene expression and proliferation in lymphocytes (Carpenter et al., 2013). The experiments in this thesis are the first to provide evidence that the telomerase RNA actually contributes to regulation of T cell survival by protecting from apoptosis independent of telomere length and telomerase activity.

FUTURE STUDIES

Localization studies

Our studies do not show if the catalytically inactive state in which hTR protects from apoptosis only occurs when hTR is unbound to hTERT, or if this catalytically inactive state can occur when hTR and hTERT are bound and expressed at endogenous levels. As discussed previously hTR is known to have multiple conformations. It is possible that hTR, though not necessarily bound to hTERT, can be in complex with hTERT, but in a catalytically inactive state to prevent apoptosis. However, since hTERT overexpression increases telomerase activity we know that hTR does exist without hTERT, so it is possible that at endogenous levels WT hTR only protects from apoptosis when unbound to hTERT.

Localization of hTR and hTERT in the cell might also help explain how hTR protects from apoptosis. Flag-tagged hTERT has been shown to localize to the mitochondria as well as the nucleus. Since the intrinsic apoptotic pathway is activated with hTR knockdown it is possible that hTR interacts with the mitochondria or influences the localization of hTERT. Unfortunately to address this question, a better antibody for hTERT must be made in order to determine the localization patterns of endogenous hTERT. Other studies using PNA FISH have visualized hTR in the nucleus of cancer cells though have not published visualization of hTR in the cytoplasm (Zhu et al., 2004). In yeast, however, the telomerase RNA has been found in the cytoplasm (Teixeira et al., 2002). Since three PNA probes targeting different regions of the telomerase RNA were needed to visualize it in the nucleus of cancer cells, it is possible that the technique is not sensitive enough to identify lower levels of the RNA in the cytoplasm (Zhu et al., 2004). As better techniques emerge, future studies must be performed to address the mechanism by which

hTR protects from apoptosis, how hTR and hTERT are localized within the cell, and if this function is specific to lymphocytes.

snoRNA studies

Several of the results described in this thesis suggest that hTR might act as a snoRNA and/or might interact with the snoRNA pathway. hTR has an H/ACA box similar to H/ACA box snoRNAs. This domain has been previously shown to be necessary for hTR stability and binding to dyskerin (Fu and Collins, 2003; Mitchell et al., 1999). The experiments in this thesis suggest that the H/ACA domain is also necessary for protection from apoptosis. Since other snoRNAs bind dyskerin and pseudouridylate other RNAs, which affects their stability, it is possible that hTR, when bound to dyskerin targets a specific RNA for pseudouridylation (Esteller, 2011). This function might protect from apoptosis in T cells. Unfortunately since mutations that affect hTR binding to dyskerin decrease hTR stability, determining a function for hTR binding to dyskerin is difficult. Furthermore dyskerin has pleiotropic functions necessary for cell survival. Therefore knocking out dyskerin reduces cell survival regardless of any role hTR might have with dyskerin in preventing apoptosis (Montanaro, 2010). Bioinformatics techniques to identify possible RNA targets of hTR acting as a snoRNA might be the best approach to determine if hTR acts as a snoRNA. These targets could be analyzed for pseudouridylation in the presence or absence of hTR to determine if hTR modifies them.

hTR binding factors and conformations

The results in this thesis are consistent with published results indicating that hTR has multiple conformations. It is possible that hTR when in an inactive conformation is able to bind

or interact with a factor involved in apoptosis. Since these results show that the 3' half of hTR is necessary for protection from apoptosis, it is possible that the P6.1 stem loop interacts with another binding partner to protect from apoptosis when in the inactive conformation. Previous studies have identified hStau and L22, two proteins that bind RNAs, to bind to hTR, however any function for these interactions is unknown (Le et al., 2000). It is possible that hTR has other unknown binding partners that could be identified with hTR pull down followed by mass spectrometry analysis.

While many more studies must be performed to identify a mechanism by which hTR protects from apoptosis, this thesis shows the first evidence that hTR protects from apoptosis independent of telomere length and telomerase activity.

CHAPTER 2: BREAST CANCER

INTRODUCTION

The mammalian telomerase ribonucleoprotein complex adds TTAGGG repeats to telomeres, the ends of linear chromosomes. The core human telomerase contains the catalytic reverse transcriptase protein component (hTERT) and telomerase RNA (called hTR, hTER or hTERC) that provides the template for telomeric DNA synthesis (Blackburn, 2000). In most human somatic cells, telomerase expression is very low. In contrast, telomerase expression is upregulated in many human cancer cells and stem cells (Kim et al., 1994). For example, we have shown that telomerase activity is upregulated in a panel of 50 breast cancer cell lines with the range of activity varying by more than 300 fold (Listerman et al., 2013). In human cancer cells, the degree of telomerase expression seems higher than would appear necessary solely for maintaining telomere length. In fact, many studies suggest telomere-independent roles for telomerase. We and others have shown that overexpression of TERT protects cells in culture from apoptosis independently of the telomere lengthening properties of telomerase (Lee et al., 2008; Listerman et al., 2013; Rahman et al., 2004). Furthermore, overexpression of mouse and human TERT promotes cell proliferation in stem, normal, and cancer cell lines (Mukherjee et al., 2011; Oh et al., 2001; Sarin et al., 2005; Smith et al., 2003; Stampfer et al., 2001; Xiang et al., 2002). Experiments overexpressing or reducing hTERT in cells in culture have suggested roles for hTERT in controlling expression of growth factor response and other genes (Kraemer et al., 2006). Gene expression changes have been reported to occur as soon as one week after ectopic hTERT overexpression (Smith et al., 2003). While taken together these results strongly suggest non-telomeric roles for telomerase, mechanisms by which telomerase might protect from apoptosis and promote proliferation remain largely unknown.

Some previous studies have linked TERT expression and Wnt/ β -catenin signaling, hereafter referred to as Wnt signaling (Choi et al., 2008b; Hoffmeyer et al., 2012; Park et al., 2009). The Wnt signaling pathway plays a central role in development, stem cell renewal, and cancer. In the absence of Wnt signaling, cytoplasmic β -catenin is bound by destruction complex proteins including AXIN, adenomatous polyposis coli (APC) and glycogen synthase kinase 3 beta (GSK3B). Consequently, β -catenin is phosphorylated and degraded by the ubiquitin-proteasome pathway. When secreted Wnt proteins bind to Frizzled and low-density lipoprotein receptor-related proteins (LRPs) at the plasma membrane, a signal is transduced to destabilize the β -catenin destruction complex. β -catenin can then translocate to the nucleus where it complexes with T-cell factor/lymphoid enhancer factor (TCF/LEF) transcription factors to promote target gene transcription (Holland et al., 2013). The Wnt pathway has been previously shown to upregulate telomerase in mouse mammary tumors and human cells (Broccoli et al., 1996; Zhang et al., 2012). Furthermore, β -catenin may contribute to telomerase upregulation in stem and cancer cells, by directly regulating TERT expression via binding to the TERT promoter in complex with Klf4, as reported in mouse adult stem cells and human carcinoma lines NTERA2 and SW480 (Hoffmeyer et al., 2012).

Reciprocally, Park et al. (Park et al., 2009) previously suggested that TERT expression promotes Wnt signaling. In that study, TERT^{-/-} knockout mice in the first generation were reported to have developmental defects such as homeotic transformations of the vertebrae. Such defects, occurring before the onset of significant telomere shortening, resembled effects of aberrant Wnt signaling. The authors additionally reported protein-protein interactions between hTERT and the chromatin remodeling factor BRG1 and between hTERT and β -catenin. It was also reported that TERT overexpression upregulated expression of a Wnt luciferase reporter in

TERT^{-/-} and TR^{-/-} mouse embryonic fibroblasts (MEFs) and human fibroblast (BJ) cells and that, in SW-13 and HeLa cancer cells, TERT overexpression hyperactivated a Wnt signaling reporter in a BRG1-dependent manner (Park et al., 2009). Consistent with these results, Hrdlickova et al. reported increased proliferation and a slight but significant increase in Wnt reporter activation upon overexpression of either hTERT or a catalytically-incompetent hTERT splice variant, in both U2OS (telomerase-deficient) and HeLa (telomerase-positive) cell lines (Hrdličková et al., 2012). BRG1 has been reported to bind to β -catenin and to promote β -catenin target gene expression (Barker et al., 2001; Mahmoudi et al., 2010). Because many growth-promoting genes are β -catenin targets, and Wnt signaling plays an important role in self renewal, proliferation, and survival, these reports suggested that TERT in concert with BRG1 might promote cell proliferation via Wnt signaling.

An influence of TERT on Wnt signaling has not been consistently reproduced in other experimental settings. Strong et al. did not detect homeotic transformations or diminished Wnt reporter activity in TERT^{-/-} knockout mice or MEFs derived from these mice (Strong et al., 2011). The discrepancies between the two mouse TERT^{-/-} knockout studies could have been due to slightly different experimental conditions, such as different mouse backgrounds and/or Wnt signaling activators (such as different mouse backgrounds and/or Wnt signaling activators; (Park et al., 2009; Strong et al., 2011)). Alternatively, the TERT overexpression system that identified a Wnt pathway interaction (Park et al., 2009) may not produce a biologically relevant phenotype. While Strong et al. disputed a TERT/Wnt signaling interaction in mice and MEFs (Strong et al., 2011), they did not address a possible TERT/Wnt signaling interaction in human cancer cells.

We utilized a well-characterized panel of breast cancer cells to examine a possible TERT/Wnt interaction and identify any other genes or pathways that might interact with

telomerase. This panel of breast cancer cells has been previously shown to closely represent the tumors from which they arise by gene expression (Heiser et al., 2012). We have further characterized this panel of breast cancer cells by measuring telomerase activity, telomere length, hTERT splicing, and hTR RNA levels (Listerman et al., 2013). Breast cancer cells are a relevant system to study Wnt signaling as Wnt signaling is often dysregulated in breast cancer (Howe and Brown, 2004) and either TERT overexpression or Wnt activation leads to mammary tumorigenesis in mice (Artandi et al., 2002; Howe and Brown, 2004). We therefore used this panel of breast cancer cells to investigate the role of telomerase in Wnt signaling and to identify new pathways or genes that interact with telomerase.

MATERIALS AND METHODS

Cell lines

HeLa cells were purchased from American Type Culture Collection (ATCC) and grown in DMEM with 10% FBS, 1% penicillin-streptomycin, 1% GlutaMax (Invitrogen). HCC3153, HCC1806, SUM149, and MCF10A were obtained from the lab of Joe W. Gray, Oregon Health and Sciences University. HCC3153 and HCC1806 were grown in RPMI with 10% FBS, 1% penicillin-streptomycin, 1% GlutaMax(Invitrogen). SUM149PT were grown in Ham's F12 with 5% FBS, 0.01 mg/ml Insulin, 500 ng/ml hydrocortisone, 1% penicillin-streptomycin. MCF10A were grown in DMEM/F12 with 5% horse serum, 20 ng/ml epidermal growth factor, 100 ng/ml cholera toxin, 0.01 mg/ml insulin, 500 ng/ml hydrocortisone, and 1% penicillin-streptomycin. All cell lines were grown at 37°C with 5% CO₂.

Light microscopy

HCC3153, HCC1806, SUM149PT, and MCF10A cell lines were grown on chamber slides (Lab-Tek II 154526) and treated with 25mM LiCl or 200 ng/ml Wnt3a (5036-WN-010/CF, R&D Systems) for 4 h. Cells were fixed in 2% paraformaldehyde in PBS and permeabilized with 0.5% NP-40 in PBS. Immunostaining was performed with anti- β -catenin antibody clone 14 (BD Biosciences) followed by secondary Alexa Flour 488 (Molecular Probes). DNA was visualized with 4',6-diamidino-2-phenylindole (DAPI; Invitrogen). Images were acquired in 0.5 μ M increments using a Deltavision RT (Applied Precision) with a 100x/1.40N PlanApo objective (Olympus). Images were deconvolved, Z-projected in Softworx (Applied Precision), and then adjusted for brightness and contrast in FIJI (Schindelin et al., 2012).

cDNA generation and quantitative PCR

Total RNA was extracted with the Qiagen RNeasy Mini Kit from cells treated with 25 mM LiCl, 200 ng/ml Wnt3a, or PBS for 4 h. cDNA synthesis was performed using 2 ug RNA, random hexamers, and SuperScript III (Invitrogen). cDNA was amplified in 10 ul reactions containing LightCycler 480 DNA SYBR Green I Master (Roche Applied Science) and 0.5-1 μ mol/L final concentration of each primer using a Light Cycler 480 (Roche Applied Science). The cycling conditions were 95°C for 5 min, 50 cycles of 95°C for 10 s, 60°C for 20 s, 72°C for 20 s. A melting curve (65-98°C) was generated at the end of each run. Relative expression was determined by the $2^{-\Delta\Delta CT}$ method (Livak and Schmittgen, 2001) and normalized to GAPDH. Primers used for AXIN2 forward: 5'-CATGTTTCGTCATGGGTGTGAACCA – 3', AXIN2 reverse: 5'- TGGCTGGTGCAAAGACATAG – 3'. Primers for GAPDH forward: 5'- CATGTTTCGTCATGGGTGTGAACCA – 3', GAPDH reverse: 5' – ATGGCATGGACTGTGGTCATGAGT – 3'. For Wnt target gene expression analysis, cell lines were transduced with control or wildtype hTERT lentivirus pHR'CMV-hTERT-IRES-PURO and selected with 1 μ g (HCC1806, SUM149PT) or 2 μ g (HCC3153) puromycin for 3 days and allowed to recover for 1-2 days. Cells were treated with 25 mM LiCl for 6 h, following total RNA extraction using the RNeasy kit (Quiagen) and cDNA generation using the RT2 First Strand Kit (Quiagen) according to the manufacturers instructions. 84 Wnt target genes were measured using qPCR human Wnt signaling target arrays (PAHS-243G, SABiosciences) according to the manufacturers instructions. A minimum cutoff of 2.5 fold change over control was used to determine significant gene changes.

Wnt luciferase reporter assays

The M50 Super TOPFlash and M51 Super FOPFlash luciferase reporter vectors were obtained from Adgene (Veeman et al., 2003). pRL-TK Renilla luciferase was used as an internal control (Invitrogen). The lentivirus plasmids pBARL (β -catenin Activated Reporter Luciferase) and pfluBARL (mutated pBARL), and the pSL9/rLuc (Renilla Luciferase) were obtained from the lab of Randall Moon, University of Washington (Biechele et al., 2009). Cells were seeded on 96 well microplates (655083, Greiner bio-one) and each well was transiently transfected with 0.5 μ g pRL-TK control along with either 50 μ g SUPER TOPFlash or 50 μ g mutated FOPFlash and with either 10 μ g empty vector or 10 μ g pcDNA3-FLAG-hTERT using X-tremeGene HP (Roche) and treated with or without 25mM of LiCl for 24 hours, followed by cell lysis with passive lysis buffer (Promega) for 10 min and analysis using the Dual-Luciferase Reporter Assay system (Promega). Firefly and Renilla luciferase was read with the Veritas Microplate Luminometer (Turner Biosystems). Lentivirus production and transduction was carried out as previously described (Li et al., 2004). Stable cell lines expressing reporter Renilla luciferase, pBARL or pfluBARL lentivirus were generated as reported previously described, using the same titer of lentivirus in all cell lines. Then, cell lines were transduced with either control or hTERT lentivirus (Biechele et al., 2009; Li et al., 2004), selected with puromycin, treated with 25 mM of LiCl for 24 hours, and analyzed as described above. Background luciferase readings were subtracted and Firefly luciferase values were normalized to Renilla luciferase.

RNAi

Lentivirus expressing shRNAs against β -catenin (5'-CCGGAGGTGCTATCTGTCTGCTCTACTCGAGTAGAGCAGACAGATAGCACCTTTTTT-3') (Firestein et al., 2008), hTERT (5'-GGAGACCACGTTTCAAAGTCTCTTGAACCTTTTGAACGTGGTCTCC-3')

and scramble shRNA (5'-GTTCTACAACG TAACGAGGTTT CTCTTGAAAACCTCGTTACGTTGTAGAAC-3') (Stohr and Blackburn, 2008) was generated as described previously (Stohr and Blackburn, 2008). Cells were transduced with shRNA and control vector lentivirus and selected with 1 μ g/ml puromycin for 3 days and were then expanded.

Immunoprecipitation and Western blotting

HeLa cells were transfected with pcDNA3 constructs containing wildtype hTERT with one N-terminal FLAG tag using Lipofectamine 2000 (Invitrogen) for 18 h, followed by treatment with 25 mM LiCl for 6 h. The following antibodies were used: anti-Flag (M2, Sigma F3165 and F1804), anti-BRG1 (H-88, SantaCruz), anti- β -catenin (clone 14; 610153, Transduction Laboratories) and anti-GAPDH (MAB374, EMD Millipore). Cell lysis, and IP procedures and immunoblotting were done as described previously (Park et al., 2009), using Western Lightening Plus ECL (Perkin Elmer) for detection of horseradish peroxidase-conjugated secondary antibodies and Gamma-Bind G Sepharose (GE Healthcare Life Sciences) for preclearing and IP.

Bioinformatics analysis

We determined the union of published BRG1 and hTR enriched regions identified by CHIP-Seq or ChIRP-Seq, respectively in HeLa S3 cells (Chu et al., 2011; Euskirchen et al., 2011) and merged any unioned regions that were separated by ≤ 100 bp using the CHIPPeakAnno R package (Zhu et al., 2010). Enriched gene sets were obtained through GREAT (McLean et al., 2010) on all 145 genomic regions. GO terms and KEGG pathways were identified using DAVID (Huang et al., 2008, 2009).

Telomere Repeat Amplification Protocol

Relative telomerase activity was determined by the real-time quantitative telomere repeat amplification protocol RQ-TRAP (Wege et al., 2003). Briefly cells were extracted at 1,000 cells/ μ l of 1X CHAPS buffer (10mM Tris HCl, pH 7.5; 1 mM MgCl₂; 1 mM EGTA; 0.1 mM Benzamidine; 5 mM β -mercaptoethanol; 0.5% CHAPS; 10% glycerol) for 30 min on ice and centrifuged for 20 minutes at 4C at 14,000 rpm and supernatant was transferred to a new tube. Each TRAP reaction was performed in triplicate with 5 μ l of cell extract and 15 μ l of master mix (1X TRAP buffer; 8 ng/ μ l TS primer; 4 ng/ μ l ACX primer; 30% glycerol; 0.5X SYBR green (Invitrogen S7563); 2.5 mM total dNTPs). 10X TRAP buffer: 200 mM Trish HCl, pH 8.3; 15 mM MgCl₂; 630 mM KCl; 0.5% Tween 20; 10 mM EGTA). TS Primer: 5'- AAT CCG TCG AGC AGA GTT - 3'. ACX primer: 5' - GCG CGG CTT ACC CTT ACC CTT ACC CTA ACC - 3'. Reactions were incubated at 30C for 30 minutes then PCR amplification was performed on a Lightcycler 480 (Roche Applied Systems) with the following cycling conditions: 95 C 2 min followed by 50 cycles of 95 C 1 sec, 50 C 7 sec (single acquisition) and 72 C 10 sec. The second derivative max Cp per reaction was compared to a standard curve of serial dilutions of 293T extracts (2500, 500, 100, 25, 5 cells/reaction).

RESULTS

Endogenous Wnt signaling competency varies among the breast cell lines MCF10A, SUM149PT, HCC1806 and HCC3153

One immortalized breast cell line with low telomerase activity and three basal breast cancer cell lines with mid-range to high levels of telomerase activity were selected: MCF10A (low telomerase activity), HCC3153 (mid-range) and SUM149PT and HCC1806 (relatively higher telomerase activity levels) (Listerman et al., 2013). First, to determine the extent of Wnt signaling in the breast cancer cell lines, we induced Wnt signaling with Wnt3a or LiCl. Wnt3a activates the pathway at the cell surface receptor level and specifically induces β -catenin signaling by binding to Frizzled and LRP receptors (Shibamoto et al., 1998). LiCl pharmacologically inhibits GSK3B kinase activity in the cytoplasm, thus leaving β -catenin unphosphorylated and stabilized (Hedgepeth et al., 1997).

Under control conditions, both SUM149PT and HCC3153 cells showed diffuse cytoplasmic and nuclear β -catenin staining, suggesting that they may have dysregulated Wnt signaling, which is found frequently in breast cancers (Lin et al., 2000). Upon Wnt3a or LiCl treatment, SUM149PT and HCC3153 cells showed stronger nuclear localization of β -catenin (Figure 1A). In accordance with this increased nuclear localization of β -catenin in these cells, both treatments increased the expression of the endogenous β -catenin target gene AXIN2 (Figure 1B). In contrast, in HCC1806 cells, β -catenin was largely membrane-bound, and remained so even after LiCl or Wnt3a treatment (Figure 1A). Consistent with these findings, HCC1806 cells did not significantly upregulate AXIN2 after Wnt signaling induction (Figure 1B). In MCF 10A cells, β -catenin was also largely membrane bound but showed weak nuclear localization after

LiCl or Wnt3A treatment (Figure 1A), and AXIN2 was moderately upregulated (Figure 1B). These results suggest that HCC1806 cells are not competent for Wnt signaling induction by LiCl or Wnt3A. We conclude that Wnt signaling can be activated in SUM149PT and HCC3153 lines, somewhat less in MCF 10A cells, but at most minimally in HCC1806 cells.

Figure 1

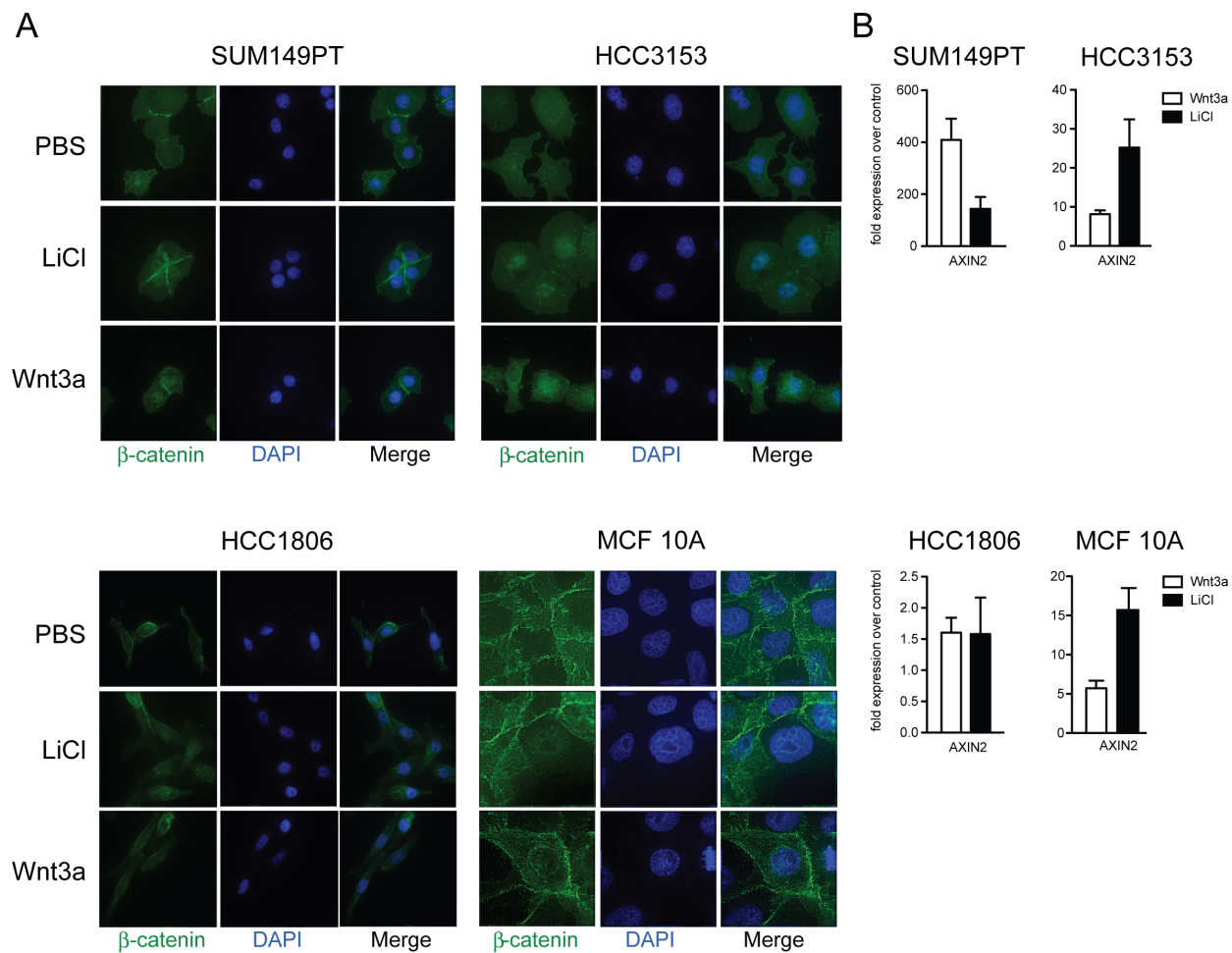


Figure 1. Endogenous Wnt/ β -catenin target gene induction varies in breast cancer cell lines. **A)** Cell lines SUM149PT (high telomerase), HCC3153 (medium telomerase), HCC1806 (high telomerase) and MCF 10A (low telomerase) were treated with PBS, 25 mM LiCl or 200 ng/ml Wnt3a for 4 h prior to staining for β -catenin (green) and DAPI (blue). **B)** Wnt/ β -catenin target

gene AXIN2 mRNA expression over PBS control treated cells was measured by qRT-PCR following activation with Wnt3a (white bars) or LiCl (black bars) for 4 h.

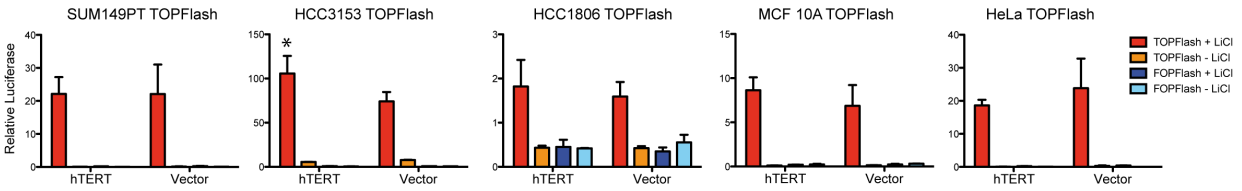
hTERT overexpression has minimal and non-concordant effects on Wnt signaling reporters in breast cancer cell lines

Having established that HCC3153, SUM149PT and MCF 10A but not HCC1806, cancer cells can strongly to moderately activate Wnt signaling, we tested whether hTERT overexpression modulated Wnt signaling reporter genes in these lines, as has been reported for MEFS, HeLa cells and U2OS cells (Hrdličková et al., 2012; Park et al., 2009). For independent verification, we employed two different Wnt signaling reporter construct systems with multimerized TCF/LEF binding sites driving luciferase expression: the M50 Super TOPFlash reporter and its control M51 Super FOPFlash Wnt reporter (Veeman et al., 2003), and the BARL (β -catenin Activated Reporter Luciferase) / fuBARL (control) system (Biechele et al., 2009). While TOPFlash contains 7 TCF/LEF binding sites and was transiently expressed via plasmid transfection, BARL contains 12 TCF/LEF binding sites and was stably integrated. Vector or hTERT plasmids were co-transfected together with TOPFlash/FOPFlash in SUM149PT, HCC5313, HCC1806, MCF10A and HeLa cells, followed by LiCl treatment (Figure 2A). As expected, LiCl treatment strongly increased luciferase activity in the vector-transfected TOPFlash SUM149PT, HCC3153, MCF 10A and HeLa cells. LiCl treatment only weakly induced the luciferase activity in HCC1806 cells, with maximum luciferase expression being 5-100-fold lower than in the other four cell lines, consistent with our observations (Figure 1) indicating that HCC1806 cells are severely impaired in Wnt signaling. Furthermore, only HCC3153 cells exhibited a statistically significant, but mild (~1.4 fold), increase of relative luciferase activity over vector control, while relative luciferase activity did not change significantly compared to vector controls in SUM149PT, HCC1806, MCF 10A or HeLa cells. In the pBARL cells, over-expressing hTERT increased luciferase activity over the vector control

cells only in HCC3153 cells (by ~2 fold; Figure 2B). Overexpression of hTERT did not detectably change the luciferase activity in SUM149PT, HCC1806 or MCF 10A cell lines expressing pBARL. In HeLa cells that stably expressed the TCF/LEF mutant (control) binding site construct, fuBARL, with hTERT overexpression we observed a ~3 fold increase in luciferase activity over control cells. However, in HeLa cells stably expressing BARL, there was only a ~2 fold increase in luciferase activity in hTERT-overexpressing cells over control cells (Figure 2B). Hence hTERT overexpression activated luciferase expression regardless of a functional TCF/LEF promoter in HeLa cells. Because hTERT overexpression led to mild hyperactivation of both Wnt signaling reporters only in HCC3153 cells and not in the four other cell lines, we conclude that Wnt reporter hyperactivation through hTERT is dependent on the context. Hence, hTERT does not hyperactivate Wnt reporters universally, but instead does so in a cell-line and context dependent manner.

Figure 2

A



B

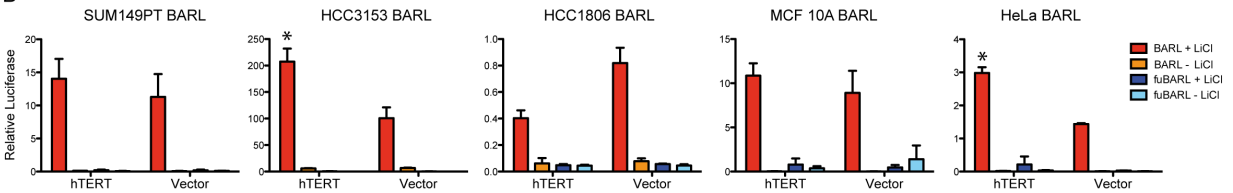


Figure 2. Effect of hTERT overexpression on two Wnt/ β -catenin reporters. **A)** SUM149PT, HCC3153, HCC1806, MCF 10A and HeLa cells were transiently transfected with pRL-TK Renilla luciferase vector (internal control), hTERT or vector, and M50 SuperTOPFlash or M51 SuperFOPFlash reporter vectors and treated with or without 25 mM LiCl for 24 h prior to luciferase measurement. **B)** Cell lines were transduced with pSL9/rLuc, pBARL or pfuBARL and either hTERT or vector control lentivirus and selected for stable expression prior to LiCl treatment and luciferase measurement.

Lack of evidence for hTERT interaction with β -catenin or BRG1 in HeLa cells

Since Park et al. (Park et al., 2009) reported that FLAG-hTERT in HeLa cells co-immunoprecipitated with BRG1, a protein previously reported to interact with β -catenin (Barker et al., 2001; Park et al., 2009), we also investigated hTERT/Wnt pathway interactions using HeLa cells. To independently verify the published results (Park et al., 2009), we transiently overexpressed FLAG-hTERT in LiCl treated HeLa cells and tested whether BRG1 or β -catenin interacted with FLAG-hTERT by co-immunoprecipitation (co-IP). Interestingly, using the same buffers as described in Park et al. (Park et al., 2009), and the non-affinity-isolated version of the anti-FLAG antibody M2 (F3165, Sigma) for IP, we observed a strong band migrating slightly slower than the β -catenin band in Western blots (M2 lanes in Figure 3A) when the FLAG-IP Western Blot was stained with the β -catenin antibody. Importantly, we also observed the same band in similar quantities independent of whether FLAG-hTERT was expressed in the HeLa cells (M2 lanes in Figure 3A), and using a variety of washing procedures in the co-IP and Western blot experiments. We extended these experiments using the affinity-isolated anti-FLAG M2 antibody (F1804, Sigma), which, while it did not enrich for this background band, instead detected another band of the expected size for β -catenin at low levels (1.7 fold over IgG control IP) that again were identical regardless of whether FLAG-hTERT was expressed (Figure 3B). We verified the identity of this cross-reacting co-immunoprecipitated protein band as β -catenin by RNAi: reducing β -catenin produced corresponding reductions in the intensity of the band pulled down by the affinity-purified M2 antibody co-IP experiments (Figure 3C). Thus, we did not detect a significant or specific interaction between hTERT and β -catenin in HeLa cells above the background signals caused by anti-FLAG antibody cross-reactivity. Using the same antibodies and IP buffers as in Park et al. (Park et al., 2009), we were also unable to detect an

interaction between overexpressed FLAG-hTERT and endogenous BRG1, despite obtaining high signals to FLAG-hTERT itself with the FLAG antibodies used (Figure 3B). In addition, we were only able to detect a weak interaction, at best, between endogenous levels of BRG1 and β -catenin; such an interaction has previously been reported only in a BRG1 overexpression context (Barker et al., 2001). We conclude, firstly, that the endogenous expression levels of BRG1 in HeLa cells were too low to detect strong interactions with β -catenin in our experiments, secondly, that M2 anti-FLAG antibody cross-reacts with a protein with a gel mobility close to that of beta-catenin, and lastly that the interaction of FLAG-hTERT with BRG1 or with β -catenin was not significantly above background IP levels.

Bottom: Western Blot of input samples from experiment. C) Top: Western Blot of HeLa cells treated with or without β -catenin shRNA following IP with specific antibodies. Bottom: Western Blot of input samples from experiment.

BRG1 and hTR do not co-localize at Wnt target genes

In human cells, the hTERT protein and the telomerase RNA hTR, together with additional proteins, assemble to form the telomerase ribonucleoprotein complex, although it has not been determined what fractions of the total levels of hTERT and hTR exist in these complexes. Previously, Chu et al. (Chu et al., 2011) used whole-genome Chromatin Isolation by RNA Purification (ChIRP) in HeLa S3 cells to detect hTR associated with chromatin at 2198 genomic locations in HeLa S3 cells. The authors additionally reported that the hTR-bound peaks they had identified were significantly enriched at loci of genes in the ‘Wnt receptor signaling pathway’ Gene Ontology (GO) term, and on this basis proposed that hTR in complex with hTERT co-occupies Wnt target genes (Chu et al., 2011). Given evidence described above that a previously reported interaction between hTERT and β -catenin protein can be explained by cross reactivity of anti-FLAG antibody rather than a bona-fide interaction, we used a bioinformatics approach to re-examine any potential connection between the published genomic localizations of BRG1 cross-linked sites, telomerase RNA cross-linked sites and Wnt signaling genes. To identify loci on the HeLa S3 genome enriched for localization sites of both BRG1 and hTR (with hTR inferred to likely be in complex with hTERT, as was described previously (Chu et al., 2011)), we merged the published BRG1 enriched localization sites identified by ChIP-Seq in HeLa S3 cells (Euskirchen et al., 2011) and the published hTR enriched localization sites (Chu et al., 2011). We applied the criterion that they were separated by ≤ 100 bp, as this same criterion was previously used to determine co-occupancy of BRG1 with other members of the SWI/SNF complex at genomic loci (Euskirchen et al., 2011). Using this criterion, 217 genes in the vicinity of the merged BRG1/hTR enriched loci were identified. However, while ‘Positive regulation of apoptosis’ was identified as a highly significant GO term among these 217 genes, Wnt signaling

was not identified as a significant GO term (Table 1). Of the 217 genes, only MYC is known to be a target gene of Wnt signaling. Thus, this analysis in HeLa S3 cells (applying the criterion of peak separation no greater than 100 base pairs) failed to verify any significant co-occupancy by hTR and BRG1 of Wnt target genes or their nearby controlling regions except for MYC. This analysis does not directly address hTERT and BRG1 co-occupancy on chromatin genomic loci. However, because some fractions of hTERT and hTR exist as telomerase complexes in HeLa S3 cells, co-localization of hTR with BRG1 at Wnt signaling gene loci might be predicted if hTERT protein and BRG1 protein interact, as suggested previously (Chu et al., 2011). Our negative finding for hTR and BRG1 co-occupancy at Wnt signaling gene loci thus did not support, but by itself does not refute, the possibility of interaction between hTERT and BRG1.

Table 1

	GO Term	P-Value
GO:0043065	positive regulation of apoptosis	0.005
GO:0006928	cell motion	0.025
GO:0051693	actin filament capping	0.027
GO:0007028	cytoplasm organization	0.035
GO:0006917	induction of apoptosis	0.035
GO:0048146	positive regulation of fibroblast proliferation	0.037
GO:0030834	regulation of actin filament depolymerization	0.040
GO:0033043	regulation of organelle organization	0.043
GO:0032272	negative regulation of protein polymerization	0.045
GO:0032271	regulation of protein polymerization	0.046

Table 1. Significant GO terms for genes close to BRG1 and hTR co-occupied loci in HeLa S3 genome.

Effects of hTERT overexpression on Wnt signaling target gene expression in cell lines do not reflect cellular Wnt signaling competency

While our bioinformatics data analysis did not identify a significant overlap of Wnt pathway genes with genomic loci cross-linkable to hTR and BRG1 in HeLa cells, this analysis did not exclude the possibility that TERT, possibly unbound to hTR, could still promote Wnt signaling. To test directly whether hTERT modulates endogenous Wnt signaling target gene expression in breast cancer cells, we stably overexpressed hTERT in the high Wnt-signaling SUM149PT and HCC3153 cells and, as a control, in the Wnt signaling-impaired HCC1806 cells. We then measured the mRNA levels of 84 endogenous Wnt downstream target genes supplied as arrays for q-RT-PCR (see Materials and Methods). First, with hTERT overexpression (Figure 4C), the Wnt-signaling-competent SUM149PT cells showed a modest overall trend to greater expression of the Wnt target genes as a group compared with vector controls; however, this trend was no greater than that seen for the Wnt-signaling-impaired HCC1806 cells, and furthermore, was not found for the Wnt-signaling-competent HCC3153 cells (Figure 4A). In addition, the genes that were significantly (at least 2.5-fold) changed by hTERT overexpression varied between the cell lines (Figure 4B). Among the 84 Wnt target genes analyzed, 10 genes were upregulated and 1 gene was downregulated in the Wnt signaling-impaired HCC1806 cells, while 9 genes were upregulated and 1 gene was downregulated in SUM149PT cells, which can strongly activate Wnt signaling (Figure 4B). In HCC3153 cells, which can also strongly activate Wnt signaling, in response to hTERT overexpression only 2 target genes were upregulated by at least 2.5 fold. Only three genes (BTRC, GDNF, MMP7) were upregulated at least 2.5 fold in any two of the cell lines, and for any of these three genes, one of the cell lines was always the Wnt

signaling-impaired cell line HCC1806. Furthermore, in SUM149PT and HCC1806 cells, IL-6 expression responded to hTERT overexpression in opposite directions.

We conclude that hTERT overexpression affects expression of some Wnt target genes, but without a discernable pattern in 3 different breast cancer cell lines with different Wnt signaling capacities, and sometimes in discordant directions between cell lines. Since hTERT overexpression also produced comparable magnitudes of effects on gene expression in the control line HCC1806, which has severely diminished Wnt-signaling, it is unlikely that hTERT changes gene expression in concert with β -catenin function.

Figure 4

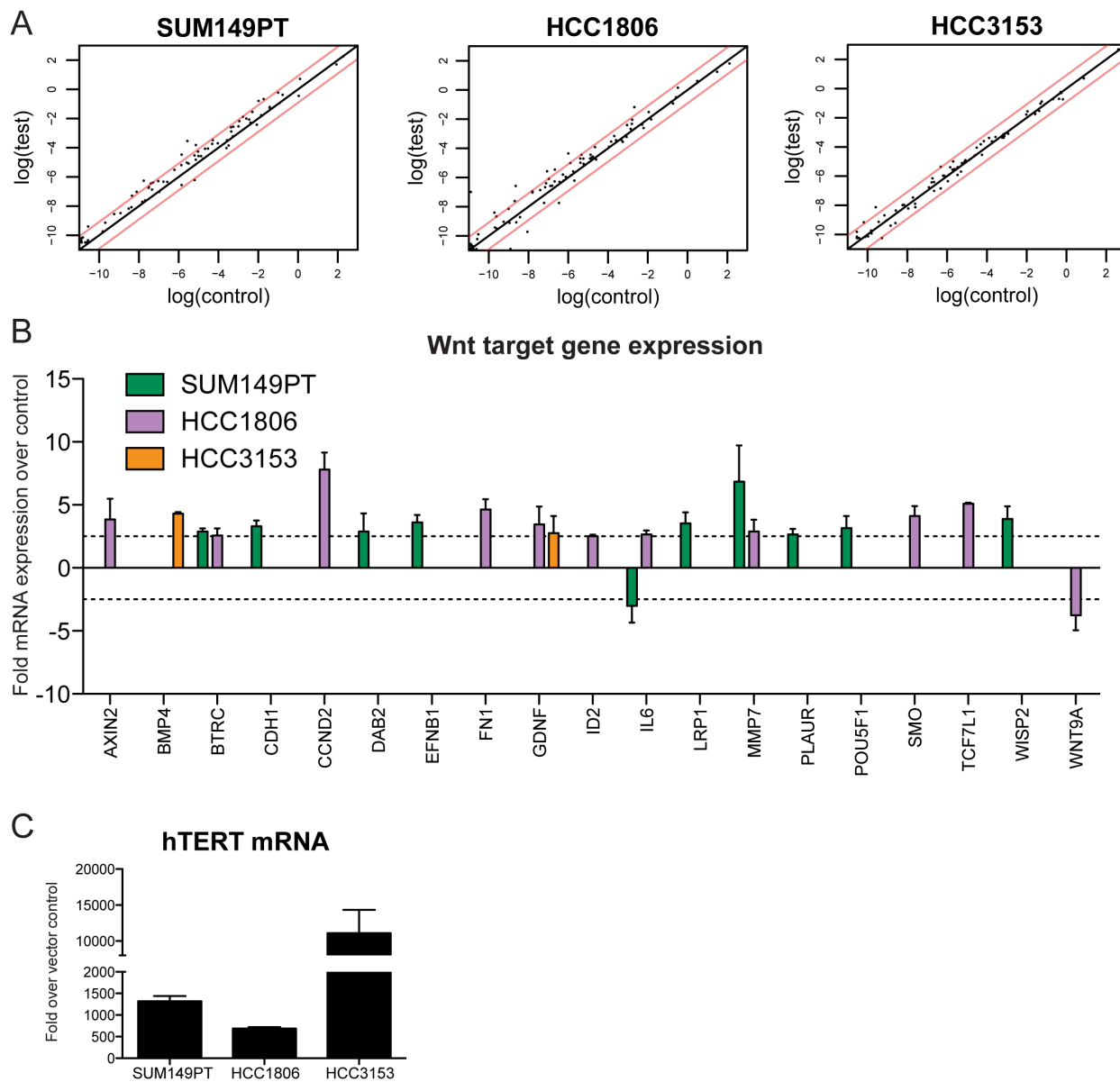


Figure 4. Effect of hTERT overexpression on Wnt target gene expression in breast cancer cell lines. SABiosciences qPCR arrays were used to measure the response of hTERT overexpression on the mRNA expression of endogenous Wnt target genes after treatment with 25 mM LiCl for 6 h. **A)** Scatter plots of log-transformed relative expression levels of each gene. Red lines indicate

a 2.5-fold change in gene expression. **B)** Wnt target genes that change +/- 2.5 fold over control (indicated by dotted line) upon hTERT overexpression in SUM149PT, HCC1806 and HCC3153 cells. **C.** hTERT mRNA expression relative to GAPDH mRNA and vector control in SUM149PT, HCC1806 and HCC3153. Bars represent mean of 3 (SUM149PT, HCC1806) and 2 (HCC3153) biological replicates. Error bars indicate SD.

We also measured the mRNA levels of a panel of 84 endogenous Wnt signaling pathway genes. As with the Wnt target gene panel, upon hTERT overexpression, the Wnt-signaling-competent SUM149PT cells showed a small trend to greater expression of the Wnt pathway genes as a group compared with vector controls; however, again, this trend was no greater than that seen for Wnt-signaling-impaired HCC1806 cells (Figure 5A). Furthermore, hTERT overexpression caused the Wnt-signaling-competent HCC3153 cells to show slightly decreased, rather than increased, expression of the Wnt pathway genes as a group. Again, among the three cell lines, hTERT overexpression caused specific Wnt pathway genes to be up- or downregulated (at least 2.5-fold) in a cell-line specific manner (Figure 5B). Additionally arguing against hTERT expression promoting Wnt signaling, knockdown of endogenous levels of hTERT (as measured by reduction of telomerase activity in Figure 6B) in SUM149PT and HCC1806 cells resulted in a corresponding decrease in gene expression of only one (Wnt11) of those genes we found to be significantly upregulated by hTERT overexpression, and furthermore, this effect occurred only in the Wnt signaling-impaired HCC1806 cells (Figure 6A).

In summary, the magnitudes of the effects of hTERT overexpression or reduction on gene expression were similar regardless of functional Wnt signaling. Furthermore, hTERT expression alterations in the cell lines examined resulted in patterns predicted to have discordant and counteractive effects on Wnt target and pathway gene expression. Thus, hTERT is unlikely to universally promote the Wnt pathway in human breast cancer cell lines.

Figure 5

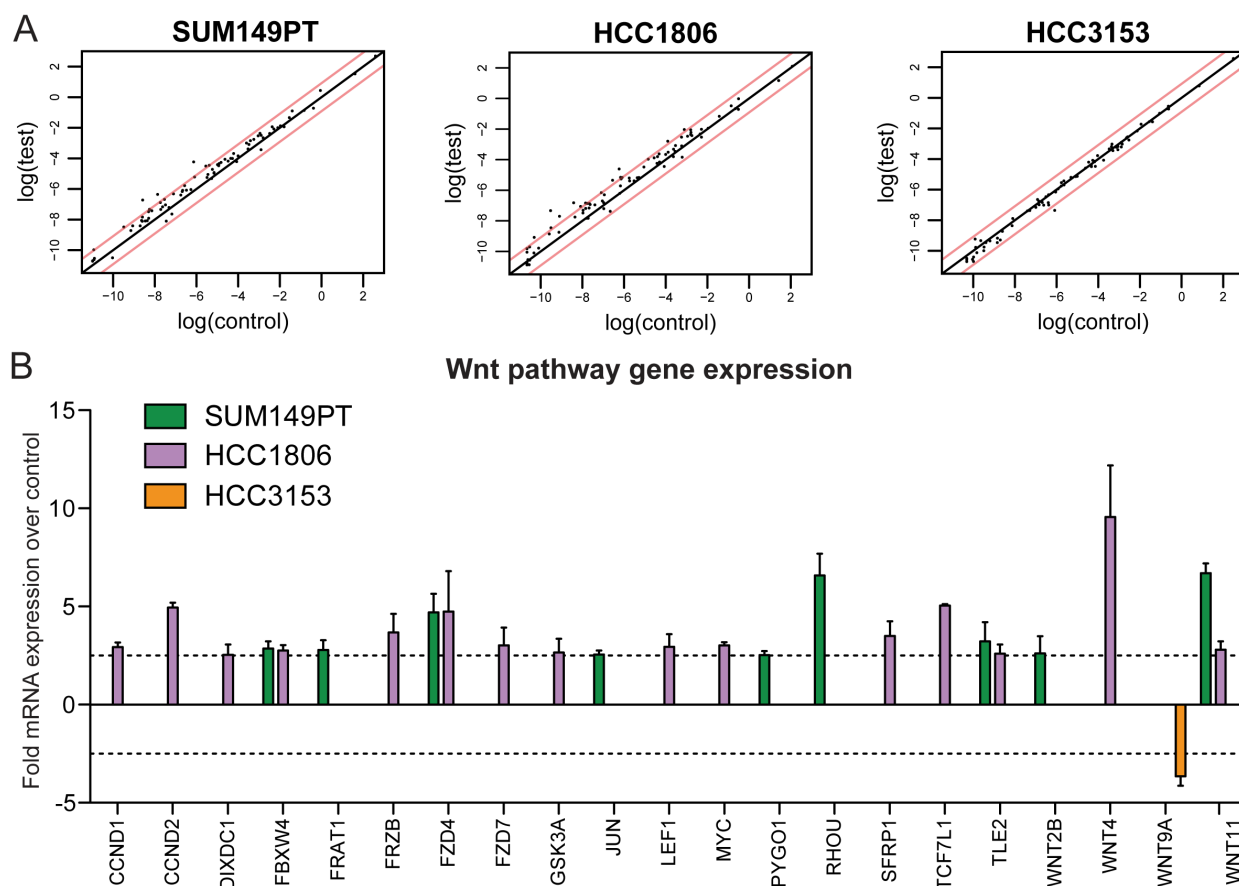


Figure 5. Effect of hTERT overexpression on Wnt pathway gene expression in breast cancer cell lines. SABiosciences qPCR arrays were used to measure the response of hTERT overexpression on the mRNA expression of endogenous Wnt pathway genes after treatment with 25 mM LiCl for 6 h, using same RNA samples as in Figure 4. **A**) Scatter plots of log-transformed relative expression levels of each gene. Red lines indicate a 2.5-fold change in gene expression. **B**) Wnt pathway genes that change +/- 2.5 fold over control (indicated by dotted line) upon hTERT overexpression in SUM149PT, HCC1806 and HCC3153 cells. Bars represent mean of 3 biological replicates. Error bars indicate SD.

Figure 6

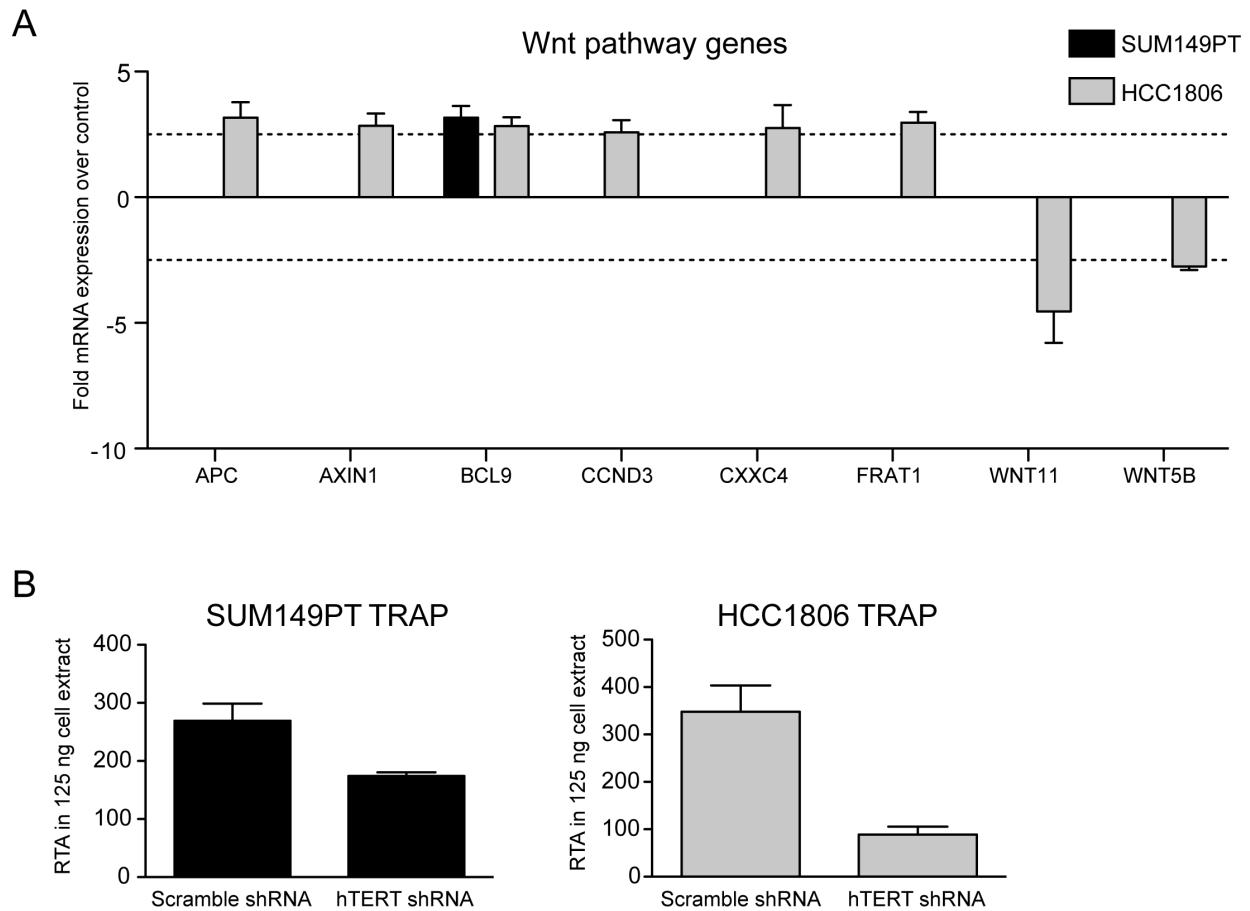


Figure 6. Effect of hTERT knockdown on Wnt pathway gene expression in SUM149PT and HCC1806 cells. SABiosciences qPCR arrays were used to measure the response of hTERT knockdown on mRNA expression of endogenous Wnt pathway genes. **A)** Wnt pathway genes that change +/- 2.5 fold over control (indicated by dotted line) upon hTERT knockdown in cells treated with 200 ng/ml Wnt3a for 6 hours. **B)** In same cells used for analysis in A, relative telomerase activity (RTA) as measured by the TRAP assay is reduced after shRNA-mediated

hTERT knockdown. Bars represent mean of 2 (SUM149PT) and 3 (HCC1806) biological replicates. Error bars indicate SD.

Telomerase activity is consistent within a wide range of confluency, extraction concentration, and passage number

Since we did not find a consistent relationship between telomerase and Wnt signaling we utilized the panel of breast cancer cell lines to identify any new pathways with which telomerase might be involved. We have already shown that telomerase activity positively correlates with full length hTERT mRNA expression, though not hTR expression in this panel of breast cancer cells (Listerman et al., 2013). Since hTERT is generally thought to be the limiting factor for telomerase activity in cancer cells, it is expected that hTERT, and not necessarily hTR, expression correlates with telomerase activity. We also found that telomere length positively correlates with telomerase activity in this panel of breast cancer cells. These results suggest that a functional readout of telomerase activity, in this case maintaining telomeres, can be obtained from this panel of breast cancer cells. Therefore we hypothesized that correlating telomerase activity with gene expression from previously published microarray data on these cell lines might identify other genes and pathways with which telomerase interacts.

Since the microarray data on these breast cancer cell lines was obtained from a different lab and potentially from cells at different passage numbers and confluencies, we first determined how these variables might affect telomerase activity. Four breast cancer cell lines with varying amounts of telomerase activity according to our published results (Listerman et al., 2013) and HEK293T cell lines (which are used as the standard in telomerase activity assays) were cultured and harvested when 10%, 25%, 50%, 100% confluent. Figure 7A shows that confluency at harvest actually does not affect telomerase activity. Figure 7B shows that passage number also does not effect telomerase activity, as expected since we have already published that passage number does not effect telomere length. Since confluency and passage number do not affect

telomerase activity in a selection of these cell lines, we conclude that correlating telomerase activity measured at a one time point with gene expression data measured at a different time point should accurately suggest genes and pathways with which telomerase might be involved.

Figure 7

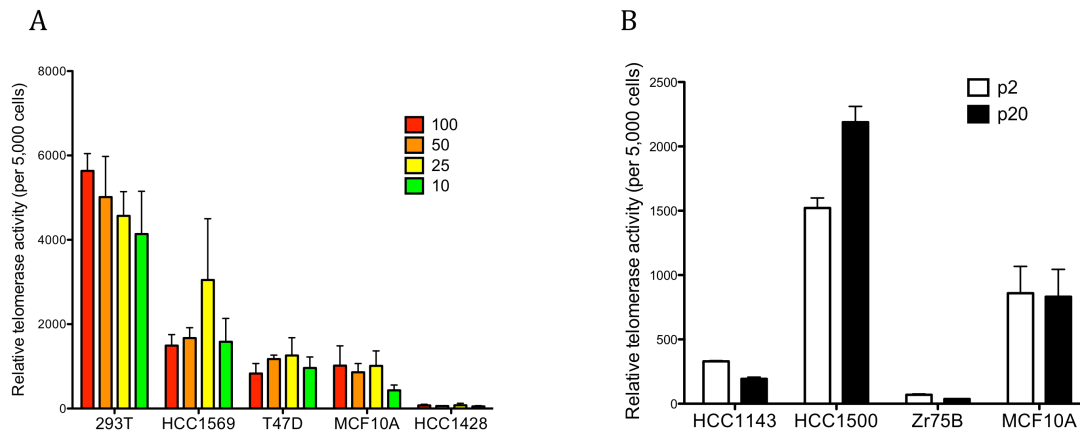


Figure 7. Confluency and passage number do not affect telomerase activity. **A)** 293T, HCC1569, T47D, MCF10A, and HCC1428 cells were harvested at confluencies of 100%, 50%, 25%, and 10% and telomerase activity was measured. Confluency at harvest does not affect telomerase activity in the five cell lines measured. **B)** HCC1143, HCC1500, ZR75B, and MCF10A were collected at passage 2 after thawing and 20 passages later and telomerase activity was measured. Passage number does not affect telomerase activity supporting our published results that telomere length does not change with passage number in breast cancer cells (Listerman et al., 2013).

Telomerase activity correlates with proliferation and differentiation

Gene expression from previously published microarray data on the panel of breast cancer cell lines was correlated with telomerase activity. Supplementary Table S3 shows the genes that significantly correlate with telomerase activity. As expected hTERT is one of the top genes that correlate with telomerase activity. Future studies should be performed to determine if telomerase interacts with any of these other genes that correlate with telomerase activity. These interactions could help determine non- telomere roles for telomerase.

DISCUSSION

While the role of telomerase in protecting and maintaining telomeres can explain the upregulation of telomerase in stem cells and tumors, it does not exclude the possibility for other, non-telomeric roles for telomerase. Recently, it was reported that hTERT interacts with BRG1 and promotes Wnt signaling (Park et al., 2009). In the present study, we set out to determine whether hTERT promotes Wnt signaling in human breast cancer cells. We tested this question using different biochemical and molecular biology approaches. Using three human basal breast cancer cell lines, breast cell line MCF10A and HeLa cells, we fail to find evidence consistent with the hypothesis that hTERT promotes Wnt signaling in a biologically significant way in these cells. While our results were not aimed at addressing the question of any interaction between TERT and Wnt signaling in the mouse system, they add some new information for the context of such investigations.

Using both transient and stably integrated Wnt reporter systems, we find that hTERT only mildly hyperactivates the reporters in a TCF/LEF-site dependent manner in only one (HCC3153) of the five cell lines tested. Although we observed a 2 fold increase in luciferase activity upon hTERT overexpression in HeLa cells using BARL, we believe this to be an insignificant result since in the control experiment, overexpression of hTERT together with the mutant control TCF/LEF fuBARL led to a 3 fold increase in luciferase activity. This result renders it unlikely that luciferase expression in HeLa cells is dependent on hTERT promoting a functional TCF/LEF promoter. One possible partial explanation for the apparent discrepancy between our study and previous reports that hTERT overexpression increases Wnt reporter activity in HeLa cells (Hrdličková et al., 2012; Park et al., 2009) may be the number of TCF/LEF

sites in the different reporters used. Park et al. utilized a transiently expressed Mega TOPFlash with 14 TCF/LEF binding sites (Park et al., 2009), and observed a 2 fold increase in luciferase activity upon hTERT overexpression. Hrdlickova et al. and the present study used SuperTOPFlash with 7 TCF/LEF binding sites (Veeman et al., 2003) and observed a small, but statistically significant ~1.5 fold increase in HeLa cells (Hrdličková et al., 2012) and ~1.4 fold increase in HCC3153 cells (this study). Mouse Wnt reporters in MEFs have also yielded varying results. A 6-fold MegaTOPFlash hyperactivation was reported with mTERT overexpression in TERT^{-/-} MEFs using LiCl to activate Wnt signaling (Park et al., 2009), while Strong et al. were unable to detect a reciprocal decrease in SuperTOPFlash activity in TERT^{-/-} MEFs using Wnt3a activation of Wnt signaling (Strong et al., 2011). We conclude that the effect of hTERT on Wnt reporters is small but not universal in cancer cells; rather, it depends on cell type and context, and on the reporter system used.

Since hTERT only mildly hyperactivated Wnt/b-catenin reporters, and only in one of the five human cancer cell lines tested, we re-examined the possible biochemical links between hTERT and Wnt signaling that were previously reported to be mediated by BRG1 (Park et al., 2009). We failed to detect a significant protein-protein interaction between our overexpressed FLAG-hTERT and endogenous BRG1 in HeLa cells, using the same buffers and antibodies as described in Park et al. Since an interaction with overexpressed and endogenous hTERT and BRG1 was reported in another study in HeLa and 293T cells (Okamoto et al., 2011), this discrepancy between the results may be due to variations in BRG1 expression in different HeLa strains. Additional considerations that may underly the discrepancy between those two reports and our results include possible cross reactivities of antibodies; in those reports (Okamoto et al., 2011; Park et al., 2009) various controls to rule out such cross-reactivities were not shown.

We were unable to detect an interaction between FLAG-hTERT and β -catenin (hypothesized to be mediated by BRG1) using an affinity purified anti-FLAG M2 antibody for IP. Instead, we detected a cross-reactivity between the immunoprecipitates from non-affinity purified anti-FLAG M2 antibody IPs and the β -catenin antibody, even (a) in the absence of FLAG-tagged hTERT and (b) when β -catenin was not stabilized with LiCl. Thus, we cannot exclude the possibility that the cross-reactivity we observed with the M2 antibody provides an explanation for the conclusion reached by Park et al. (Park et al., 2009) that FLAG-hTERT interacts biochemically with β -catenin. Furthermore, we detected only a very weak interaction between endogenously expressed BRG1 and β -catenin. To our knowledge, the only published evidence of a protein-protein interaction between BRG1 and β -catenin was reported only under conditions where BRG1 was overexpressed in 293T and DK11 cells (Barker et al., 2001). Furthermore, native BRG1 did not bind to GST-tagged β -catenin in vitro (Kadam and Emerson, 2003). Our negative findings are thus consistent with the possibility that BRG1 is only transiently associated with β -catenin, which may hinder the detection of an interaction using immunoprecipitation. Alternatively, BRG1 may not be expressed at high enough levels under normal circumstances to allow detection of its interaction with hTERT or β -catenin.

A model was previously proposed by which the telomerase complex interacts with BRG1 to promote β -catenin gene expression (Chu et al., 2011; Park et al., 2009). If hTERT interacts with BRG1 to directly bind to β -catenin target genes, it is reasonable to postulate that the telomerase ribonucleoprotein complex (as monitored by hTR cross-linking to chromatin (Chu et al., 2011)) would be co-localized with at least some genomic positions together with BRG1. However, in our re-analysis of published data to seek simultaneous enrichment of hTR and BRG1, Wnt signaling was not among the significant GO terms for the 217 genes that we

identified in the vicinity of the overlap between BRG1- and hTR-enriched genomic sites. Among these 217 genes, only one Wnt target gene, MYC, was identified as an hTR- and BRG1-enriched cross-linked locus. Since enrichment peaks of hTR (mean peak size = 761 bps) and BRG1 (mean peak size = 1245 bps) were analyzed and reported by different groups using slightly different background correction, this does not rule out the possibility that hTR and BRG1 co-occupy sites in the genome further apart than the 100 bp spacing between hTR and BRG1 enriched regions that we allowed for in our analysis. However, given the report that hTERT and BRG1 interact directly, it was reasonable to investigate whether BRG1 and hTR may be localized at the same genomic sites, as has been reported for BRG1 and other members of the SWI/SNF complex (Euskirchen et al., 2011). Merged regions encompassing BRG1 and hTR peaks with ≤ 100 bp separation span a distance of 1700 bps on average, a distance that can incorporate ~ 11 to 12 nucleosomes. By this criterion we were only able to detect co-occupancy of BRG1 and hTR (potentially in a complex with hTERT) in HeLa S3 cells at one Wnt target gene, MYC. However, this analysis does not exclude the possibility that hTR might be localized at Wnt genes that are not bound by BRG1, and does not address directly whether hTERT is bound to BRG1-bound sites.

We found that hTERT overexpression and depletion did change the expression of some Wnt pathway or target genes, but independently of whether the cell line was strongly activating Wnt signaling or not, and not in directions predicted to have concordant effects on Wnt signaling. These data suggest that while hTERT seems to affect gene expression, these changes are not necessarily β -catenin signaling related. Interestingly, even though overexpression of hTERT in human mammary epithelial cells (hMECs) provided a proliferative advantage under low-mitogen conditions and led to gene expression changes (Smith et al., 2003), another study

failed to find upregulation of the Wnt target gene AXIN2 after hTERT overexpression in hMECs (Mukherjee et al., 2011). Furthermore, hTERT has been reported to bind to and regulate NFkB1 target genes directly (Ghosh et al., 2012). Since many Wnt signaling target genes are also regulated by other pathways, such as the transforming growth factor-beta (TGF- β) pathway (Guo and Wang, 2009), we propose that hTERT may promote the expression of certain genes but not necessarily by acting solely in Wnt signaling. MYC, which emerged as the strongest candidate regulated by BRG1 in combination with hTERT/hTR, is for example an important transcriptional activator for cell growth and proliferation and is downstream of other receptor signal transduction pathways such as receptor tyrosine kinase and T cell receptor pathways (Dang, 2012).

In summary, we consistently failed to find evidence that hTERT expression promotes Wnt signaling in three human breast cancer lines, an immortalized human breast cell line and HeLa cells. Our results conflict with previous studies reporting such an effect of TERT in HeLa cells, and also suggest that any effect of TERT on Wnt signaling may be context- and cell-line specific.

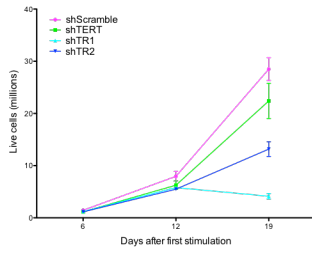
FUTURE STUDIES

While the studies described in the introduction to this section strongly suggest a non-telomere role for telomerase in apoptosis, proliferation, and mitochondrial function, we were unable to find an interaction with telomerase and Wnt signaling. Instead we found that telomerase activity correlates with almost 1,000 genes in a panel of breast cancer cells. We therefore suggest that future studies on the interactions between telomerase and these genes to identify any non-canonical roles for telomerase.

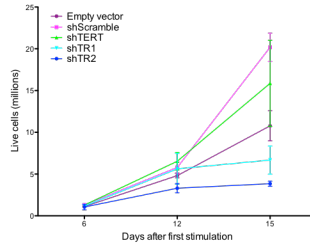
APPENDIX

Supplementary Figure 1

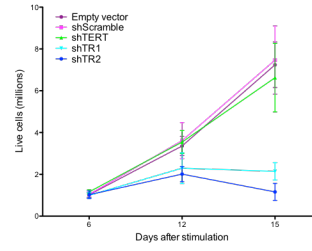
A



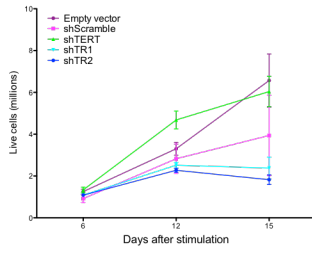
B



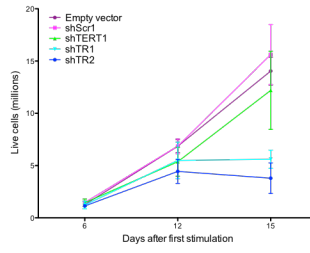
C



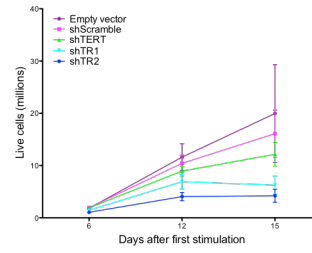
D



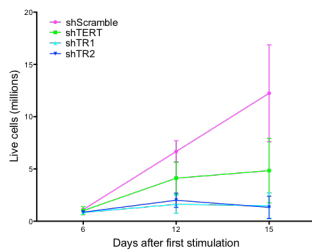
E



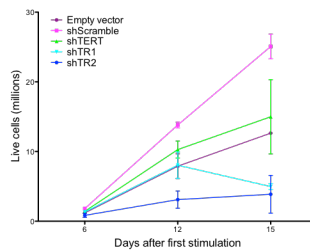
F



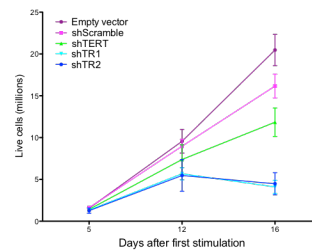
G



H

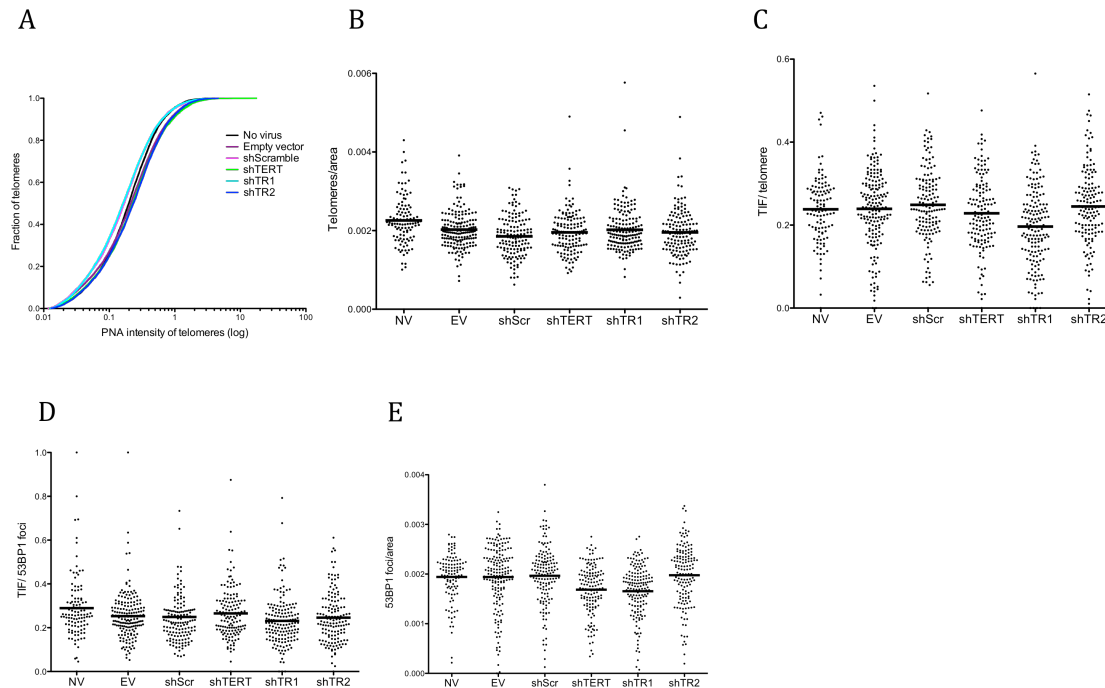


I



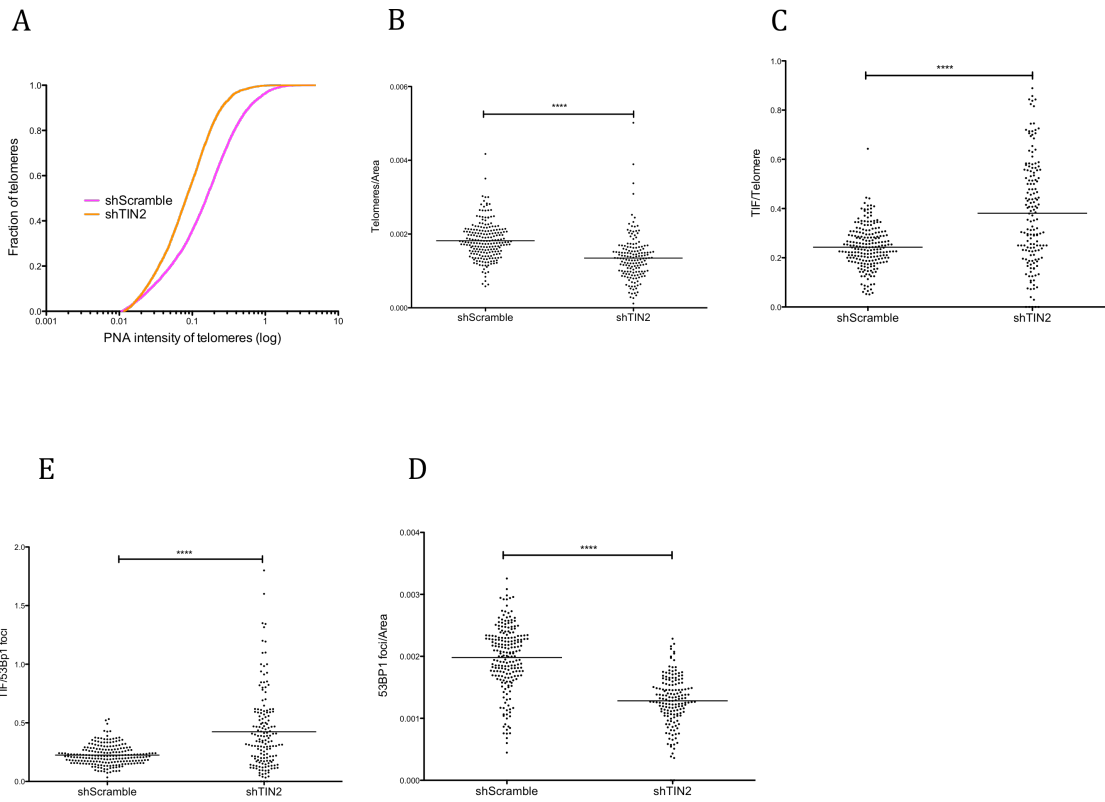
Supplementary Figure S1. hTR knockdown, but not hTERT knockdown reduces T cell survival in T cells from six additional donors. All experiments were performed in triplicate. Live cell cells were counted by trypan blue exclusion. Error bars represent standard deviation. **A)** Donor of unknown age **B)** 25 year old donor **C)** Repeat of donor from B **D)** Repeat of donor from B **E)** 19 year old donor **F)** Repeat of donor from E **G)** 24 year old donor **H)** donor of unknown age **I)** 16 year old donor.

Supplementary Figure S2



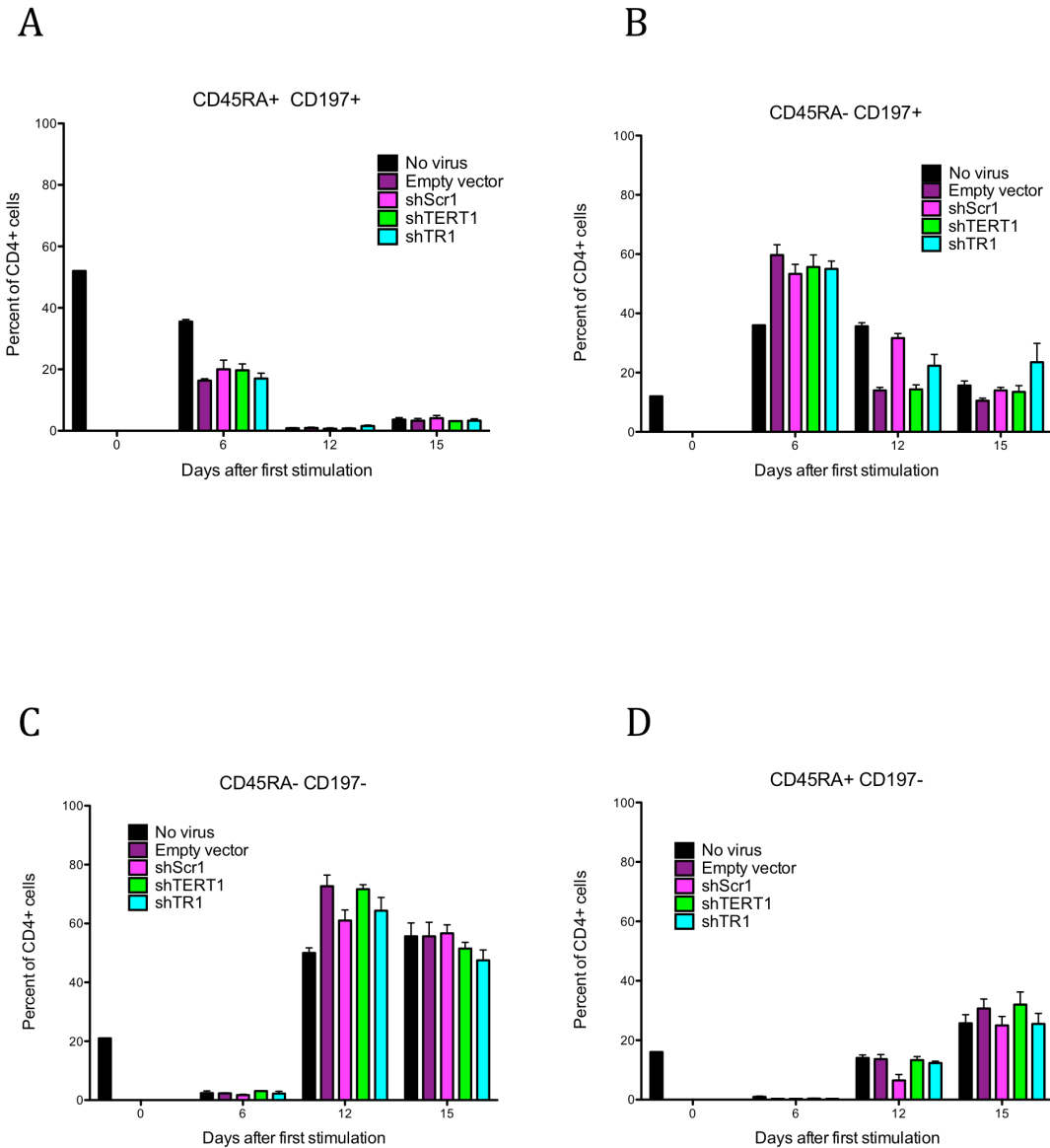
Supplementary Figure S2. Telomere length and TIF measurements with 53BP1. **A)** Cumulative frequency of PNA intensity of telomere lengths with hTR knockdown are not significantly shorter than controls. **B)** Telomeres/area do not significantly differ between hTR knockdown and shTERT, EV, or shScramble. **C)** The amount of TIFs/telomere are not significantly higher with hTR knockdown compared to controls in the timeframe of this experiment. **D)** TIF/53BP1 foci are not significantly higher with hTR knockdown. **E)** The amount of 53BP1 foci/area is not significantly higher with hTR knockdown. Statistical significance was assessed using one way ANOVA and Dunn's multiple comparison test with a significance cutoff of $p < 0.05$ in Prism (GraphPad).

Supplementary Figure S3



Supplementary Figure S3. shTIN2 acts as a positive control for telomere shortening and detection of TIFs. **A)** Cumulative frequency of PNA intensity of telomeres is significantly shorter with TIN2 knockdown compared to shScramble control. **B)** Telomeres/area are significantly reduced with TIN2 knockdown indicating that TIN2 knockdown causes more telomeres to short to be detected by the telomeric PNA probe. **C)** TIF/Telomere significantly increase with TIN2 knockdown. **D)** TIF/53BP1 foci increase with TIN2 knockdown. **E)** 53BP1 foci/area decrease with TIN2 knockdown indicating that most 53BP1 foci are located at the telomere with TIN2 knockdown. Statistical analysis was assessed using an unpaired T test. **** represents $p < 0.0001$.

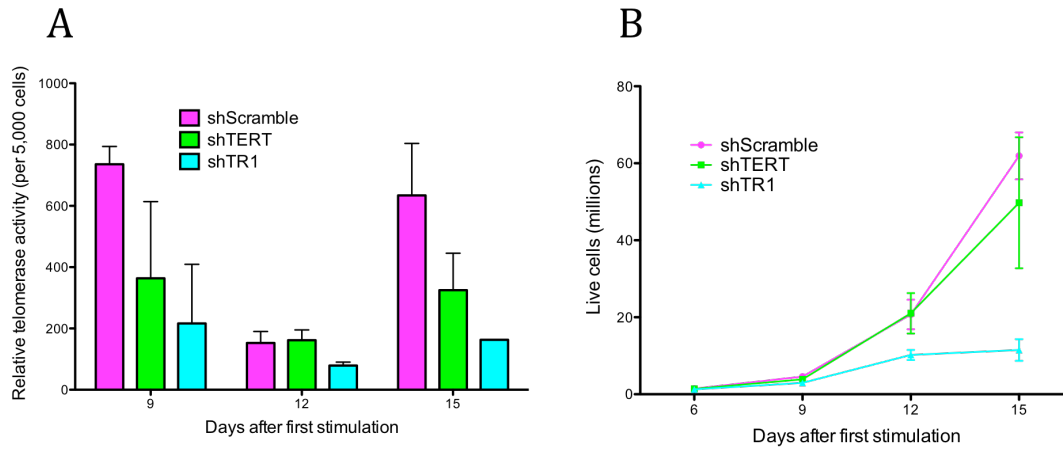
Supplementary Figure S4



Supplementary Figure S4. hTR knockdown does not affect CD4+T cell development from naïve to effector memory T cells in culture. Cells were stained with anti-CD4+ APC, anti-CD197 PE, anti-CD45RA PerCp Cy5.5 and analyzed by flow cytometry. **A)** The percent of naïve CD45RA+ CD197+ CD4+ T cells in culture over time **B)** The percent of CD45RA- CD197+

CD4⁺ central memory T cells in culture over time **C)** The percent of CD45RA⁻ CD197⁻ CD4⁺ effector memory T cells in culture over time **D)** The percent of CD45RA⁺ CD197⁻ CD4⁺ effector memory T cells in culture over time.

Figure S5



Supplementary Figure S5. hTR knockdown reduces T cell survival in culture when starting with naïve T cell population. Naïve CD4⁺ T cells were isolated from buffy coat with the Miltenyi Naïve CD4⁺ T Cell Isolation Kit. **A)** Telomerase activity over time in CD4⁺ T cells from an initial naïve CD4⁺ T cell population **B)** Live cell proliferation measured by trypan blue exclusion of CD4⁺ T cells over time starting from an initial naïve CD4⁺ T cell population.

Figure S6

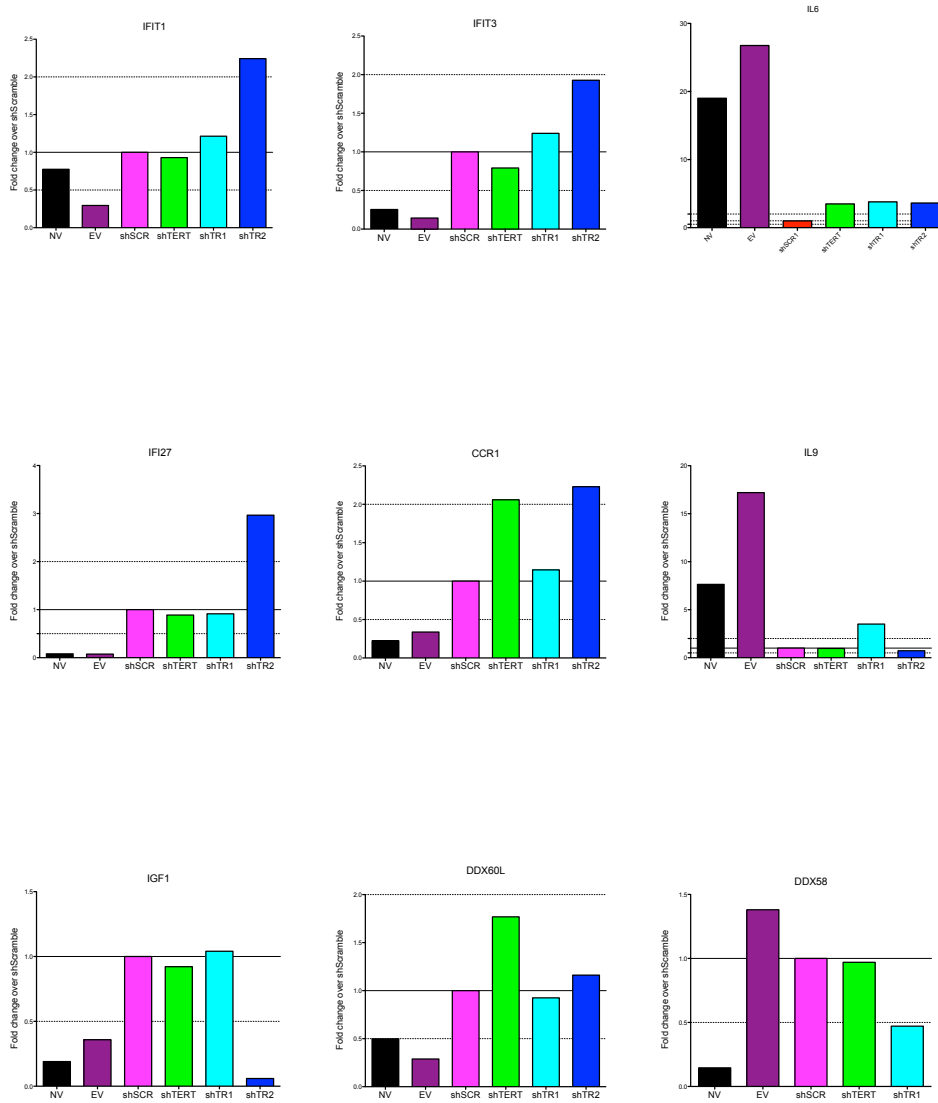
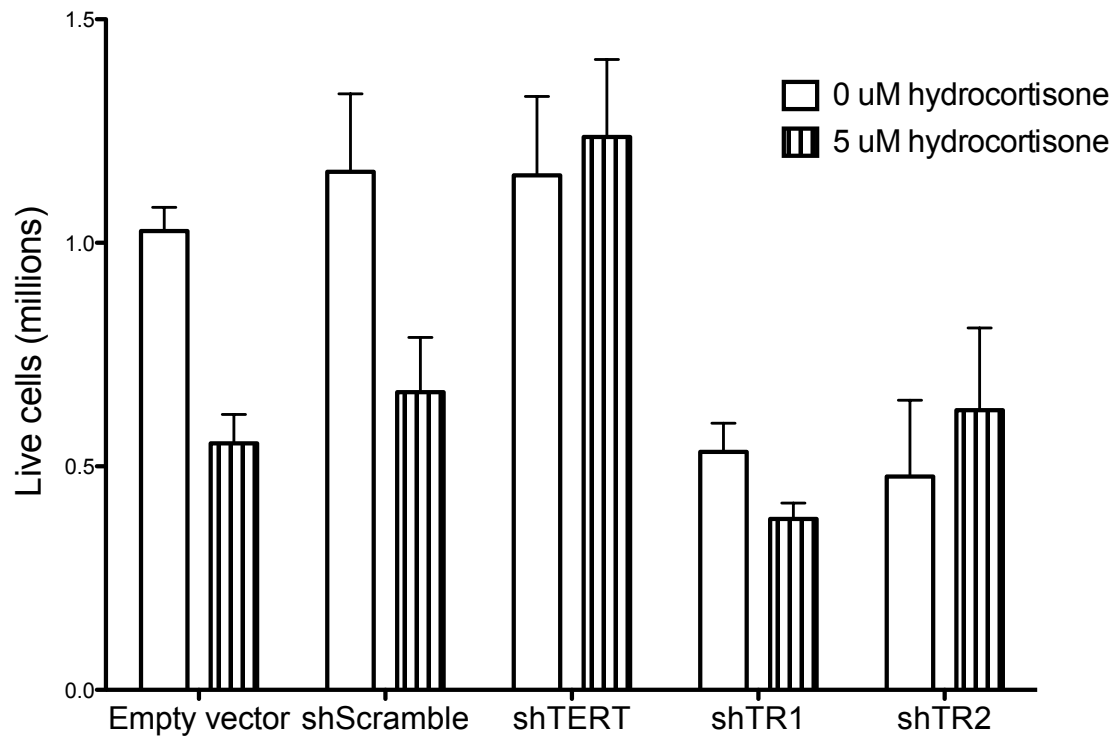


Figure S6. qRT-PCR of several genes identified by the microarray as significantly changed.

This analysis revealed most genes identified were actually not significantly changed (data not shown) or appear to be affected by lentivirus or the shRNA pathway in general and not specific to hTR knockdown as shown above.

Supplementary Figure S7



Supplementary Figure S7. Cell counts of Day 15 shRNAs with 72 hours of 5 μ M cortisol treatment. shTERT increases cell survival with hydrocortisone treatment, supporting Figure 6F showing that shTERT combined with shScr protect from dexamethasone induced apoptosis.

Supplementary Table 1. Names and descriptions of plasmids

Plasmid name	Description	EHB number (use for plasmid requests from Blackburn Lab)
Empty vector	pHR'EF1 α -puromycin	pEHB28008
Empty vector	pHR'EF1 α -puromycin	pEHB28012
shScramble	pHR' U6-shScramble-EF1 α -puromycin	pEHB28002
shScramble	pHR' U6-shScramble-EF1 α -GFP	pEHB28013
shTERT	pHR' U6-shTERT-EF1 α -puromycin	pEHB28003
shTERT	pHR' U6-shTERT-EF1 α -GFP	pEHB28014
shTR1	pHR' U6-shTR1-EF1 α -puromycin	pEHB28003
shTR1	pHR' U6-shTR1-EF1 α -GFP	pEHB28015
shTR2	pHR' U6-shTR2-EF1 α -puromycin	pEHB18007
shTR2	pHR' U6-shTR2-EF1 α -GFP	pEHB28016
shBim	pHR' U6-shBim-EF1 α -GFP	pEHB28017
WT hTR	pHR'U3-hTR-500- EF1 α -puromycin	pEHB28018
Δ 96-7	pHR'U3- Δ 96-7-500- EF1 α -puromycin	pEHB28019
C204G	pHR'U3- C204G-500- EF1 α -puromycin	pEHB28020
G305A	pHR'U3- G305A-500- EF1 α -puromycin	pEHB28021
hTR-U64 fusion	pHR'U3-hTR-U64-500	pEHB28022
Luciferase vector	pHR'CMV-Luciferase-IRES-puromycin	pEHB23010
TERT	pHR'CMV-TERT-IRES-GFP	pEHB23055
GFP vector	pHR'CMV-GFP-IRES-puromycin	pEHB28023
TERT	pHR'CMV-TERT-IRES-puromycin	pEHB28024

Supplementary table 2. Primers for qRT-PCR

Primer	Forward	Reverse
TERT	5'- CCAAGTTCCTGCACTGGCTGA – 3'	5'- TTCCCGATGCTGCCTGACC -3'
β-splice variant	5' – TGTACTTTGTCAAGGTGGATGTG - 3'	5' – GGCACTGGACGTAGGACGTGG -3'
TR	5'- TTG CGG AGG GTG GGC CT -3'	5'- CGG GCC AGC AGC TGA CAT T -3'
Bim	5'- CAGATATGCGCCCAGAGATA-3'	5'- ACCAGGCGGACAATGTAAC- 3'
GAPDH	5'- CATGTTTCGTCATGGGTGTGAACCA – 3'	5' – ATGGCATGGACTGTGGTCATGAGT – 3'
W element	5'- CATGCTATTGCTTCCCGTATGGCT - 3'	5'- ACAACGGGCCACAACCTCCTCATAA – 3'
TS primer for TRAP	5- AAT CCG TCG AGC AGA GTT – 3'	
ACX primer for TRAP		5'- GCG CGG CTT ACC CTT ACC CTT ACC CTA ACC -3'

Supplementary Table 3. Genes that correlate with telomerase activity in a panel of breast cancer cells

Gene Symbol	Gene Name	Correlation Coef.	P-Value
PSEN1	presenilin 1	-0.680	9.51E-05
HTR3D	5-hydroxytryptamine (serotonin) receptor 3 family member D	0.679	9.90E-05
SRP68	signal recognition particle 68kDa	-0.678	1.03E-04
GOSR1	golgi SNAP receptor complex member 1	-0.670	1.30E-04
LRRTM4	leucine rich repeat transmembrane neuronal 4	0.664	1.61E-04
C10orf107	chromosome 10 open reading frame 107	-0.653	2.21E-04
OSBPL5	oxysterol binding protein-like 5	-0.650	2.46E-04
TERT	telomerase reverse transcriptase	0.639	3.34E-04
PSMA2	proteasome (prosome, macropain) subunit, alpha type, 2	-0.631	4.14E-04
DNAJB7	DnaJ (Hsp40) homolog, subfamily B, member 7	0.627	4.66E-04
ANKRD49	ankyrin repeat domain 49	-0.615	6.34E-04
SCYL2	SCY1-like 2 (<i>S. cerevisiae</i>)	-0.611	7.09E-04
HN1	hematological and neurological expressed 1	-0.611	7.20E-04
NANS	N-acetylneuraminic acid synthase	-0.609	7.43E-04
SSH2	slingshot homolog 2 (<i>Drosophila</i>)	-0.606	8.03E-04
JKAMP	JNK1/MAPK8-associated membrane protein	-0.604	8.41E-04
FZR1	fizzy/cell division cycle 20 related 1 (<i>Drosophila</i>)	-0.602	8.85E-04
UEVLD	UEV and lactate/malate dehydrogenase domains	-0.602	8.94E-04
FAM64A	family with sequence similarity 64, member A	0.600	9.36E-04
WDR26	WD repeat domain 26	-0.600	9.50E-04
KCNAB1	potassium voltage-gated channel, shaker-related subfamily, beta member 1	0.596	1.04E-03
CDK12	cyclin-dependent kinase 12	-0.594	1.09E-03
NOX3	NADPH oxidase 3	0.593	1.13E-03
FTL	ferritin, light polypeptide	0.591	1.17E-03
ZNF678	zinc finger protein 678	-0.590	1.21E-03
C19orf50	chromosome 19 open reading frame 50	0.587	1.28E-03
SH3KBP1	SH3-domain kinase binding protein 1	-0.587	1.28E-03
CCDC57	coiled-coil domain containing 57	-0.587	1.30E-03
TRPC6	transient receptor potential cation channel, subfamily C, member 6	-0.586	1.32E-03
RIT2	Ras-like without CAAX 2	-0.585	1.35E-03
KDM4B	lysine (K)-specific demethylase 4B	-0.584	1.37E-03
PRKAG1	protein kinase, AMP-activated, gamma 1 non-catalytic subunit	-0.584	1.39E-03
PSEN2	presenilin 2 (Alzheimer disease 4)	-0.583	1.41E-03
RGN	regucalcin (senescence marker protein-30)	-0.582	1.46E-03
CPD	carboxypeptidase D	-0.581	1.48E-03
PPAP2B	phosphatidic acid phosphatase type 2B	0.580	1.52E-03
ATXN7	ataxin 7	0.579	1.54E-03
PCSK5	proprotein convertase subtilisin/kexin type 5	0.579	1.55E-03
VPS41	vacuolar protein sorting 41 homolog (<i>S. cerevisiae</i>)	-0.576	1.68E-03
COLEC11	collectin sub-family member 11	0.574	1.76E-03

ARL15	ADP-ribosylation factor-like 15	-0.573	1.80E-03
HACL1	2-hydroxyacyl-CoA lyase 1	0.573	1.80E-03
CINP	cyclin-dependent kinase 2 interacting protein	-0.572	1.82E-03
CHRAC1	chromatin accessibility complex 1	0.569	1.95E-03
CYTH1	cytohesin 1	-0.569	1.95E-03
TAS2R16	taste receptor, type 2, member 16	0.569	1.95E-03
NTF3	neurotrophin 3	0.568	1.98E-03
SPTLC2	serine palmitoyltransferase, long chain base subunit 2	-0.568	1.98E-03
TRAV8-3	T cell receptor alpha variable 8-3	-0.567	2.06E-03
ACOX1	acyl-CoA oxidase 1, palmitoyl	-0.565	2.12E-03
PLIN3	perilipin 3	-0.564	2.18E-03
PODXL	podocalyxin-like	0.564	2.18E-03
ZNF441	zinc finger protein 441	-0.563	2.24E-03
NR2C2	nuclear receptor subfamily 2, group C, member 2	0.562	2.30E-03
NUDCD3	NudC domain containing 3	-0.562	2.30E-03
AFAP1-AS	AFAP1 antisense RNA (non-protein coding)	0.560	2.39E-03
UBXN6	UBX domain protein 6	-0.560	2.39E-03
PEMT	phosphatidylethanolamine N-methyltransferase	0.559	2.43E-03
ENGASE	endo-beta-N-acetylglucosaminidase	-0.557	2.52E-03
DNAJB14	DnaJ (Hsp40) homolog, subfamily B, member 14	-0.557	2.56E-03
TYRP1	tyrosinase-related protein 1	-0.557	2.56E-03
ZNF578	zinc finger protein 578	-0.555	2.66E-03
C14orf179	chromosome 14 open reading frame 179	-0.555	2.66E-03
NFKBIZ	nuclear factor of kappa light polypeptide gene enhancer in B-cells inhibitor, zeta	0.555	2.66E-03
TFDP3	transcription factor Dp family, member 3	-0.554	2.70E-03
C1orf21	chromosome 1 open reading frame 21	0.554	2.73E-03
C10orf76	chromosome 10 open reading frame 76	-0.554	2.73E-03
NDUFA4	NADH dehydrogenase (ubiquinone) 1 alpha subcomplex, 4, 9kDa	-0.554	2.73E-03
IFT20	intraflagellar transport 20 homolog (Chlamydomonas)	-0.551	2.88E-03
ANKRD45	ankyrin repeat domain 45	-0.549	2.99E-03
DNAJC3	DnaJ (Hsp40) homolog, subfamily C, member 3	-0.549	2.99E-03
LOC100131217	NINP6167	0.547	3.15E-03
CANT1	calcium activated nucleotidase 1	-0.544	3.36E-03
NSUN4	NOP2/Sun domain family, member 4	0.543	3.44E-03
KRTAP21-1	keratin associated protein 21-1	-0.542	3.49E-03
BLVRA	biliverdin reductase A	-0.542	3.53E-03
SNX13	sorting nexin 13	-0.542	3.53E-03
MMP8	matrix metalloproteinase 8 (neutrophil collagenase)	-0.540	3.62E-03
TMEM99	transmembrane protein 99	-0.539	3.71E-03
ICT1	immature colon carcinoma transcript 1	-0.538	3.81E-03
GPC4	glypican 4	0.537	3.86E-03
NCAPG2	non-SMC condensin II complex, subunit G2	0.537	3.90E-03
WSB1	WD repeat and SOCS box-containing 1	-0.536	3.95E-03
ESYT1	extended synaptotagmin-like protein 1	-0.534	4.10E-03
GPRC5C	G protein-coupled receptor, family C, group 5, member C	-0.534	4.10E-03
RHBDL3	rhomboid, veinlet-like 3 (Drosophila)	-0.534	4.15E-03

BMP6	bone morphogenetic protein 6	0.533	4.21E-03
KATNA1	katanin p60 (ATPase-containing) subunit A 1	0.533	4.21E-03
COG1	component of oligomeric golgi complex 1	-0.532	4.26E-03
OR9G1	olfactory receptor, family 9, subfamily G, member 1	0.532	4.26E-03
XPA	xeroderma pigmentosum, complementation group A	-0.532	4.31E-03
CTHF18	CTF18, chromosome transmission fidelity factor 18 homolog (S. cerevisiae)	0.530	4.47E-03
IGFL2	IGF-like family member 2	-0.529	4.53E-03
NUDT13	nudix (nucleoside diphosphate linked moiety X)-type motif 13	-0.529	4.53E-03
RALA	v-ral simian leukemia viral oncogene homolog A (ras related)	-0.529	4.53E-03
JMJD6	jumonji domain containing 6	-0.529	4.58E-03
TBX19	T-box 19	0.529	4.58E-03
EN1	engrailed homeobox 1	0.528	4.64E-03
ZFYVE20	zinc finger, FYVE domain containing 20	0.528	4.64E-03
NFYB	nuclear transcription factor Y, beta	-0.527	4.69E-03
DDX23	DEAD (Asp-Glu-Ala-Asp) box polypeptide 23	-0.527	4.75E-03
NUFIP2	nuclear fragile X mental retardation protein interacting protein 2	-0.527	4.75E-03
CELF2	CUGBP, Elav-like family member 2	0.526	4.81E-03
NAT8L	N-acetyltransferase 8-like (GCN5-related, putative)	0.526	4.87E-03
SDF2	stromal cell-derived factor 2	-0.526	4.87E-03
SLC22A23	solute carrier family 22, member 23	-0.526	4.87E-03
FXYP7	FXYP domain containing ion transport regulator 7	0.525	4.91E-03
QPCTL	glutaminyl-peptide cyclotransferase-like	0.524	5.04E-03
FAH	fumarylacetoacetate hydrolase (fumarylacetoacetase)	-0.524	5.04E-03
MS4A8B	membrane-spanning 4-domains, subfamily A, member 8B	0.524	5.04E-03
CCDC40	coiled-coil domain containing 40	-0.523	5.10E-03
COPZ1	coatamer protein complex, subunit zeta 1	-0.523	5.17E-03
C7orf25	chromosome 7 open reading frame 25	-0.520	5.48E-03
HYAL3	hyaluronoglucosaminidase 3	0.520	5.48E-03
MAX	MYC associated factor X	-0.519	5.55E-03
SPAG5	sperm associated antigen 5	-0.518	5.61E-03
ANKRD28	ankyrin repeat domain 28	0.518	5.68E-03
OPA1	optic atrophy 1 (autosomal dominant)	-0.518	5.68E-03
IRAK1	interleukin-1 receptor-associated kinase 1	0.516	5.81E-03
YLPM1	YLP motif containing 1	-0.516	5.81E-03
SCGB1D4	secretoglobin, family 1D, member 4	-0.516	5.88E-03
TGFB3	transforming growth factor, beta 3	-0.516	5.88E-03
TMEM158	transmembrane protein 158 (gene/pseudogene)	0.515	5.95E-03
ZDHHC18	zinc finger, DHHC-type containing 18	0.515	5.95E-03
FGGY	FGGY carbohydrate kinase domain containing	0.515	6.02E-03
HTR3E	5-hydroxytryptamine (serotonin) receptor 3, family member E	0.515	6.02E-03
KHDRBS3	KH domain containing, RNA binding, signal transduction associated 3	0.512	6.31E-03
NTS	neurotensin	-0.510	6.53E-03
C11orf41	chromosome 11 open reading frame 41	0.510	6.60E-03
DEFB119	defensin, beta 119	0.509	6.64E-03
CACNG7	calcium channel, voltage-dependent, gamma subunit 7	0.509	6.68E-03

NFYC	nuclear transcription factor Y, gamma	-0.509	6.68E-03
OR8J1	olfactory receptor, family 8, subfamily J, member 1	-0.509	6.76E-03
MAP9	microtubule-associated protein 9	-0.508	6.83E-03
MRPL32	mitochondrial ribosomal protein L32	-0.508	6.83E-03
CTNND1	catenin (cadherin-associated protein), delta 1	-0.507	6.99E-03
OR4A5	olfactory receptor, family 4, subfamily A, member 5	0.507	6.99E-03
LAP3	leucine aminopeptidase 3	0.506	7.07E-03
ESRRB	estrogen-related receptor beta	0.506	7.14E-03
C12orf62	chromosome 12 open reading frame 62	-0.505	7.15E-03
SLC6A2	solute carrier family 6 (neurotransmitter transporter, noradrenalin), member 2	0.504	7.32E-03
NR1I3	nuclear receptor subfamily 1, group I, member 3	0.504	7.40E-03
RUFY3	RUN and FYVE domain containing 3	-0.504	7.40E-03
TGIF2LY	TGFB-induced factor homeobox 2-like, Y-linked	-0.504	7.40E-03
UBE2N	ubiquitin-conjugating enzyme E2N (UBC13 homolog, yeast)	-0.504	7.40E-03
NUMBL	numb homolog (Drosophila)-like	0.503	7.48E-03
PPP1CC	protein phosphatase 1, catalytic subunit, gamma isozyme	-0.503	7.48E-03
FAM198B	family with sequence similarity 198, member B	-0.501	7.74E-03
RNF135	ring finger protein 135	-0.501	7.74E-03
B3GNT9	UDP-GlcNAc:betaGal beta-1,3-N-acetylglucosaminyltransferase 9	-0.501	7.82E-03
OR4C6	olfactory receptor, family 4, subfamily C, member 6	0.499	8.08E-03
BAP1	BRCA1 associated protein-1 (ubiquitin carboxy-terminal hydrolase)	0.499	8.09E-03
USO1	USO1 vesicle docking protein homolog (yeast)	-0.499	8.09E-03
RNASEL	ribonuclease L (2',5'-oligoadenylate synthetase-dependent)	-0.498	8.18E-03
SLC25A18	solute carrier family 25 (mitochondrial carrier), member 18	-0.498	8.18E-03
ZZZ3	zinc finger, ZZ-type containing 3	0.498	8.27E-03
GRK6	G protein-coupled receptor kinase 6	0.497	8.36E-03
DPH3	DPH3, KTI11 homolog (S. cerevisiae)	0.496	8.55E-03
MGAT4B	mannosyl (alpha-1,3-)-glycoprotein beta-1,4-N-acetylglucosaminyltransferase, isozyme B	0.496	8.55E-03
TSPAN9	tetraspanin 9	-0.496	8.55E-03
RUNDC1	RUN domain containing 1	-0.495	8.65E-03
TCEB3B	transcription elongation factor B polypeptide 3B (elongin A2)	-0.495	8.65E-03
DOK1	docking protein 1, 62kDa (downstream of tyrosine kinase 1)	0.495	8.74E-03
C6orf168	chromosome 6 open reading frame 168	-0.493	8.92E-03
DBNL	drebrin-like	-0.493	8.93E-03
MRPS7	mitochondrial ribosomal protein S7	-0.493	8.93E-03
GNPDA2	glucosamine-6-phosphate deaminase 2	-0.493	9.03E-03
MAP3K8	mitogen-activated protein kinase kinase kinase 8	0.493	9.03E-03
TCTN1	tectonic family member 1	-0.493	9.03E-03
MAPKSP1	MAPK scaffold protein 1	-0.492	9.13E-03
OR52B4	olfactory receptor, family 52, subfamily B, member 4	0.491	9.23E-03
TNKS1BP1	tankyrase 1 binding protein 1, 182kDa	-0.491	9.33E-03
MON2	MON2 homolog (S. cerevisiae)	-0.490	9.43E-03
TIGD5	tigger transposable element derived 5	0.490	9.43E-03
BLOC1S1	biogenesis of lysosomal organelles complex-1, subunit 1	-0.490	9.54E-03
G3BP2	GTPase activating protein (SH3 domain) binding protein 2	-0.490	9.54E-03

NLRP12	NLR family, pyrin domain containing 12	0.489	9.58E-03
EAF1	ELL associated factor 1	0.489	9.64E-03
LRRFIP1	leucine rich repeat (in FLII) interacting protein 1	-0.489	9.64E-03
CD22	CD22 molecule	0.488	9.74E-03
HCFC2	host cell factor C2	-0.487	1.01E-02
CCNT1	cyclin T1	-0.486	1.02E-02
COX3	cytochrome c oxidase III	-0.485	1.03E-02
ADAP2	ArfGAP with dual PH domains 2	-0.485	1.04E-02
C1orf27	chromosome 1 open reading frame 27	-0.485	1.04E-02
NXPH2	neurexophilin 2	-0.485	1.04E-02
PSTPIP2	proline-serine-threonine phosphatase interacting protein 2	-0.485	1.04E-02
TBK1	TANK-binding kinase 1	-0.485	1.04E-02
SLC39A9	solute carrier family 39 (zinc transporter), member 9	-0.484	1.05E-02
POLDIP2	polymerase (DNA-directed), delta interacting protein 2	-0.484	1.06E-02
ASAH2	N-acylsphingosine amidohydrolase (non-lysosomal ceramidase) 2	0.483	1.07E-02
KCNJ4	potassium inwardly-rectifying channel, subfamily J, member 4	0.483	1.07E-02
ITGAL	integrin, alpha L (antigen CD11A (p180), lymphocyte function-associated antigen 1; alpha polypeptide)	-0.482	1.08E-02
PUS7L	pseudouridylyl synthase 7 homolog (<i>S. cerevisiae</i>)-like	-0.482	1.08E-02
ATP6V1G3	ATPase, H ⁺ transporting, lysosomal 13kDa, V1 subunit G3	-0.482	1.10E-02
MYL6	myosin, light chain 6, alkali, smooth muscle and non-muscle	-0.482	1.10E-02
SLC26A9	solute carrier family 26, member 9	0.481	1.10E-02
CCDC57	coiled-coil domain containing 57	-0.481	1.11E-02
IDE	insulin-degrading enzyme	-0.481	1.11E-02
KLF15	Kruppel-like factor 15	0.481	1.11E-02
KCNAB2	potassium voltage-gated channel, shaker-related subfamily, beta member 2	0.480	1.12E-02
NFKBIE	nuclear factor of kappa light polypeptide gene enhancer in B-cells inhibitor, epsilon	0.480	1.12E-02
USP53	ubiquitin specific peptidase 53	-0.480	1.12E-02
KAZ	kazrin	0.480	1.13E-02
LAT	linker for activation of T cells	0.480	1.13E-02
LRRIQ1	leucine-rich repeats and IQ motif containing 1	-0.480	1.13E-02
RNF220	ring finger protein 220	0.480	1.13E-02
ND5	NADH dehydrogenase, subunit 5 (complex I)	-0.479	1.14E-02
OR52K1	olfactory receptor, family 52, subfamily K, member 1	-0.479	1.14E-02
OR8K3	olfactory receptor, family 8, subfamily K, member 3	-0.479	1.14E-02
RANBP17	RAN binding protein 17	0.479	1.14E-02
CHRNA4	cholinergic receptor, nicotinic, alpha 4	-0.479	1.15E-02
FLJ46026	FLJ46026 protein	-0.479	1.16E-02
GOLGA6L1	golgin A6 family-like 1	-0.479	1.16E-02
LMLN	leishmanolysin-like (metallopeptidase M8 family)	-0.479	1.16E-02
RAB5C	RAB5C, member RAS oncogene family	-0.479	1.16E-02
STARD3	StAR-related lipid transfer (START) domain containing 3	-0.479	1.16E-02
SLC25A3	solute carrier family 25 (mitochondrial carrier; phosphate carrier), member 3	-0.478	1.17E-02
NFYB	nuclear transcription factor Y, beta	-0.478	1.17E-02
RAB5B	RAB5B, member RAS oncogene family	-0.477	1.18E-02

IFRD1	interferon-related developmental regulator 1	0.477	1.19E-02
KPNA5	karyopherin alpha 5 (importin alpha 6)	0.477	1.19E-02
KRTAP15-1	keratin associated protein 15-1	-0.477	1.19E-02
RASGRP1	RAS guanyl releasing protein 1 (calcium and DAG-regulated)	0.477	1.19E-02
TOMM20L	translocase of outer mitochondrial membrane 20 homolog (yeast)-like	-0.477	1.19E-02
FANCA	Fanconi anemia, complementation group A	0.476	1.20E-02
GNA11	guanine nucleotide binding protein (G protein), alpha 11 (Gq class)	-0.476	1.20E-02
SUPT6H	suppressor of Ty 6 homolog (S. cerevisiae)	-0.476	1.20E-02
PECI	peroxisomal D3,D2-enoyl-CoA isomerase	-0.476	1.22E-02
GPR35	G protein-coupled receptor 35	0.475	1.23E-02
MGAT4C	mannosyl (alpha-1,3-)-glycoprotein beta-1,4-N-acetylglucosaminyltransferase, isozyme C (putative)	-0.475	1.23E-02
PSPN	persephin	-0.475	1.23E-02
TM9SF3	transmembrane 9 superfamily member 3	-0.475	1.23E-02
C1orf182	chromosome 1 open reading frame 182	0.474	1.24E-02
APAF1	apoptotic peptidase activating factor 1	-0.474	1.24E-02
FZD8	frizzled homolog 8 (Drosophila)	0.474	1.24E-02
C12orf48	chromosome 12 open reading frame 48	-0.474	1.26E-02
TMBIM4	transmembrane BAX inhibitor motif containing 4	-0.474	1.26E-02
COL9A2	collagen, type IX, alpha 2	-0.473	1.27E-02
FRS3	fibroblast growth factor receptor substrate 3	0.473	1.28E-02
DGAT2	diacylglycerol O-acyltransferase 2	0.472	1.29E-02
CCDC65	coiled-coil domain containing 65	-0.472	1.29E-02
MGC16703	tubulin, alpha pseudogene	-0.471	1.31E-02
TAF10	TAF10 RNA polymerase II, TATA box binding protein (TBP)-associated factor, 30kDa	-0.471	1.31E-02
LARP6	La ribonucleoprotein domain family, member 6	0.471	1.32E-02
CCDC28A	coiled-coil domain containing 28A	0.470	1.34E-02
FANCG	Fanconi anemia, complementation group G	0.470	1.35E-02
EPHB1	EPH receptor B1	0.469	1.35E-02
DCT	dopachrome tautomerase (dopachrome delta-isomerase, tyrosine-related protein 2)	0.469	1.36E-02
C14orf156	chromosome 14 open reading frame 156	-0.468	1.38E-02
GATAD2A	GATA zinc finger domain containing 2A	0.468	1.38E-02
MLPH	melanophilin	-0.468	1.38E-02
NUDT4	nudix (nucleoside diphosphate linked moiety X)-type motif 4	-0.468	1.38E-02
PIP4K2B	phosphatidylinositol-5-phosphate 4-kinase, type II, beta	-0.468	1.38E-02
IFT88	intraflagellar transport 88 homolog (Chlamydomonas)	-0.468	1.39E-02
SLC7A10	solute carrier family 7, (neutral amino acid transporter, y+ system) member 10	-0.468	1.39E-02
CXorf23	chromosome X open reading frame 23	-0.467	1.40E-02
HMOX2	heme oxygenase (decycling) 2	-0.467	1.40E-02
TMEM135	transmembrane protein 135	-0.467	1.40E-02
MRS2	MRS2 magnesium homeostasis factor homolog (S. cerevisiae)	-0.466	1.42E-02
SP1	Sp1 transcription factor	-0.466	1.42E-02
CALML4	calmodulin-like 4	0.466	1.43E-02
GPBP1L1	GC-rich promoter binding protein 1-like 1	0.466	1.43E-02

USP15	ubiquitin specific peptidase 15	-0.465	1.45E-02
ZNF438	zinc finger protein 438	0.465	1.45E-02
MT1X	metallothionein 1X	0.465	1.46E-02
C1orf59	chromosome 1 open reading frame 59	0.465	1.46E-02
DKK4	dickkopf homolog 4 (<i>Xenopus laevis</i>)	-0.465	1.46E-02
STIL	SCL/TAL1 interrupting locus	0.465	1.46E-02
C17orf56	chromosome 17 open reading frame 56	-0.464	1.48E-02
C7orf36	chromosome 7 open reading frame 36	-0.464	1.48E-02
COQ6	coenzyme Q6 homolog, monooxygenase (<i>S. cerevisiae</i>)	-0.464	1.48E-02
SDR16C5	short chain dehydrogenase/reductase family 16C, member 5	-0.464	1.48E-02
NOX4	NADPH oxidase 4	-0.464	1.48E-02
EHHADH	enoyl-CoA, hydratase/3-hydroxyacyl CoA dehydrogenase	-0.463	1.49E-02
FAM104B	family with sequence similarity 104, member B	-0.463	1.49E-02
GGA3	golgi-associated, gamma adaptin ear containing, ARF binding protein 3	-0.463	1.49E-02
KIAA0391	KIAA0391	-0.463	1.49E-02
MUTYH	mutY homolog (<i>E. coli</i>)	0.463	1.49E-02
HVCN1	hydrogen voltage-gated channel 1	-0.463	1.51E-02
SPG21	spastic paraplegia 21 (autosomal recessive, Mast syndrome)	0.463	1.51E-02
ATP2A2	ATPase, Ca ⁺⁺ transporting, cardiac muscle, slow twitch 2	-0.463	1.51E-02
FOS	FBJ murine osteosarcoma viral oncogene homolog	0.463	1.51E-02
SLC45A2	solute carrier family 45, member 2	0.463	1.51E-02
MUSTN1	musculoskeletal, embryonic nuclear protein 1	0.462	1.52E-02
ISCA2	iron-sulfur cluster assembly 2 homolog (<i>S. cerevisiae</i>)	-0.462	1.54E-02
SEC62	SEC62 homolog (<i>S. cerevisiae</i>)	-0.462	1.54E-02
SEL1L	sel-1 suppressor of lin-12-like (<i>C. elegans</i>)	-0.462	1.54E-02
SOLH	small optic lobes homolog (<i>Drosophila</i>)	0.462	1.54E-02
C3orf17	chromosome 3 open reading frame 17	0.461	1.55E-02
TMEM217	transmembrane protein 217	0.461	1.55E-02
IRAK4	interleukin-1 receptor-associated kinase 4	-0.460	1.57E-02
PLEKHJ1	pleckstrin homology domain containing, family J member 1	-0.460	1.57E-02
ALKBH1	alkB, alkylation repair homolog 1 (<i>E. coli</i>)	-0.460	1.58E-02
PFDN5	prefoldin subunit 5	-0.460	1.58E-02
RPAP3	RNA polymerase II associated protein 3	-0.460	1.58E-02
STOML2	stomatin (EPB72)-like 2	0.460	1.58E-02
TSPAN31	tetraspanin 31	-0.460	1.58E-02
ZFYVE28	zinc finger, FYVE domain containing 28	0.460	1.58E-02
SLC24A2	solute carrier family 24 (sodium/potassium/calcium exchanger), member 2	0.459	1.59E-02
HS6ST2	heparan sulfate 6-O-sulfotransferase 2	0.459	1.60E-02
ARHGEF7	Rho guanine nucleotide exchange factor (GEF) 7	-0.458	1.62E-02
ASB8	ankyrin repeat and SOCS box-containing 8	-0.458	1.62E-02
ATP5B	ATP synthase, H ⁺ transporting, mitochondrial F1 complex, beta polypeptide	-0.458	1.62E-02
MC2R	melanocortin 2 receptor (adrenocorticotrophic hormone)	-0.458	1.62E-02
SRF	serum response factor (c-fos serum response element-binding transcription factor)	0.458	1.62E-02
NAALAD2	N-acetylated alpha-linked acidic dipeptidase 2	-0.458	1.62E-02
CYP1A1	cytochrome P450, family 1, subfamily A, polypeptide 1	0.458	1.63E-02

LASP1	LIM and SH3 protein 1	-0.458	1.63E-02
PSMD3	proteasome (prosome, macropain) 26S subunit, non-ATPase, 3	-0.458	1.63E-02
TMEM204	transmembrane protein 204	0.458	1.63E-02
FAM127B	family with sequence similarity 127, member B	0.457	1.65E-02
RPTOR	regulatory associated protein of MTOR, complex 1	-0.457	1.65E-02
SMARCE1	SWI/SNF related, matrix associated, actin dependent regulator of chromatin, subfamily e, member 1	-0.457	1.65E-02
TM9SF2	transmembrane 9 superfamily member 2	-0.457	1.66E-02
ALKBH5	alkB, alkylation repair homolog 5 (E. coli)	0.456	1.68E-02
DNM2	dynamamin 2	0.456	1.68E-02
NCBP2	nuclear cap binding protein subunit 2, 20kDa	-0.456	1.68E-02
PLSCR2	phospholipid scramblase 2	0.456	1.68E-02
PRKAR1A	protein kinase, cAMP-dependent, regulatory, type I, alpha (tissue specific extinguisher 1)	-0.456	1.68E-02
ADAMTS9	ADAM metalloproteinase with thrombospondin type 1 motif, 9	0.455	1.70E-02
CLEC11A	C-type lectin domain family 11, member A	-0.455	1.71E-02
PCLO	piccolo (presynaptic cytomatrix protein)	-0.455	1.71E-02
SLC30A9	solute carrier family 30 (zinc transporter), member 9	-0.455	1.71E-02
EEPDI	endonuclease/exonuclease/phosphatase family domain containing 1	0.454	1.73E-02
AMBP	alpha-1-microglobulin/bikunin precursor	-0.454	1.73E-02
OR4N5	olfactory receptor, family 4, subfamily N, member 5	-0.454	1.73E-02
TGFBR1	transforming growth factor, beta receptor 1	-0.454	1.73E-02
UBE2CBP	ubiquitin-conjugating enzyme E2C binding protein	0.454	1.73E-02
HDAC1	histone deacetylase 1	0.454	1.75E-02
MGAT5	mannosyl (alpha-1,6-)-glycoprotein beta-1,6-N-acetylglucosaminyltransferase	0.454	1.75E-02
OXER1	oxoeicosanoid (OXE) receptor 1	0.454	1.75E-02
JRK	jerky homolog (mouse)	0.453	1.77E-02
LSM4 // LSM4	LSM4 homolog, U6 small nuclear RNA associated (S. cerevisiae) // LSM4 homolog, U6 small nuclear RNA associated (S. cerevisiae)	0.453	1.77E-02
PIGG	phosphatidylinositol glycan anchor biosynthesis, class G	-0.453	1.77E-02
C17orf62	chromosome 17 open reading frame 62	-0.452	1.78E-02
GABRP	gamma-aminobutyric acid (GABA) A receptor, pi	0.452	1.78E-02
OXNAD1	oxidoreductase NAD-binding domain containing 1	0.452	1.78E-02
PLEKHA8	pleckstrin homology domain containing, family A (phosphoinositide binding specific) member 8	-0.452	1.78E-02
PAPLN	papilin, proteoglycan-like sulfated glycoprotein	-0.452	1.80E-02
CCDC55	coiled-coil domain containing 55	0.452	1.80E-02
GTDC1	glycosyltransferase-like domain containing 1	0.452	1.80E-02
NDUFA12	NADH dehydrogenase (ubiquinone) 1 alpha subcomplex, 12	-0.452	1.80E-02
PGPEP1	pyroglutamyl-peptidase I	0.452	1.80E-02
PRTFDC1	phosphoribosyl transferase domain containing 1	0.452	1.80E-02
TAF1A	TATA box binding protein (TBP)-associated factor, RNA polymerase I, A, 48kDa	0.452	1.80E-02
GCDH	glutaryl-CoA dehydrogenase	0.452	1.81E-02
CDT1	chromatin licensing and DNA replication factor 1	0.451	1.82E-02
ABHD13	abhydrolase domain containing 13	-0.451	1.82E-02

DDX53	DEAD (Asp-Glu-Ala-Asp) box polypeptide 53	-0.451	1.82E-02
SEC62	SEC62 homolog (<i>S. cerevisiae</i>)	-0.451	1.82E-02
EXOC7	exocyst complex component 7	-0.451	1.84E-02
SNAPIN	SNAP-associated protein	-0.451	1.84E-02
PGAP3	post-GPI attachment to proteins 3	-0.450	1.85E-02
PRPF38A	PRP38 pre-mRNA processing factor 38 (yeast) domain containing A	0.450	1.85E-02
SERTAD2	SERTA domain containing 2	0.450	1.85E-02
NPR1	natriuretic peptide receptor A/guanylate cyclase A (atriuretic peptide receptor A)	0.449	1.87E-02
DGKZ	diacylglycerol kinase, zeta 104kDa	-0.449	1.87E-02
DLST	dihydrolipoamide S-succinyltransferase (E2 component of 2-oxo-glutarate complex)	-0.449	1.87E-02
FRMD3	FERM domain containing 3	0.449	1.87E-02
FOXQ1	forkhead box Q1	0.449	1.89E-02
SMARCD1	SWI/SNF related, matrix associated, actin dependent regulator of chromatin, subfamily d, member 1	-0.449	1.89E-02
TNRC6C	trinucleotide repeat containing 6C	-0.449	1.89E-02
DIXDC1	DIX domain containing 1	-0.448	1.91E-02
GPAT2	glycerol-3-phosphate acyltransferase 2, mitochondrial	0.448	1.91E-02
C9orf68	chromosome 9 open reading frame 68	-0.447	1.93E-02
DSTN	destrin (actin depolymerizing factor)	-0.447	1.93E-02
FOXN1	forkhead box N1	-0.447	1.93E-02
GPR101	G protein-coupled receptor 101	-0.447	1.93E-02
LEMD3	LEM domain containing 3	-0.447	1.93E-02
TNFRSF21	tumor necrosis factor receptor superfamily, member 21	0.447	1.93E-02
DEFB127	defensin, beta 127	-0.447	1.94E-02
ADD2	adducin 2 (beta)	0.447	1.94E-02
OR1Q1	olfactory receptor, family 1, subfamily Q, member 1	0.447	1.94E-02
SAMD1	sterile alpha motif domain containing 1	0.447	1.94E-02
CPSF1	cleavage and polyadenylation specific factor 1, 160kDa	0.446	1.96E-02
TRIM3	tripartite motif-containing 3	-0.446	1.96E-02
ADAD1	adenosine deaminase domain containing 1 (testis-specific)	0.445	2.00E-02
CNKSR3	CNKSR family member 3	0.445	2.00E-02
AGAP3	ArfGAP with GTPase domain, ankyrin repeat and PH domain 3	0.444	2.02E-02
ERAL1	Era G-protein-like 1 (<i>E. coli</i>)	-0.444	2.02E-02
RNASE8	ribonuclease, RNase A family, 8	0.444	2.04E-02
SERPINB7	serpin peptidase inhibitor, clade B (ovalbumin), member 7	0.444	2.04E-02
SHOC2	soc-2 suppressor of clear homolog (<i>C. elegans</i>)	-0.444	2.04E-02
CHURC1	churchill domain containing 1	-0.444	2.05E-02
SLC46A2	solute carrier family 46, member 2	-0.443	2.06E-02
SMURF1	SMAD specific E3 ubiquitin protein ligase 1	0.443	2.06E-02
TTC15	tetratricopeptide repeat domain 15	-0.443	2.06E-02
CLIC5	chloride intracellular channel 5	0.443	2.08E-02
ABCD4	ATP-binding cassette, sub-family D (ALD), member 4	-0.443	2.08E-02
PCCA	propionyl CoA carboxylase, alpha polypeptide	-0.443	2.08E-02
MATN1	matrilin 1, cartilage matrix protein	0.442	2.09E-02
C2orf52	chromosome 2 open reading frame 52	0.442	2.10E-02

C7orf53	chromosome 7 open reading frame 53	0.442	2.10E-02
ADAM7	ADAM metallopeptidase domain 7	0.441	2.12E-02
SLCO4A1	solute carrier organic anion transporter family, member 4A1	0.441	2.12E-02
ZNF540	zinc finger protein 540	-0.441	2.12E-02
PPP1R8	protein phosphatase 1, regulatory (inhibitor) subunit 8	0.441	2.13E-02
GPS1	G protein pathway suppressor 1	-0.441	2.14E-02
MRPL27	mitochondrial ribosomal protein L27	-0.441	2.14E-02
C12orf36	chromosome 12 open reading frame 36	0.440	2.16E-02
DAZAP2	DAZ associated protein 2	-0.440	2.16E-02
FAF1	Fas (TNFRSF6) associated factor 1	0.440	2.16E-02
DNAJC10	DnaJ (Hsp40) homolog, subfamily C, member 10	-0.440	2.18E-02
HLA-DRA	major histocompatibility complex, class II, DR alpha	0.440	2.18E-02
PARP6	poly (ADP-ribose) polymerase family, member 6	0.440	2.18E-02
ZNF702P	zinc finger protein 702, pseudogene	-0.440	2.18E-02
SLC28A2	solute carrier family 28 (sodium-coupled nucleoside transporter), member 2	-0.439	2.19E-02
CDK17	cyclin-dependent kinase 17	-0.439	2.20E-02
KRTAP16-1	keratin associated protein 16-1	-0.439	2.20E-02
TECPR2	tectonin beta-propeller repeat containing 2	-0.439	2.20E-02
BMPR1A	bone morphogenetic protein receptor, type IA	-0.438	2.22E-02
EEA1	early endosome antigen 1	-0.438	2.22E-02
LGR4	leucine-rich repeat-containing G protein-coupled receptor 4	-0.438	2.22E-02
PLA2G4E	phospholipase A2, group IVE	-0.438	2.22E-02
PIP	prolactin-induced protein	-0.438	2.24E-02
RACGAP1P	Rac GTPase activating protein 1 pseudogene	-0.438	2.24E-02
REEP3	receptor accessory protein 3	-0.438	2.24E-02
SLC41A2	solute carrier family 41, member 2	-0.438	2.24E-02
SNRNP48	small nuclear ribonucleoprotein 48kDa (U11/U12)	0.438	2.24E-02
ST6GALNAC5	ST6 (alpha-N-acetyl-neuraminy1-2,3-beta-galactosyl-1,3)-N-acetylgalactosaminide alpha-2,6-sialyltransferase 5	0.437	2.26E-02
TOP1MT	topoisomerase (DNA) I, mitochondrial	0.437	2.26E-02
TAS2R38	taste receptor, type 2, member 38	0.436	2.30E-02
LRRTM3	leucine rich repeat transmembrane neuronal 3	-0.435	2.33E-02
MRPL38	mitochondrial ribosomal protein L38	-0.435	2.33E-02
TAF6	TAF6 RNA polymerase II, TATA box binding protein (TBP)-associated factor, 80kDa	0.435	2.33E-02
YIPF2	Yip1 domain family, member 2	0.435	2.33E-02
HPX	hemopexin	-0.435	2.35E-02
ASTN1	astrotactin 1	0.434	2.36E-02
ARFIP2	ADP-ribosylation factor interacting protein 2	-0.434	2.37E-02
KCTD2	potassium channel tetramerisation domain containing 2	-0.434	2.37E-02
MASTL	microtubule associated serine/threonine kinase-like	0.434	2.37E-02
PARK7	Parkinson disease (autosomal recessive, early onset) 7	-0.434	2.37E-02
SYAP1	synapse associated protein 1	-0.434	2.37E-02
NCOA7	nuclear receptor coactivator 7	0.433	2.39E-02
ORMDL3	ORM1-like 3 (S. cerevisiae)	-0.433	2.39E-02
TRAK1	trafficking protein, kinesin binding 1	0.433	2.39E-02
EXD1	exonuclease 3'-5' domain containing 1	-0.433	2.41E-02

FLJ35220	hypothetical protein FLJ35220	-0.433	2.41E-02
RNF26	ring finger protein 26	0.433	2.41E-02
C19orf70	chromosome 19 open reading frame 70	-0.432	2.43E-02
CDK13	cyclin-dependent kinase 13	-0.432	2.43E-02
VPS13D	vacuolar protein sorting 13 homolog D (S. cerevisiae)	-0.432	2.44E-02
BCL2	B-cell CLL/lymphoma 2	0.432	2.46E-02
FLJ42393	hypothetical LOC401105	0.432	2.46E-02
LTN1	listerin E3 ubiquitin protein ligase 1	-0.432	2.46E-02
PAPOLA	poly(A) polymerase alpha	-0.432	2.46E-02
TDPI	tyrosyl-DNA phosphodiesterase 1	-0.432	2.46E-02
ANKH	ankylosis, progressive homolog (mouse)	0.431	2.48E-02
OR56A4	olfactory receptor, family 56, subfamily A, member 4	0.431	2.48E-02
REV3L	REV3-like, catalytic subunit of DNA polymerase zeta (yeast)	0.431	2.48E-02
SLC25A13	solute carrier family 25, member 13 (citrin)	-0.431	2.48E-02
CACHD1	cache domain containing 1	0.430	2.50E-02
C10orf116	chromosome 10 open reading frame 116	-0.430	2.50E-02
C1orf64	chromosome 1 open reading frame 64	-0.430	2.50E-02
DHRS7	dehydrogenase/reductase (SDR family) member 7	-0.430	2.50E-02
RARB	retinoic acid receptor, beta	0.430	2.50E-02
SOX18	SRY (sex determining region Y)-box 18	-0.430	2.50E-02
C6orf25	chromosome 6 open reading frame 25	0.430	2.51E-02
OK/SW-CL.58	OK/SW-CL.58	0.430	2.51E-02
HSPA6	heat shock 70kDa protein 6 (HSP70B')	0.430	2.53E-02
AKIRIN2	akirin 2	0.429	2.55E-02
SNAP23	synaptosomal-associated protein, 23kDa	-0.429	2.55E-02
GZMK	granzyme K (granzyme 3; tryptase II)	0.429	2.57E-02
MAP3K3	mitogen-activated protein kinase kinase kinase 3	-0.429	2.57E-02
RRP8	ribosomal RNA processing 8, methyltransferase, homolog (yeast)	-0.429	2.57E-02
SOD2	superoxide dismutase 2, mitochondrial	0.429	2.57E-02
SYNJ2	synaptojanin 2	0.429	2.57E-02
TDG	thymine-DNA glycosylase	-0.429	2.57E-02
DEFB125	defensin, beta 125	-0.428	2.60E-02
MAPK12	mitogen-activated protein kinase 12	0.428	2.60E-02
SERBP1	SERPINE1 mRNA binding protein 1	0.428	2.60E-02
MYOZ2	myozenin 2	0.428	2.60E-02
C8orf34	chromosome 8 open reading frame 34	-0.427	2.62E-02
PNPLA4	patatin-like phospholipase domain containing 4	-0.427	2.62E-02
SSBP2	single-stranded DNA binding protein 2	-0.427	2.62E-02
VEZT	vezatin, adherens junctions transmembrane protein	-0.427	2.62E-02
ZMYM6	zinc finger, MYM-type 6	0.427	2.62E-02
ZNF707	zinc finger protein 707	0.427	2.62E-02
NUBPL // NUBPL	nucleotide binding protein-like // nucleotide binding protein-like	-0.427	2.64E-02
OAZ1	ornithine decarboxylase antizyme 1	-0.427	2.64E-02
KDM6A	lysine (K)-specific demethylase 6A	-0.426	2.67E-02
SLC4A4	solute carrier family 4, sodium bicarbonate cotransporter, member 4	0.426	2.68E-02

LRRC20	leucine rich repeat containing 20	0.426	2.69E-02
TRMT2B	TRM2 tRNA methyltransferase 2 homolog B (<i>S. cerevisiae</i>)	0.426	2.69E-02
CTDSP2	CTD (carboxy-terminal domain, RNA polymerase II, polypeptide A) small phosphatase 2	-0.425	2.72E-02
MEF2C	myocyte enhancer factor 2C	0.425	2.72E-02
PSCA	prostate stem cell antigen	-0.425	2.72E-02
RG9MTD2	RNA (guanine-9-) methyltransferase domain containing 2	-0.425	2.72E-02
CYP3A43	cytochrome P450, family 3, subfamily A, polypeptide 43	0.424	2.75E-02
ARID5A	AT rich interactive domain 5A (MRF1-like)	0.424	2.76E-02
C17orf101	chromosome 17 open reading frame 101	-0.424	2.76E-02
GPR173	G protein-coupled receptor 173	0.424	2.76E-02
IFT81	intraflagellar transport 81 homolog (<i>Chlamydomonas</i>)	-0.424	2.76E-02
IL18R1	interleukin 18 receptor 1	0.424	2.76E-02
IL1F9	interleukin 1 family, member 9	0.424	2.76E-02
KRT33B	keratin 33B	0.424	2.76E-02
NCKIPSD	NCK interacting protein with SH3 domain	0.424	2.76E-02
ND4	NADH dehydrogenase, subunit 4 (complex I)	-0.424	2.76E-02
ZNF491	zinc finger protein 491	-0.424	2.76E-02
C9orf125	chromosome 9 open reading frame 125	-0.423	2.79E-02
B4GALT7	xylosylprotein beta 1,4-galactosyltransferase, polypeptide 7 (galactosyltransferase I)	0.423	2.79E-02
FGFR3	fibroblast growth factor receptor 3	-0.423	2.79E-02
NEURL3	neuralized homolog 3 (<i>Drosophila</i>) pseudogene	0.423	2.79E-02
OR10G4	olfactory receptor, family 10, subfamily G, member 4	-0.423	2.79E-02
OR5AN1	olfactory receptor, family 5, subfamily AN, member 1	-0.423	2.79E-02
TSNAXIP1	translin-associated factor X interacting protein 1	-0.423	2.79E-02
C1orf228	chromosome 1 open reading frame 228	0.422	2.81E-02
ACER1	alkaline ceramidase 1	-0.422	2.81E-02
LOC100129726	hypothetical LOC100129726	0.422	2.81E-02
MTERFD3	MTERF domain containing 3	-0.422	2.81E-02
TMEM184C	transmembrane protein 184C	-0.422	2.81E-02
FOXC2	forkhead box C2 (MFH-1, mesenchyme forkhead 1)	0.422	2.84E-02
SENPI	SUMO1/sentrin specific peptidase 1	-0.422	2.84E-02
SLC7A13	solute carrier family 7, (cationic amino acid transporter, y ⁺ system) member 13	-0.422	2.84E-02
ZFAND2B	zinc finger, AN1-type domain 2B	0.422	2.84E-02
ZNF276	zinc finger protein 276	0.422	2.84E-02
ANO4	anoctamin 4	-0.422	2.85E-02
CNNM1	cyclin M1	0.421	2.87E-02
CCDC56	coiled-coil domain containing 56	-0.421	2.87E-02
LIMA1	LIM domain and actin binding 1	-0.421	2.87E-02
WDR54	WD repeat domain 54	0.421	2.87E-02
AOAH	acyloxyacyl hydrolase (neutrophil)	-0.421	2.88E-02
C3orf26	chromosome 3 open reading frame 26	0.421	2.89E-02
ZNF555	zinc finger protein 555	-0.421	2.89E-02
BST1	bone marrow stromal cell antigen 1	0.420	2.92E-02
FBXL20	F-box and leucine-rich repeat protein 20	-0.420	2.92E-02
IARS2	isoleucyl-tRNA synthetase 2, mitochondrial	-0.420	2.92E-02

PLCG2	phospholipase C, gamma 2 (phosphatidylinositol-specific)	0.420	2.92E-02
POLR1E	polymerase (RNA) I polypeptide E, 53kDa	0.420	2.92E-02
RUNX1	runt-related transcription factor 1	0.420	2.92E-02
TMEM169	transmembrane protein 169	0.420	2.92E-02
ZFYVE21	zinc finger, FYVE domain containing 21	-0.420	2.92E-02
ZNF266	zinc finger protein 266	-0.420	2.92E-02
C17orf106	chromosome 17 open reading frame 106	-0.419	2.94E-02
CSNK1D	casein kinase 1, delta	-0.419	2.94E-02
FAM104A	family with sequence similarity 104, member A	-0.419	2.94E-02
MAP2K3	mitogen-activated protein kinase kinase 3	0.419	2.94E-02
PCYT1A	phosphate cytidylyltransferase 1, choline, alpha	-0.419	2.94E-02
SRSF6	serine/arginine-rich splicing factor 6	-0.419	2.94E-02
SSTR2	somatostatin receptor 2	-0.419	2.94E-02
MMD2	monocyte to macrophage differentiation-associated 2	0.419	2.95E-02
OTUB2	OTU domain, ubiquitin aldehyde binding 2	-0.419	2.97E-02
RPL23AP32	ribosomal protein L23a pseudogene 32	0.419	2.97E-02
SCAMP4	secretory carrier membrane protein 4	-0.419	2.97E-02
TSPAN9	tetraspanin 9	-0.419	2.97E-02
ACBD5	acyl-CoA binding domain containing 5	0.418	2.99E-02
KIAA1161	KIAA1161	-0.418	2.99E-02
TRIP11	thyroid hormone receptor interactor 11	-0.418	2.99E-02
YTHDF2	YTH domain family, member 2	0.418	2.99E-02
ABCG5	ATP-binding cassette, sub-family G (WHITE), member 5	0.418	3.01E-02
DNAH3	dynein, axonemal, heavy chain 3	-0.418	3.02E-02
CDK18	cyclin-dependent kinase 18	0.418	3.02E-02
CUL3	cullin 3	-0.418	3.02E-02
FUT5	fucosyltransferase 5 (alpha (1,3) fucosyltransferase)	0.418	3.02E-02
PIH1D2	PIH1 domain containing 2	-0.418	3.02E-02
THAP10	THAP domain containing 10	0.418	3.02E-02
TOMM7 // TOMM7	translocase of outer mitochondrial membrane 7 homolog (yeast) // translocase of outer mitochondrial membrane 7 homolog (yeast)	-0.418	3.02E-02
MMRN2	multimerin 2	-0.417	3.05E-02
PRDM9	PR domain containing 9	0.417	3.05E-02
ARHGEF10	Rho guanine nucleotide exchange factor (GEF) 10	0.416	3.08E-02
FCGRT	Fc fragment of IgG, receptor, transporter, alpha	-0.416	3.08E-02
NAT9	N-acetyltransferase 9 (GCN5-related, putative)	-0.416	3.08E-02
RGS7	regulator of G-protein signaling 7	0.416	3.08E-02
NADK	NAD kinase	0.416	3.09E-02
TRPC7	transient receptor potential cation channel, subfamily C, member 7	0.416	3.09E-02
C17orf80	chromosome 17 open reading frame 80	-0.416	3.10E-02
RAB3IL1	RAB3A interacting protein (rabin3)-like 1	0.416	3.10E-02
AGAP11	ankyrin repeat and GTPase domain Arf GTPase activating protein 11	-0.415	3.13E-02
C19orf25	chromosome 19 open reading frame 25	-0.415	3.13E-02
GSTZ1	glutathione transferase zeta 1	-0.415	3.13E-02
TBX20	T-box 20	0.415	3.13E-02

TEKT1	tektin 1	-0.415	3.13E-02
PGLYRP4	peptidoglycan recognition protein 4	0.415	3.14E-02
IPCEF1	interaction protein for cytohesin exchange factors 1	0.415	3.16E-02
TEX9	testis expressed 9	-0.415	3.16E-02
TMCC2	transmembrane and coiled-coil domain family 2	0.415	3.16E-02
TSHZ2	teashirt zinc finger homeobox 2	0.415	3.16E-02
ZNF44	zinc finger protein 44	-0.415	3.16E-02
ANXA10	annexin A10	0.414	3.17E-02
C17orf39	chromosome 17 open reading frame 39	0.414	3.18E-02
ADAM29	ADAM metallopeptidase domain 29	-0.414	3.18E-02
C14orf43	chromosome 14 open reading frame 43	-0.414	3.18E-02
EYA4	eyes absent homolog 4 (Drosophila)	0.414	3.18E-02
PSMB3	proteasome (prosome, macropain) subunit, beta type, 3	-0.414	3.18E-02
RCOR1	REST corepressor 1	-0.414	3.18E-02
SGPP1	sphingosine-1-phosphate phosphatase 1	-0.414	3.18E-02
SIN3B	SIN3 homolog B, transcription regulator (yeast)	0.414	3.18E-02
ZNF615	zinc finger protein 615	-0.414	3.18E-02
C20orf108	chromosome 20 open reading frame 108	-0.413	3.21E-02
FAM8A1	family with sequence similarity 8, member A1	-0.413	3.21E-02
LRRC42	leucine rich repeat containing 42	0.413	3.21E-02
PTK2	PTK2 protein tyrosine kinase 2	0.413	3.21E-02
RCHY1	ring finger and CHY zinc finger domain containing 1	-0.413	3.21E-02
TAOK1	TAO kinase 1	-0.413	3.21E-02
LRRC18	leucine rich repeat containing 18	0.413	3.24E-02
C11orf87	chromosome 11 open reading frame 87	-0.413	3.24E-02
ERN2	endoplasmic reticulum to nucleus signaling 2	-0.413	3.24E-02
CRCT1	cysteine-rich C-terminal 1	0.412	3.27E-02
PNMA2	paraneoplastic antigen MA2	0.412	3.27E-02
TM4SF1	transmembrane 4 L six family member 1	0.412	3.27E-02
ABRA	actin-binding Rho activating protein	0.411	3.30E-02
IMMP1L	IMP1 inner mitochondrial membrane peptidase-like (S. cerevisiae)	-0.411	3.30E-02
PPIL2	peptidylprolyl isomerase (cyclophilin)-like 2	-0.411	3.30E-02
TMCO1	transmembrane and coiled-coil domains 1	-0.411	3.30E-02
TRIM68	tripartite motif-containing 68	-0.411	3.30E-02
TRIML1	tripartite motif family-like 1	0.411	3.30E-02
ASF1A	ASF1 anti-silencing function 1 homolog A (S. cerevisiae)	0.411	3.33E-02
ASNS	asparagine synthetase (glutamine-hydrolyzing)	0.411	3.33E-02
CCDC3	coiled-coil domain containing 3	0.411	3.33E-02
GUK1	guanylate kinase 1	-0.411	3.33E-02
MCM2	minichromosome maintenance complex component 2	0.411	3.33E-02
RETSAT	retinol saturase (all-trans-retinol 13,14-reductase)	-0.411	3.33E-02
ITK	IL2-inducible T-cell kinase	0.411	3.34E-02
C18orf34	chromosome 18 open reading frame 34	-0.411	3.34E-02
TRPM6	transient receptor potential cation channel, subfamily M, member 6	0.411	3.34E-02
ACAT2	acetyl-CoA acetyltransferase 2	0.410	3.35E-02
CMPK1	cytidine monophosphate (UMP-CMP) kinase 1, cytosolic	0.410	3.35E-02

EPHX1	epoxide hydrolase 1, microsomal (xenobiotic)	-0.410	3.35E-02
GRM2	glutamate receptor, metabotropic 2	0.410	3.35E-02
HNRNPA1	heterogeneous nuclear ribonucleoprotein A1	-0.410	3.35E-02
PRPF38B	PRP38 pre-mRNA processing factor 38 (yeast) domain containing B	0.410	3.35E-02
RCC1	regulator of chromosome condensation 1	0.410	3.35E-02
ZDHHC15	zinc finger, DHHC-type containing 15	-0.410	3.35E-02
ZNF92	zinc finger protein 92	-0.409	3.40E-02
PUM1	pumilio homolog 1 (Drosophila)	0.409	3.41E-02
ATXN2	ataxin 2	-0.409	3.41E-02
OR1L3	olfactory receptor, family 1, subfamily L, member 3	-0.409	3.41E-02
TACO1	translational activator of mitochondrially encoded cytochrome c oxidase I	-0.409	3.41E-02
PAX5	paired box 5	0.409	3.42E-02
C4orf17	chromosome 4 open reading frame 17	0.408	3.44E-02
C9orf11	chromosome 9 open reading frame 11	-0.408	3.44E-02
RAP2A	RAP2A, member of RAS oncogene family	-0.408	3.44E-02
CYP3A7	cytochrome P450, family 3, subfamily A, polypeptide 7	0.408	3.47E-02
CS	citrate synthase	-0.408	3.47E-02
GMEB1	glucocorticoid modulatory element binding protein 1	0.408	3.47E-02
KRTAP9-4	keratin associated protein 9-4	-0.408	3.47E-02
MORC4	MORC family CW-type zinc finger 4	-0.408	3.47E-02
MRPL17	mitochondrial ribosomal protein L17	-0.408	3.47E-02
NAPEPLD	N-acyl phosphatidylethanolamine phospholipase D	0.408	3.47E-02
TNFAIP1	tumor necrosis factor, alpha-induced protein 1 (endothelial)	-0.408	3.47E-02
PGC	progastricsin (pepsinogen C)	0.407	3.50E-02
DNAI1	dynein, axonemal, intermediate chain 1	-0.407	3.50E-02
FANK1	fibronectin type III and ankyrin repeat domains 1	-0.407	3.50E-02
OLAH	oleoyl-ACP hydrolase	-0.407	3.50E-02
ANP32C	acidic (leucine-rich) nuclear phosphoprotein 32 family, member C	0.407	3.53E-02
ARAF	v-raf murine sarcoma 3611 viral oncogene homolog	-0.407	3.53E-02
FOXJ3	forkhead box J3	0.407	3.53E-02
PCDH17	protocadherin 17	-0.407	3.53E-02
SMC1A	structural maintenance of chromosomes 1A	-0.407	3.53E-02
SMYD4	SET and MYND domain containing 4	0.407	3.53E-02
ZNF696	zinc finger protein 696	0.407	3.53E-02
APBA1	amyloid beta (A4) precursor protein-binding, family A, member 1	0.406	3.56E-02
BHLHA15	basic helix-loop-helix family, member a15	0.406	3.56E-02
GABRG1	gamma-aminobutyric acid (GABA) A receptor, gamma 1	0.406	3.56E-02
KIT	v-kit Hardy-Zuckerman 4 feline sarcoma viral oncogene homolog	0.406	3.56E-02
MTHFD1L	methylenetetrahydrofolate dehydrogenase (NADP+ dependent) 1-like	0.406	3.56E-02
PPM1A	protein phosphatase, Mg ²⁺ /Mn ²⁺ dependent, 1A	-0.406	3.56E-02
IL12RB2	interleukin 12 receptor, beta 2	0.406	3.58E-02
CD300C	CD300c molecule	0.405	3.59E-02
DCAF15	DDB1 and CUL4 associated factor 15	0.405	3.59E-02

SPAG11B	sperm associated antigen 11B	-0.405	3.59E-02
TCTN2	tectonic family member 2	-0.405	3.59E-02
UBE2E3	ubiquitin-conjugating enzyme E2E 3 (UBC4/5 homolog, yeast)	0.405	3.59E-02
ACRBP	acrosin binding protein	0.405	3.62E-02
CD93	CD93 molecule	-0.405	3.62E-02
SLC26A11	solute carrier family 26, member 11	-0.405	3.62E-02
STX17	syntaxin 17	-0.405	3.62E-02
ARID1B	AT rich interactive domain 1B (SWI1-like)	0.404	3.65E-02
ATXN2L	ataxin 2-like	0.404	3.65E-02
PGRMC2	progesterone receptor membrane component 2	-0.404	3.65E-02
CSTF2T	cleavage stimulation factor, 3' pre-RNA, subunit 2, 64kDa, tau variant	-0.404	3.69E-02
GPT2	glutamic pyruvate transaminase (alanine aminotransferase) 2	0.404	3.69E-02
SCAP	SREBF chaperone	0.404	3.69E-02
TFAP2D	transcription factor AP-2 delta (activating enhancer binding protein 2 delta)	0.404	3.69E-02
ADAM17	ADAM metallopeptidase domain 17	0.403	3.72E-02
LOC100131541	hypothetical LOC100131541	0.403	3.72E-02
MITF	microphthalmia-associated transcription factor	0.403	3.72E-02
MORN2	MORN repeat containing 2	-0.403	3.72E-02
PAGE1	P antigen family, member 1 (prostate associated)	-0.403	3.72E-02
PRPF4B	PRP4 pre-mRNA processing factor 4 homolog B (yeast)	-0.403	3.72E-02
RAD54L	RAD54-like (<i>S. cerevisiae</i>)	0.403	3.72E-02
RPS6KA2	ribosomal protein S6 kinase, 90kDa, polypeptide 2	0.403	3.72E-02
C1orf35	chromosome 1 open reading frame 35	-0.403	3.73E-02
FAM131C	family with sequence similarity 131, member C	0.402	3.75E-02
FLJ41170	hypothetical LOC440200	-0.402	3.75E-02
SLC17A8	solute carrier family 17 (sodium-dependent inorganic phosphate cotransporter), member 8	-0.402	3.75E-02
TSPYL6	TSPY-like 6	0.402	3.75E-02
XYLT1	xylosyltransferase I	0.402	3.75E-02
IGFBP3	insulin-like growth factor binding protein 3	0.402	3.78E-02
RPL13	ribosomal protein L13	0.402	3.78E-02
SH3PXD2A	SH3 and PX domains 2A	0.402	3.78E-02
ZBTB2	zinc finger and BTB domain containing 2	0.402	3.78E-02
C11orf40	chromosome 11 open reading frame 40	0.401	3.81E-02
DIP2B	DIP2 disco-interacting protein 2 homolog B (<i>Drosophila</i>)	-0.401	3.81E-02
MEST	mesoderm specific transcript homolog (mouse)	-0.401	3.81E-02
SLC7A11	solute carrier family 7, (cationic amino acid transporter, y ⁺ system) member 11	0.401	3.81E-02
TRAPPC8	trafficking protein particle complex 8	-0.401	3.81E-02
USP1	ubiquitin specific peptidase 1	0.401	3.81E-02
ZNF169	zinc finger protein 169	-0.401	3.83E-02
ATXN7L2	ataxin 7-like 2	0.400	3.84E-02
EIF2C2	eukaryotic translation initiation factor 2C, 2	0.400	3.84E-02
CXorf58	chromosome X open reading frame 58	-0.400	3.84E-02
MFSD5	major facilitator superfamily domain containing 5	-0.400	3.84E-02
MKNK2	MAP kinase interacting serine/threonine kinase 2	-0.400	3.84E-02

OBP2B	odorant binding protein 2B	0.400	3.84E-02
ZNF177	zinc finger protein 177	-0.400	3.84E-02
SLC6A20	solute carrier family 6 (proline IMINO transporter), member 20	0.400	3.86E-02
COX16	COX16 cytochrome c oxidase assembly homolog (S. cerevisiae)	-0.400	3.88E-02
GOLGA5	golgin A5	-0.400	3.88E-02
GPRIN1	G protein regulated inducer of neurite outgrowth 1	0.400	3.88E-02
RRP9	ribosomal RNA processing 9, small subunit (SSU) processome component, homolog (yeast)	0.400	3.88E-02
SULT1A1	sulfotransferase family, cytosolic, 1A, phenol-preferring, member 1	-0.400	3.88E-02
ARMC7	armadillo repeat containing 7	-0.399	3.91E-02
HACE1	HECT domain and ankyrin repeat containing, E3 ubiquitin protein ligase 1	0.399	3.91E-02
TTN	titin	-0.399	3.91E-02
YKT6	YKT6 v-SNARE homolog (S. cerevisiae)	-0.399	3.91E-02
ALG11	asparagine-linked glycosylation 11, alpha-1,2-mannosyltransferase homolog (yeast)	-0.399	3.94E-02
DPCD	deleted in primary ciliary dyskinesia homolog (mouse)	-0.399	3.94E-02
GSTA3	glutathione S-transferase alpha 3	-0.399	3.94E-02
SPRY1	sprouty homolog 1, antagonist of FGF signaling (Drosophila)	-0.399	3.94E-02
THOC7	THO complex 7 homolog (Drosophila)	0.399	3.94E-02
AXIN2	axin 2	-0.398	3.98E-02
PIP5K1C	phosphatidylinositol-4-phosphate 5-kinase, type I, gamma	-0.398	3.98E-02
RECQL4	RecQ protein-like 4	0.398	3.98E-02
SRRT	serrate RNA effector molecule homolog (Arabidopsis)	0.398	3.98E-02
CNTN4	contactin 4	0.397	4.01E-02
MTHFD2	methylenetetrahydrofolate dehydrogenase (NADP+ dependent) 2, methenyltetrahydrofolate cyclohydrolase	0.397	4.01E-02
NAA50	N(alpha)-acetyltransferase 50, NatE catalytic subunit	0.397	4.01E-02
PPP1R14A	protein phosphatase 1, regulatory (inhibitor) subunit 14A	0.397	4.01E-02
STRN4	striatin, calmodulin binding protein 4	0.397	4.01E-02
TMCO3	transmembrane and coiled-coil domains 3	-0.397	4.01E-02
CC2D1B	coiled-coil and C2 domain containing 1B	0.397	4.04E-02
C19orf18	chromosome 19 open reading frame 18	-0.397	4.04E-02
C9orf156	chromosome 9 open reading frame 156	-0.397	4.04E-02
MLH3	mutL homolog 3 (E. coli)	-0.397	4.04E-02
KERA	keratocan	0.397	4.05E-02
C19orf43	chromosome 19 open reading frame 43	0.396	4.08E-02
EPB41L2	erythrocyte membrane protein band 4.1-like 2	0.396	4.08E-02
ATAD1	ATPase family, AAA domain containing 1	-0.396	4.08E-02
COPB2	coatamer protein complex, subunit beta 2 (beta prime)	-0.396	4.08E-02
PDE1A	phosphodiesterase 1A, calmodulin-dependent	-0.396	4.08E-02
FOSB	FBJ murine osteosarcoma viral oncogene homolog B	0.396	4.09E-02
C10orf55	chromosome 10 open reading frame 55	0.396	4.11E-02
BIVM	basic, immunoglobulin-like variable motif containing	-0.396	4.11E-02
DSG1	desmoglein 1	-0.396	4.11E-02
LIG3	ligase III, DNA, ATP-dependent	-0.396	4.11E-02

NRD1	nardilysin (N-arginine dibasic convertase)	0.396	4.11E-02
PHF5A	PHD finger protein 5A	0.396	4.11E-02
TMEM49	transmembrane protein 49	-0.396	4.11E-02
TTC30B	tetratricopeptide repeat domain 30B	-0.396	4.11E-02
FMO1	flavin containing monooxygenase 1	-0.395	4.12E-02
ADRA1A	adrenergic, alpha-1A-, receptor	-0.395	4.13E-02
KIF21A	kinesin family member 21A	-0.395	4.14E-02
BRPF1	bromodomain and PHD finger containing, 1	0.395	4.14E-02
CASP12	caspase 12 (gene/pseudogene)	0.395	4.14E-02
AHSA1	AHA1, activator of heat shock 90kDa protein ATPase homolog 1 (yeast)	-0.395	4.14E-02
C16orf78	chromosome 16 open reading frame 78	-0.395	4.14E-02
PKLR	pyruvate kinase, liver and RBC	0.395	4.14E-02
PLA2G12A	phospholipase A2, group XIIA	0.395	4.14E-02
RNF11	ring finger protein 11	0.395	4.14E-02
LMBR1L	limb region 1 homolog (mouse)-like	-0.395	4.16E-02
CHRNE	cholinergic receptor, nicotinic, epsilon	0.394	4.18E-02
MOBK2A	MOB1, Mps One Binder kinase activator-like 2A (yeast)	-0.394	4.18E-02
TNP1	transition protein 1 (during histone to protamine replacement)	0.394	4.18E-02
GPHN	gephyrin	-0.394	4.21E-02
HSP90AA1	heat shock protein 90kDa alpha (cytosolic), class A member 1	-0.394	4.21E-02
LGI4	leucine-rich repeat LGI family, member 4	-0.394	4.21E-02
MCRS1	microspherule protein 1	-0.394	4.21E-02
NDUFB1	NADH dehydrogenase (ubiquinone) 1 beta subcomplex, 1, 7kDa	-0.394	4.21E-02
PIGS	phosphatidylinositol glycan anchor biosynthesis, class S	-0.394	4.21E-02
RBM43	RNA binding motif protein 43	-0.394	4.21E-02
AGXT2	alanine--glyoxylate aminotransferase 2	-0.393	4.24E-02
USP7	ubiquitin specific peptidase 7 (herpes virus-associated)	-0.393	4.24E-02
CBX8	chromobox homolog 8	-0.393	4.25E-02
FKBP3	FK506 binding protein 3, 25kDa	-0.393	4.25E-02
FKBP8	FK506 binding protein 8, 38kDa	0.393	4.25E-02
GGCT	gamma-glutamylcyclotransferase	-0.393	4.25E-02
PHF8	PHD finger protein 8	-0.393	4.25E-02
PRKCQ	protein kinase C, theta	0.393	4.25E-02
RDH13	retinol dehydrogenase 13 (all-trans/9-cis)	-0.393	4.25E-02
RGP1	RGP1 retrograde golgi transport homolog (S. cerevisiae)	0.393	4.25E-02
TMED1	transmembrane emp24 protein transport domain containing 1	0.393	4.25E-02
TMEM25	transmembrane protein 25	-0.393	4.25E-02
IL1RAPL1	interleukin 1 receptor accessory protein-like 1	-0.393	4.26E-02
ADPRH	ADP-ribosylarginine hydrolase	0.393	4.28E-02
C17orf37	chromosome 17 open reading frame 37	-0.393	4.28E-02
LOC150197	hypothetical LOC150197	0.393	4.28E-02
OCR1	ovarian cancer-related protein 1	-0.393	4.28E-02
PDXP	pyridoxal (pyridoxine, vitamin B6) phosphatase	0.393	4.28E-02
SCRIB	scribbled homolog (Drosophila)	0.393	4.28E-02
TMEM149	transmembrane protein 149	-0.393	4.28E-02
SAA3P	serum amyloid A3 pseudogene	-0.393	4.28E-02

ESYT2	extended synaptotagmin-like protein 2	0.392	4.31E-02
CD3E	CD3e molecule, epsilon (CD3-TCR complex)	-0.392	4.32E-02
FNBP1L	formin binding protein 1-like	-0.392	4.32E-02
OR5M3	olfactory receptor, family 5, subfamily M, member 3	0.392	4.32E-02
PTPN13	protein tyrosine phosphatase, non-receptor type 13 (APO-1/CD95 (Fas)-associated phosphatase)	-0.392	4.32E-02
RPIA	ribose 5-phosphate isomerase A	0.392	4.32E-02
SYNJ2BP	synaptojanin 2 binding protein	-0.392	4.32E-02
DNAJC8	DnaJ (Hsp40) homolog, subfamily C, member 8	0.392	4.33E-02
ATAD2B	ATPase family, AAA domain containing 2B	-0.391	4.35E-02
C15orf63	chromosome 15 open reading frame 63	-0.391	4.35E-02
FPR3	formyl peptide receptor 3	-0.391	4.35E-02
GNB5	guanine nucleotide binding protein (G protein), beta 5	0.391	4.35E-02
GNPAT	glyceronephosphate O-acyltransferase	-0.391	4.35E-02
PMP22	peripheral myelin protein 22	0.391	4.35E-02
PPARA	peroxisome proliferator-activated receptor alpha	0.391	4.35E-02
SOX30	SRY (sex determining region Y)-box 30	0.391	4.35E-02
UNC5B	unc-5 homolog B (C. elegans)	-0.391	4.35E-02
C14orf21	chromosome 14 open reading frame 21	0.391	4.39E-02
C1orf161	chromosome 1 open reading frame 161	0.391	4.39E-02
C14orf129	chromosome 14 open reading frame 129	-0.391	4.39E-02
CES2	carboxylesterase 2	-0.391	4.39E-02
GPD1L	glycerol-3-phosphate dehydrogenase 1-like	-0.391	4.39E-02
IFITM2	interferon induced transmembrane protein 2 (1-8D)	-0.391	4.39E-02
SOST	sclerostin	-0.391	4.39E-02
STRA13	stimulated by retinoic acid 13 homolog (mouse)	-0.391	4.39E-02
VSX2	visual system homeobox 2	-0.391	4.39E-02
GSPT1	G1 to S phase transition 1	-0.390	4.43E-02
MAP3K2	mitogen-activated protein kinase kinase kinase 2	0.390	4.43E-02
ST6GAL1	ST6 beta-galactosamide alpha-2,6-sialyltransferase 1	-0.390	4.43E-02
TNFSF8	tumor necrosis factor (ligand) superfamily, member 8	-0.390	4.43E-02
FAM53C	family with sequence similarity 53, member C	0.389	4.46E-02
GBX2	gastrulation brain homeobox 2	0.389	4.46E-02
KRT35	keratin 35	0.389	4.46E-02
SNRNP40	small nuclear ribonucleoprotein 40kDa (U5)	0.389	4.46E-02
TRAPPC3	trafficking protein particle complex 3	0.389	4.46E-02
CCDC110	coiled-coil domain containing 110	-0.389	4.50E-02
LRRC19	leucine rich repeat containing 19	-0.389	4.50E-02
RAG1	recombination activating gene 1	-0.389	4.51E-02
TSLP	thymic stromal lymphopoietin	0.389	4.52E-02
TMEM71	transmembrane protein 71	0.388	4.53E-02
C13orf18	chromosome 13 open reading frame 18	0.388	4.53E-02
C1orf86	chromosome 1 open reading frame 86	0.388	4.53E-02
CBX3	chromobox homolog 3	-0.388	4.53E-02
HIF1AN	hypoxia inducible factor 1, alpha subunit inhibitor	-0.388	4.53E-02
NDUFS7	NADH dehydrogenase (ubiquinone) Fe-S protein 7, 20kDa (NADH-coenzyme Q reductase)	-0.388	4.53E-02
NKAIN4	Na ⁺ /K ⁺ transporting ATPase interacting 4	-0.388	4.53E-02

PPT2	palmitoyl-protein thioesterase 2	0.388	4.53E-02
RASSF8	Ras association (RalGDS/AF-6) domain family (N-terminal) member 8	0.388	4.53E-02
TMEM198	transmembrane protein 198	0.388	4.53E-02
USP30	ubiquitin specific peptidase 30	-0.388	4.53E-02
ROPN1	ropporin, rhophilin associated protein 1	0.388	4.56E-02
ELF4	E74-like factor 4 (ets domain transcription factor)	0.388	4.57E-02
MRPL12	mitochondrial ribosomal protein L12	-0.388	4.57E-02
NPLOC4	nuclear protein localization 4 homolog (S. cerevisiae)	-0.388	4.57E-02
TIMM17B	translocase of inner mitochondrial membrane 17 homolog B (yeast)	-0.388	4.57E-02
TP53I11	tumor protein p53 inducible protein 11	-0.388	4.57E-02
TPD52L3	tumor protein D52-like 3	-0.388	4.57E-02
VILL	villin-like	0.388	4.57E-02
WFDC10A	WAP four-disulfide core domain 10A	0.388	4.57E-02
C17orf70	chromosome 17 open reading frame 70	-0.387	4.61E-02
EGF	epidermal growth factor	-0.387	4.61E-02
PABPN1	poly(A) binding protein, nuclear 1	0.387	4.61E-02
TPRA1	transmembrane protein, adipocyte associated 1	0.387	4.61E-02
ZNF605	zinc finger protein 605	-0.387	4.61E-02
AKAP8L	A kinase (PRKA) anchor protein 8-like	0.386	4.65E-02
ARID3B	AT rich interactive domain 3B (BRIGHT-like)	-0.386	4.65E-02
FAM111A	family with sequence similarity 111, member A	-0.386	4.65E-02
GABBR2	gamma-aminobutyric acid (GABA) B receptor, 2	0.386	4.65E-02
HDAC2	histone deacetylase 2	0.386	4.65E-02
IQCE	IQ motif containing E	-0.386	4.65E-02
RAP1GAP2	RAP1 GTPase activating protein 2	0.386	4.65E-02
RPS6KB1	ribosomal protein S6 kinase, 70kDa, polypeptide 1	-0.386	4.65E-02
SLC40A1	solute carrier family 40 (iron-regulated transporter), member 1	-0.386	4.65E-02
TRIM56	tripartite motif-containing 56	0.386	4.65E-02
UBE2O	ubiquitin-conjugating enzyme E2O	-0.386	4.65E-02
ABHD14A	abhydrolase domain containing 14A	0.386	4.68E-02
C7orf55	chromosome 7 open reading frame 55	0.386	4.68E-02
AGGF1	angiogenic factor with G patch and FHA domains 1	-0.386	4.68E-02
DNAJB13	DnaJ (Hsp40) homolog, subfamily B, member 13	-0.386	4.68E-02
GAS2	growth arrest-specific 2	0.386	4.68E-02
LCE1B	late cornified envelope 1B	0.386	4.68E-02
NAP1L4	nucleosome assembly protein 1-like 4	-0.386	4.68E-02
SGSH	N-sulfoglucosamine sulfohydrolase	-0.386	4.68E-02
TRPM7	transient receptor potential cation channel, subfamily M, member 7	0.386	4.68E-02
CCDC67	coiled-coil domain containing 67	-0.386	4.70E-02
SERPINF2	serpin peptidase inhibitor, clade F (alpha-2 antiplasmin, pigment epithelium derived factor), member 2	-0.386	4.70E-02
C12orf29	chromosome 12 open reading frame 29	-0.385	4.72E-02
C17orf87	chromosome 17 open reading frame 87	-0.385	4.72E-02
PLCXD2	phosphatidylinositol-specific phospholipase C, X domain containing 2	0.385	4.72E-02
PMAIP1	phorbol-12-myristate-13-acetate-induced protein 1	0.385	4.72E-02

C9orf98	chromosome 9 open reading frame 98	-0.385	4.76E-02
COX6B1	cytochrome c oxidase subunit VIb polypeptide 1 (ubiquitous)	-0.385	4.76E-02
DCXR	dicarbonyl/L-xylulose reductase	-0.385	4.76E-02
OR10K2	olfactory receptor, family 10, subfamily K, member 2	0.385	4.76E-02
SHF	Src homology 2 domain containing F	0.385	4.76E-02
SST	somatostatin	0.385	4.76E-02
DNAJB6	DnaJ (Hsp40) homolog, subfamily B, member 6	0.384	4.80E-02
EXOSC1	exosome component 1	-0.384	4.80E-02
FGF2	fibroblast growth factor 2 (basic)	0.384	4.80E-02
GEMIN8	gem (nuclear organelle) associated protein 8	-0.384	4.80E-02
SLC4A9	solute carrier family 4, sodium bicarbonate cotransporter, member 9	0.384	4.80E-02
ATOH1	atonal homolog 1 (Drosophila)	0.383	4.84E-02
BRSK2	BR serine/threonine kinase 2	0.383	4.84E-02
ACTR10	actin-related protein 10 homolog (S. cerevisiae)	-0.383	4.84E-02
LPAL2	lipoprotein, Lp(a)-like 2, pseudogene	0.383	4.84E-02
MAN1B1	mannosidase, alpha, class 1B, member 1	0.383	4.84E-02
SELPLG	selectin P ligand	0.383	4.84E-02
UBE3C	ubiquitin protein ligase E3C	0.383	4.84E-02
FOXL1	forkhead box L1	0.383	4.85E-02
PHGDH	phosphoglycerate dehydrogenase	0.383	4.87E-02
ADCY7	adenylate cyclase 7	0.383	4.88E-02
ARHGAP1	Rho GTPase activating protein 1	-0.383	4.88E-02
DIP2B	DIP2 disco-interacting protein 2 homolog B (Drosophila)	-0.383	4.88E-02
DNAJB3	DnaJ (Hsp40) homolog, subfamily B, member 3	-0.383	4.88E-02
GLI4	GLI family zinc finger 4	0.383	4.88E-02
LRRC8C	leucine rich repeat containing 8 family, member C	0.383	4.88E-02
PLCD4	phospholipase C, delta 4	-0.383	4.88E-02
RGNEF	190 kDa guanine nucleotide exchange factor	0.383	4.88E-02
SLC28A3	solute carrier family 28 (sodium-coupled nucleoside transporter), member 3	0.383	4.88E-02
SLC7A1	solute carrier family 7 (cationic amino acid transporter, y+ system), member 1	0.383	4.88E-02
USE1	unconventional SNARE in the ER 1 homolog (S. cerevisiae)	0.383	4.88E-02
VLDLR	very low density lipoprotein receptor	0.383	4.88E-02
ZCCHC16	zinc finger, CCHC domain containing 16	-0.383	4.88E-02
ALAS1	aminolevulinate, delta-, synthase 1	0.382	4.92E-02
NPM2	nucleophosmin/nucleoplasmin 2	0.382	4.92E-02
TPD52L2	tumor protein D52-like 2	0.382	4.92E-02
VPS29	vacuolar protein sorting 29 homolog (S. cerevisiae)	-0.382	4.92E-02
VKORC1	vitamin K epoxide reductase complex, subunit 1	0.382	4.95E-02
C14orf79	chromosome 14 open reading frame 79	-0.382	4.95E-02
RP2	retinitis pigmentosa 2 (X-linked recessive)	-0.382	4.95E-02
DCAF5	DDB1 and CUL4 associated factor 5	-0.381	4.99E-02
PEX6	peroxisomal biogenesis factor 6	-0.381	4.99E-02
RARS2	arginyl-tRNA synthetase 2, mitochondrial	0.381	4.99E-02
TUBAL3	tubulin, alpha-like 3	-0.381	4.99E-02
C14orf105	chromosome 14 open reading frame 105	-0.381	5.00E-02

REFERENCES

- Armanios, M. (2013). Telomeres and age-related disease: how telomere biology informs clinical paradigms. *J. Clin. Invest.* *123*, 996–1002.
- Armanios, M., and Blackburn, E.H. (2012). The telomere syndromes. *Nat. Rev. Genet.* *13*, 693–704.
- Artandi, S.E., Alson, S., Tietze, M.K., Sharpless, N.E., Ye, S., Greenberg, R.A., Castrillon, D.H., Horner, J.W., Weiler, S.R., Carrasco, R.D., et al. (2002). Constitutive telomerase expression promotes mammary carcinomas in aging mice. *Proc. Natl. Acad. Sci. U. S. A.* *99*, 8191–8196.
- Barker, N., Hurlstone, A., Musisi, H., Miles, A., Bienz, M., and Clevers, H. (2001). The chromatin remodelling factor Brg-1 interacts with β -catenin to promote target gene activation. *EMBO J.* *20*, 4935–4943.
- Biechele, T.L., Adams, A.M., and Moon, R.T. (2009). Transcription-Based Reporters of Wnt/ β -Catenin Signaling. *Cold Spring Harb. Protoc.* *2009*, pdb.prot5223.
- Blackburn, E.H. (2000). Telomere states and cell fates. *Nature* *408*, 53–56.
- Blackburn, E.H. (2001). Switching and signaling at the telomere. *Cell* *106*, 661–673.
- Blackburn, E.H., and Collins, K. (2011). Telomerase: An RNP Enzyme Synthesizes DNA. *Cold Spring Harb. Perspect. Biol.* *3*, a003558.
- Blasco, M.A. (2005). Telomeres and human disease: ageing, cancer and beyond. *Nat. Rev. Genet.* *6*, 611–622.
- Broccoli, D., Godley, L.A., Donehower, L.A., Varmus, H.E., and de Lange, T. (1996). Telomerase activation in mouse mammary tumors: lack of detectable telomere shortening and evidence for regulation of telomerase RNA with cell proliferation. *Mol. Cell. Biol.* *16*, 3765–3772.
- Carpenter, S., Aiello, D., Atianand, M.K., Ricci, E.P., Gandhi, P., Hall, L.L., Byron, M., Monks, B., Henry-Bezy, M., Lawrence, J.B., et al. (2013). A Long Noncoding RNA Mediates Both Activation and Repression of Immune Response Genes. *Science* *341*, 789–792.
- Chebel, A., Bauwens, S., Gerland, L.-M., Belleville, A., Urbanowicz, I., de Climens, A.R., Tourneur, Y., Chien, W.W., Catallo, R., Salles, G., et al. (2009). Telomere uncapping during in vitro T-lymphocyte senescence. *Aging Cell* *8*, 52–64.
- Chen, J.L., Blasco, M.A., and Greider, C.W. (2000). Secondary structure of vertebrate telomerase RNA. *Cell* *100*, 503–514.
- Choi, J., Fauce, S.R., and Effros, R.B. (2008a). Reduced telomerase activity in human T lymphocytes exposed to cortisol. *Brain. Behav. Immun.* *22*, 600–605.

- Choi, J., Southworth, L.K., Sarin, K.Y., Venteicher, A.S., Ma, W., Chang, W., Cheung, P., Jun, S., Artandi, M.K., Shah, N., et al. (2008b). TERT Promotes Epithelial Proliferation through Transcriptional Control of a Myc- and Wnt-Related Developmental Program. *PLoS Genet* 4, e10.
- Chu, C., Qu, K., Zhong, F.L., Artandi, S.E., and Chang, H.Y. (2011). Genomic Maps of Long Noncoding RNA Occupancy Reveal Principles of RNA-Chromatin Interactions. *Mol. Cell* 44, 667–678.
- Dang, C.V. (2012). MYC on the Path to Cancer. *Cell* 149, 22–35.
- Daubenmier, J., Lin, J., Blackburn, E., Hecht, F.M., Kristeller, J., Maninger, N., Kuwata, M., Bacchetti, P., Havel, P.J., and Epel, E. (2012). Changes in stress, eating, and metabolic factors are related to changes in telomerase activity in a randomized mindfulness intervention pilot study. *Psychoneuroendocrinology* 37, 917–928.
- Diolaiti, M.E., Cimini, B.A., Kageyama, R., Charles, F.A., and Stohr, B.A. (2013). In situ visualization of telomere elongation patterns in human cells. *Nucleic Acids Res.* 41, e176.
- Epel, E.S., Blackburn, E.H., Lin, J., Dhabhar, F.S., Adler, N.E., Morrow, J.D., and Cawthon, R.M. (2004). Accelerated telomere shortening in response to life stress. *Proc. Natl. Acad. Sci. U. S. A.* 101, 17312–17315.
- Erlacher, M., Labi, V., Manzl, C., Böck, G., Tzankov, A., Häcker, G., Michalak, E., Strasser, A., and Villunger, A. (2006b). Puma cooperates with Bim, the rate-limiting BH3-only protein in cell death during lymphocyte development, in apoptosis induction. *J. Exp. Med.* 203, 2939–2951.
- Erlacher, M., Labi, V., Manzl, C., Böck, G., Tzankov, A., Häcker, G., Michalak, E., Strasser, A., and Villunger, A. (2006a). Puma cooperates with Bim, the rate-limiting BH3-only protein in cell death during lymphocyte development, in apoptosis induction. *J. Exp. Med.* 203, 2939–2951.
- Esteller, M. (2011). Non-coding RNAs in human disease. *Nat. Rev. Genet.* 12, 861–874.
- Euskirchen, G.M., Auerbach, R.K., Davidov, E., Gianoulis, T.A., Zhong, G., Rozowsky, J., Bhardwaj, N., Gerstein, M.B., and Snyder, M. (2011). Diverse Roles and Interactions of the SWI/SNF Chromatin Remodeling Complex Revealed Using Global Approaches. *PLoS Genet* 7, e1002008.
- Feng, J., Funk, W.D., Wang, S.S., Weinrich, S.L., Avilion, A.A., Chiu, C.P., Adams, R.R., Chang, E., Allsopp, R.C., Yu, J., et al. (1995). The RNA component of human telomerase. *Science* 269, 1236–1241.
- Firestein, R., Bass, A.J., Kim, S.Y., Dunn, I.F., Silver, S.J., Guney, I., Freed, E., Ligon, A.H., Vena, N., Ogino, S., et al. (2008). CDK8 is a colorectal cancer oncogene that regulates β -catenin activity. *Nature* 455, 547–551.

- Fu, D., and Collins, K. (2003). Distinct biogenesis pathways for human telomerase RNA and H/ACA small nucleolar RNAs. *Mol. Cell* *11*, 1361–1372.
- Del Gaizo Moore, V., Brown, J.R., Certo, M., Love, T.M., Novina, C.D., and Letai, A. (2007). Chronic lymphocytic leukemia requires BCL2 to sequester prodeath BIM, explaining sensitivity to BCL2 antagonist ABT-737. *J. Clin. Invest.* *117*, 112–121.
- Gazzaniga, F.S., Listerman, I., and Blackburn, E.H. (2013). An investigation of the effects of the telomerase core protein TERT on Wnt signaling in human breast cancer cells. *Mol. Cell Biol.*
- Ghosh, A., Saginc, G., Leow, S.C., Khattar, E., Shin, E.M., Yan, T.D., Wong, M., Zhang, Z., Li, G., Sung, W.-K., et al. (2012). Telomerase directly regulates NF- κ B-dependent transcription. *Nat. Cell Biol.* *14*, 1270–1281.
- Goytisolo, F.A., and Blasco, M.A. (2002). Many ways to telomere dysfunction: in vivo studies using mouse models. *Oncogene* *21*, 584–591.
- Groom, J.R., and Luster, A.D. (2011). CXCR3 ligands: redundant, collaborative and antagonistic functions. *Immunol. Cell Biol.* *89*, 207–215.
- Guo, X., and Wang, X.-F. (2009). Signaling cross-talk between TGF- β /BMP and other pathways. *Cell Res.* *19*, 71–88.
- Harley, C.B., Futcher, A.B., and Greider, C.W. (1990). Telomeres shorten during ageing of human fibroblasts. *Nature* *345*, 458–460.
- Harper, J.W., and Elledge, S.J. (2007). The DNA Damage Response: Ten Years After. *Mol. Cell* *28*, 739–745.
- Hedgepeth, C.M., Conrad, L.J., Zhang, J., Huang, H.-C., Lee, V.M.Y., and Klein, P.S. (1997). Activation of the Wnt Signaling Pathway: A Molecular Mechanism for Lithium Action. *Dev. Biol.* *185*, 82–91.
- Heidari, N., Miller, A.V., Hicks, M.A., Marking, C.B., and Harada, H. (2012). Glucocorticoid-mediated BIM induction and apoptosis are regulated by Runx2 and c-Jun in leukemia cells. *Cell Death Dis.* *3*, e349.
- Heiser, L.M., Sadanandam, A., Kuo, W.-L., Benz, S.C., Goldstein, T.C., Ng, S., Gibb, W.J., Wang, N.J., Ziyad, S., Tong, F., et al. (2012). Subtype and pathway specific responses to anticancer compounds in breast cancer. *Proc. Natl. Acad. Sci.* *109*, 2724–2729.
- Hengesbach, M., Kim, N.-K., Feigon, J., and Stone, M.D. (2012). Single-Molecule FRET Reveals the Folding Dynamics of the Human Telomerase RNA Pseudoknot Domain. *Angew. Chem. Int. Ed.* *51*, 5876–5879.

- Hoffmeyer, K., Raggioli, A., Rudloff, S., Anton, R., Hierholzer, A., Valle, I.D., Hein, K., Vogt, R., and Kemler, R. (2012). Wnt/ β -Catenin Signaling Regulates Telomerase in Stem Cells and Cancer Cells. *Science* 336, 1549–1554.
- Holland, J.D., Klaus, A., Garratt, A.N., and Birchmeier, W. (2013). Wnt signaling in stem and cancer stem cells. *Curr. Opin. Cell Biol.* 25, 254–264.
- Horn, S., Figl, A., Rachakonda, P.S., Fischer, C., Sucker, A., Gast, A., Kadel, S., Moll, I., Nagore, E., Hemminki, K., et al. (2013). TERT Promoter Mutations in Familial and Sporadic Melanoma. *Science* 339, 959–961.
- Howe, L.R., and Brown, A.M.C. (2004). Wnt Signaling and Breast Cancer. *Cancer Biol. Ther.* 3, 36–41.
- Hrdličková, R., Nehyba, J., and Bose, H.R. (2012). Alternatively Spliced Telomerase Reverse Transcriptase Variants Lacking Telomerase Activity Stimulate Cell Proliferation. *Mol. Cell Biol.* 32, 4283–4296.
- Huang, D.W., Sherman, B.T., and Lempicki, R.A. (2008). Systematic and integrative analysis of large gene lists using DAVID bioinformatics resources. *Nat. Protoc.* 4, 44–57.
- Huang, D.W., Sherman, B.T., and Lempicki, R.A. (2009). Bioinformatics enrichment tools: paths toward the comprehensive functional analysis of large gene lists. *Nucleic Acids Res.* 37, 1–13.
- Huang, F.W., Hodis, E., Xu, M.J., Kryukov, G.V., Chin, L., and Garraway, L.A. (2013). Highly Recurrent TERT Promoter Mutations in Human Melanoma. *Science* 339, 957–959.
- Kadam, S., and Emerson, B.M. (2003). Transcriptional Specificity of Human SWI/SNF BRG1 and BRM Chromatin Remodeling Complexes. *Mol. Cell* 11, 377–389.
- Kedde, M., le Sage, C., Duursma, A., Zlotorynski, E., van Leeuwen, B., Nijkamp, W., Beijersbergen, R., and Agami, R. (2006). Telomerase-independent regulation of ATR by human telomerase RNA. *J. Biol. Chem.* 281, 40503–40514.
- Killela, P.J., Reitman, Z.J., Jiao, Y., Bettegowda, C., Agrawal, N., Diaz, L.A., Friedman, A.H., Friedman, H., Gallia, G.L., Giovannella, B.C., et al. (2013). TERT promoter mutations occur frequently in gliomas and a subset of tumors derived from cells with low rates of self-renewal. *Proc. Natl. Acad. Sci.* 110, 6021–6026.
- Kim, N.-K., Theimer, C.A., Mitchell, J.R., Collins, K., and Feigon, J. (2010). Effect of pseudouridylation on the structure and activity of the catalytically essential P6.1 hairpin in human telomerase RNA. *Nucleic Acids Res.* 38, 6746–6756.
- Kim, N.W., Piatyszek, M.A., Prowse, K.R., Harley, C.B., West, M.D., Ho, P.L., Coviello, G.M., Wright, W.E., Weinrich, S.L., and Shay, J.W. (1994). Specific association of human telomerase activity with immortal cells and cancer. *Science* 266, 2011–2015.

- Kosciolek, B.A., and Rowley, P.T. (1999). Telomere-related components are coordinately synthesized during human T-lymphocyte activation. *Leuk. Res.* *23*, 1097–1103.
- Kraemer, K., Schmidt, U., Fuessel, S., Herr, A., Wirth, M.P., and Meye, A. (2006). Microarray analyses in bladder cancer cells: Inhibition of hTERT expression down-regulates EGFR. *Int. J. Cancer* *119*, 1276–1284.
- Lange, T. de (2009a). How Telomeres Solve the End-Protection Problem. *Science* *326*, 948–952.
- Lange, T. de (2009b). How Telomeres Solve the End-Protection Problem. *Science* *326*, 948–952.
- Lavretsky, H., Epel, E.S., Siddarth, P., Nazarian, N., Cyr, N.S., Khalsa, D.S., Lin, J., Blackburn, E., and Irwin, M.R. (2013). A pilot study of yogic meditation for family dementia caregivers with depressive symptoms: effects on mental health, cognition, and telomerase activity. *Int. J. Geriatr. Psychiatry* *28*, 57–65.
- Le, S., Sternglanz, R., and Greider, C.W. (2000). Identification of Two RNA-binding Proteins Associated with Human Telomerase RNA. *Mol. Biol. Cell* *11*, 999–1010.
- Lee, J., Sung, Y.H., Cheong, C., Choi, Y.S., Jeon, H.K., Sun, W., Hahn, W.C., Ishikawa, F., and Lee, H.-W. (2008). TERT promotes cellular and organismal survival independently of telomerase activity. *Oncogene* *27*, 3754–3760.
- Leeper, T., Leulliot, N., and Varani, G. (2003). The solution structure of an essential stem-loop of human telomerase RNA. *Nucleic Acids Res.* *31*, 2614–2621.
- Li, S., Rosenberg, J.E., Donjacour, A.A., Botchkina, I.L., Hom, Y.K., Cunha, G.R., and Blackburn, E.H. (2004). Rapid inhibition of cancer cell growth induced by lentiviral delivery and expression of mutant-template telomerase RNA and anti-telomerase short-interfering RNA. *Cancer Res.* *64*, 4833–4840.
- Lin, S.-Y., Xia, W., Wang, J.C., Kwong, K.Y., Spohn, B., Wen, Y., Pestell, R.G., and Hung, M.-C. (2000). β -Catenin, a novel prognostic marker for breast cancer: Its roles in cyclin D1 expression and cancer progression. *Proc. Natl. Acad. Sci.* *97*, 4262–4266.
- Listerman, I., Sun, J., Gazzaniga, F.S., Lukas, J.L., and Blackburn, E.H. (2013). The major reverse transcriptase-incompetent splice variant of the human telomerase protein inhibits telomerase activity but protects from apoptosis. *Cancer Res.* *73*, 2817–2828.
- Liu, K., Schoonmaker, M.M., Levine, B.L., June, C.H., Hodes, R.J., and Weng, N.P. (1999). Constitutive and regulated expression of telomerase reverse transcriptase (hTERT) in human lymphocytes. *Proc. Natl. Acad. Sci. U. S. A.* *96*, 5147–5152.
- Livak, K.J., and Schmittgen, T.D. (2001). Analysis of Relative Gene Expression Data Using Real-Time Quantitative PCR and the $2^{-\Delta\Delta CT}$ Method. *Methods* *25*, 402–408.

- Mahmoudi, T., Boj, S.F., Hatzis, P., Li, V.S.W., Taouatas, N., Vries, R.G.J., Teunissen, H., Begthel, H., Korving, J., Mohammed, S., et al. (2010). The Leukemia-Associated Mllt10/Af10-Dot11 Are Tcf4/ β -Catenin Coactivators Essential for Intestinal Homeostasis. *PLoS Biol* 8, e1000539.
- McLean, C.Y., Bristor, D., Hiller, M., Clarke, S.L., Schaar, B.T., Lowe, C.B., Wenger, A.M., and Bejerano, G. (2010). GREAT improves functional interpretation of cis-regulatory regions. *Nat. Biotechnol.* 28, 495–501.
- Menzel, O., Migliaccio, M., Goldstein, D.R., Dahoun, S., Delorenzi, M., and Rufer, N. (2006). Mechanisms Regulating the Proliferative Potential of Human CD8+ T Lymphocytes Overexpressing Telomerase. *J. Immunol.* 177, 3657–3668.
- Mitchell, J.R., and Collins, K. (2000). Human Telomerase Activation Requires Two Independent Interactions between Telomerase RNA and Telomerase Reverse Transcriptase. *Mol. Cell* 6, 361–371.
- Mitchell, J.R., Cheng, J., and Collins, K. (1999). A Box H/ACA Small Nucleolar RNA-Like Domain at the Human Telomerase RNA 3' End. *Mol. Cell. Biol.* 19, 567–576.
- Montanaro, L. (2010). Dyskerin and cancer: more than telomerase. The defect in mRNA translation helps in explaining how a proliferative defect leads to cancer. *J. Pathol.* 222, 345–349.
- Morrison, S.J., Prowse, K.R., Ho, P., and Weissman, I.L. (1996). Telomerase activity in hematopoietic cells is associated with self-renewal potential. *Immunity* 5, 207–216.
- Mukherjee, S., Firpo, E.J., Wang, Y., and Roberts, J.M. (2011). Separation of telomerase functions by reverse genetics. *Proc. Natl. Acad. Sci.* 108, E1363–E1371.
- Oh, H., Taffet, G.E., Youker, K.A., Entman, M.L., Overbeek, P.A., Michael, L.H., and Schneider, M.D. (2001). Telomerase reverse transcriptase promotes cardiac muscle cell proliferation, hypertrophy, and survival. *Proc. Natl. Acad. Sci.* 98, 10308–10313.
- Okamoto, N., Yasukawa, M., Nguyen, C., Kasim, V., Maida, Y., Possemato, R., Shibata, T., Ligon, K.L., Fukami, K., Hahn, W.C., et al. (2011). Maintenance of tumor initiating cells of defined genetic composition by nucleostemin. *Proc. Natl. Acad. Sci.* 108, 20388–20393.
- Ornish, D., Lin, J., Daubenmier, J., Weidner, G., Epel, E., Kemp, C., Magbanua, M.J.M., Marlin, R., Yglecias, L., Carroll, P.R., et al. (2008). Increased telomerase activity and comprehensive lifestyle changes: a pilot study. *Lancet Oncol.* 9, 1048–1057.
- Park, J.-I., Venteicher, A.S., Hong, J.Y., Choi, J., Jun, S., Shkreli, M., Chang, W., Meng, Z., Cheung, P., Ji, H., et al. (2009). Telomerase modulates Wnt signalling by association with target gene chromatin. *Nature* 460, 66–72.

Perillo, N.L., Walford, R.L., Newman, M.A., and Effros, R.B. (1989). Human T lymphocytes possess a limited in vitro life span. *Exp. Gerontol.* *24*, 177–187.

Qiao, F., and Cech, T.R. (2008). Triple-helix structure in telomerase RNA contributes to catalysis. *Nat. Struct. Mol. Biol.* *15*, 634–640.

Rahman, R., Latonen, L., and Wiman, K.G. (2004). hTERT antagonizes p53-induced apoptosis independently of telomerase activity. *Oncogene* *24*, 1320–1327.

Robart, A.R., and Collins, K. (2010). Investigation of human telomerase holoenzyme assembly, activity, and processivity using disease-linked subunit variants. *J. Biol. Chem.* *285*, 4375–4386.

Röth, A., Yssel, H., Pène, J., Chavez, E.A., Schertzer, M., Lansdorp, P.M., Spits, H., and Luiten, R.M. (2003). Telomerase levels control the lifespan of human T lymphocytes. *Blood* *102*, 849–857.

Röth, A., Baerlocher, G.M., Schertzer, M., Chavez, E., Dührsen, U., and Lansdorp, P.M. (2005). Telomere loss, senescence, and genetic instability in CD4⁺ T lymphocytes overexpressing hTERT. *Blood* *106*, 43–50.

Saebøe-Larsen, S., Fossberg, E., and Gaudernack, G. (2006). Characterization of novel alternative splicing sites in human telomerase reverse transcriptase (hTERT): analysis of expression and mutual correlation in mRNA isoforms from normal and tumour tissues. *BMC Mol. Biol.* *7*, 26.

Sarin, K.Y., Cheung, P., Gilson, D., Lee, E., Tennen, R.I., Wang, E., Artandi, M.K., Oro, A.E., and Artandi, S.E. (2005). Conditional telomerase induction causes proliferation of hair follicle stem cells. *Nature* *436*, 1048–1052.

Schindelin, J., Arganda-Carreras, I., Frise, E., Kaynig, V., Longair, M., Pietzsch, T., Preibisch, S., Rueden, C., Saalfeld, S., Schmid, B., et al. (2012). Fiji: an open-source platform for biological-image analysis. *Nat. Methods* *9*, 676–682.

Shay, J.W., and Bacchetti, S. (1997). A survey of telomerase activity in human cancer. *Eur. J. Cancer Oxf. Engl.* *1990* *33*, 787–791.

Shibamoto, Higano, K., Takada, R., Ito, F., Takeichi, M., and Takada, S. (1998). Cytoskeletal reorganization by soluble Wnt-3a protein signalling. *Genes Cells* *3*, 659–670.

Smith, L.L., Coller, H.A., and Roberts, J.M. (2003). Telomerase modulates expression of growth-controlling genes and enhances cell proliferation. *Nat. Cell Biol.* *5*, 474–479.

Stampfer, M.R., Garbe, J., Levine, G., Lichtsteiner, S., Vasserot, A.P., and Yaswen, P. (2001). Expression of the telomerase catalytic subunit, hTERT, induces resistance to transforming growth factor β growth inhibition in p16INK4A(-) human mammary epithelial cells. *Proc. Natl. Acad. Sci.* *98*, 4498–4503.

- Stohr, B.A., and Blackburn, E.H. (2008). ATM Mediates Cytotoxicity of a Mutant Telomerase RNA in Human Cancer Cells. *Cancer Res.* *68*, 5309–5317.
- Strong, M.A., Vidal-Cardenas, S.L., Karim, B., Yu, H., Guo, N., and Greider, C.W. (2011). Phenotypes in mTERT+/- and mTERT-/- Mice Are Due to Short Telomeres, Not Telomere-Independent Functions of Telomerase Reverse Transcriptase. *Mol. Cell. Biol.* *31*, 2369–2379.
- Teixeira, M.T., Förstemann, K., Gasser, S.M., and Lingner, J. (2002). Intracellular trafficking of yeast telomerase components. *EMBO Rep.* *3*, 652–659.
- Ueda, C.T., and Roberts, R.W. (2004). Analysis of a long-range interaction between conserved domains of human telomerase. *RNA* *10*, 139–147.
- Veeman, M.T., Slusarski, D.C., Kaykas, A., Louie, S.H., and Moon, R.T. (2003). Zebrafish Prickle, a Modulator of Noncanonical Wnt/Fz Signaling, Regulates Gastrulation Movements. *Curr. Biol.* *13*, 680–685.
- Watson, J.D. (1972). Origin of concatemeric T7 DNA. *Nature. New Biol.* *239*, 197–201.
- Wege, H., Chui, M.S., Le, H.T., Tran, J.M., and Zern, M.A. (2003). SYBR Green real-time telomeric repeat amplification protocol for the rapid quantification of telomerase activity. *Nucleic Acids Res.* *31*, E3–3.
- Weng, N.P., Levine, B.L., June, C.H., and Hodes, R.J. (1996). Regulated expression of telomerase activity in human T lymphocyte development and activation. *J. Exp. Med.* *183*, 2471–2479.
- Weng, N.P., Palmer, L.D., Levine, B.L., Lane, H.C., June, C.H., and Hodes, R.J. (1997). Tales of tails: regulation of telomere length and telomerase activity during lymphocyte development, differentiation, activation, and aging. *Immunol. Rev.* *160*, 43–54.
- Xiang, H., Wang, J., Mao, Y., Liu, M., Reddy, V.N., and Li, D.W.-C. (2002). Human telomerase accelerates growth of lens epithelial cells through regulation of the genes mediating RB/E2F pathway. *Oncogene* *21*, 3784–3791.
- Yeoman, J.A., Orte, A., Ashbridge, B., Klenerman, D., and Balasubramanian, S. (2010). RNA Conformation in Catalytically Active Human Telomerase. *J. Am. Chem. Soc.* *132*, 2852–2853.
- Yu, J., and Zhang, L. (2008). PUMA, a potent killer with or without p53. *Oncogene* *27*, S71–S83.
- Zhang, Y., Toh, L., Lau, P., and Wang, X. (2012). Human Telomerase Reverse Transcriptase (hTERT) Is a Novel Target of the Wnt/ β -Catenin Pathway in Human Cancer. *J. Biol. Chem.* *287*, 32494–32511.

Zhu, J., and Paul, W.E. (2008). CD4 T cells: fates, functions, and faults. *Blood* *112*, 1557–1569.

Zhu, L.J., Gazin, C., Lawson, N.D., Pagès, H., Lin, S.M., Lapointe, D.S., and Green, M.R. (2010). CHIPpeakAnno: a Bioconductor package to annotate CHIP-seq and CHIP-chip data. *BMC Bioinformatics* *11*, 237.

Zhu, Y., Tomlinson, R.L., Lukowiak, A.A., Terns, R.M., and Terns, M.P. (2004). Telomerase RNA accumulates in Cajal bodies in human cancer cells. *Mol. Biol. Cell* *15*, 81–90.

Zufferey, R., Nagy, D., Mandel, R.J., Naldini, L., and Trono, D. (1997). Multiply attenuated lentiviral vector achieves efficient gene delivery in vivo. *Nat. Biotechnol.* *15*, 871–875.


LIBRARY RELEASE FORM

Publishing Agreement

It is the policy of the University to encourage the distribution of all theses, dissertations, and manuscripts. Copies of all UCSF theses, dissertations, and manuscripts will be routed to the library via the Graduate Division. The library will make all theses, dissertations, and manuscripts accessible to the public and will preserve these to the best of their abilities, in perpetuity.

Please sign the following statement:

I hereby grant permission to the Graduate Division of the University of California, San Francisco to release copies of my thesis, dissertation, or manuscript to the Campus Library to provide access and preservation, in whole or in part, in perpetuity.



Author Signature

12-16-13
Date